

MULTI-OBJECTIVE OPTIMIZATION OF LASER CUTTING PARAMETERS USING PARTICLE SWARM OPTIMIZATION

A thesis submitted towards partial fulfilment of the requirements for the degree of

MTECH IN LASER TECHNOLOGY

by

AMLAN DIPTA CHAKRAVARTY

Examination Roll No.: M1LST21001

Registration No.: 154568 of 2020-2021

Under the guidance of

Dr.Paramasivan .K

School of Laser Science and Engineering

Faculty of Interdisciplinary Studies, Law and Management

Jadavpur University

Kolkata -700032

India

2022

DECLARATION OF ORIGINALITY

I hereby declare that this thesis is completed and written by me with the help of my co-guide Dr. Paramasivan.K entitling “MULTI-OBJECTIVE OPTIMIZATION OF LASER CUTTING PARAMETERS USING PARTICLE SWARM OPTIMIZATION” . This thesis is not submitted previously to any other professor or other university or examination body.

I give consent to this copy of my thesis, for the future research use of Jadavpur University.

.....
AMLAN DIPTA CHAKRAVARTY
M.Tech in Laser Technology
Roll No- M1LST21001

**FACULTY OF INTERDISCIPLINARY STUDIES LAW & MANAGEMENT
SCHOOL OF LASER SCIENCE AND ENGINEERING**

**JADAVPUR UNIVERSITY
KOLKATA -700032**

CERTIFICATE OF RECOMMENDATION

I HEREBY CERTIFY THAT THE THESIS PREPARED UNDER MY SUPERVISION BY AMLAN DIPTA CHAKRAVARTY ENTITLED MULTI OBJECTIVE OPTIMIZATION OF LASER CUTTING PARAMETERS USING PARTICLE SWARM OPTIMIZATION BE ACCEPTED IN THE PARTIAL FULFILLMENT OF THE REQUIREMENTS FOR THE DEGREE OF MASTER OF TECHNOLOGY IN LASER TECHNOLOGY DURING THE ACADEMIC SESSION 2019-2021.

THESIS SUPERVISOR

Dr.Paramasivan .K

School of Laser Science and Engineering
Jadavpur University, Kolkata-7000032

Countersigned

DIRECTOR

DIPTEN MISRA

School of Laser Science and Engineering

Jadavpur University, Kolkata-700 032

DEAN

Faculty of Interdisciplinary Studies, Law and Management Jadavpur University, Kolkata-700 032

FACULTY OF INTERDISCIPLINARY STUDIES, LAW AND MANAGEMENT

JADAVPUR UNIVERSITY

SCHOOL OF LASER SCIENCE AND ENGINEERING

KOLKATA -700032

CERTIFICATE OF APPROVAL

In this regard, the foregoing thesis is approved as a creditable study of an engineering subject that was conducted and presented in a satisfactory manner to warrant its acceptance as a prerequisite to the degree for which it was submitted. Those signing the thesis understand that it is not necessarily an endorsement or approval of any statement made in the thesis, or of any opinion expressed, or of any conclusion drawn, but accepts it only for the purpose for which it is submitted.

COMMITTEE OF FINAL EXAMINATION

FOR EVALUATION OF THE THESIS

Acknowledgement

It is a great privilege to express my profound and sincere gratitude to all the faculty members of the School of Laser Science and Engineering. I am also grateful to Dr.Paramasivan .K, Thesis Supervisor, School of Laser Science and Engineering unless whose enormous encouragement and guidance I may not complete the project in time. I would also like to show my gratitude to Prof.Dipten Misra, Director of School of Laser Science and Engineering for sharing his pearls of wisdom during this thesis submission .

Although any errors found in this thesis are my own and should not tarnish the reputation of these esteemed professors.

.....
AMLAN DIPTA CHAKRAVARTY
M.Tech in Laser Technology
Roll No- M1LST21001

Contents

DECLARATION OF ORIGINALITY	II
CERTIFICATE OF RECOMMENDATION.....	III
CERTIFICATE OF APPROVAL.....	IV
ACKNOWLEDGEMENT	V
ABSTRACT	IX
1. INTRODUCTION TO LASER CUTTING	2
1.1 WORKING PRINCIPLE OF LASER CUTTING	2
1.2 TYPES OF LASER CUTTING.....	3
1.2.1 Vaporization Cutting	4
1.2.2 Fusion cutting – Melt & Blow.....	4
1.2.3 Reactive Fusion Cutting	5
1.2.4 Controlled Fracture.....	5
1.2.5 Scribing	5
1.2.6 Cold Cutting.....	6
1.2.7 LASOX.....	7
1.2.8 Sublimation cutting	7
1.3 METHODS OF CUTTING.....	8
1.4 CONVENTIONAL CUTTING METHODS	8
1.5 NON-CONVENTIONAL CUTTING METHODS.....	9
1.5.1 Hybrid Cutting Methods	9
1.6 CUTTING WITH LASERS.....	9
1.6.1 ND:YAG Laser	10
1.6.2 Co2 Laser.....	10
1.6.3 Fibre Laser.....	10
1.7 PROCESS VARIATIONS.....	11
1.7.1 Arc Augmented Laser Cutting	11
1.7.2 Hot Machining.....	11
1.8 MECHANISM OF MATERIAL REMOVAL	11
1.8.1 Vaporization.....	12
1.8.2 Melting/Boiling	12
1.8.3 Ablation	12
1.8.4 Phasor Explosion	12
1.9 PARAMETERS OF LASER CUTTING	13
1.9.1 Beam Characteristics.....	13
1.9.2 Transport Characteristics.....	15
1.9.3 Gas Characteristics.....	16
1.9.4 Material Property.....	17
1.10 CHARACTERISTICS OF LASER CUT	17
1.10.1 Kerf Depth	17
1.10.2 Heat Affected Zone	18
1.10.3 Recast Layer	18
1.10.4 Surface Roughness.....	18
1.10.5 Taper Angle	18
1.11 APPLICATION OF LASER CUTTING.....	18
1.12 ADVANTAGES OF LASER CUTTING.....	19
1.13 DISADVANTAGES OF LASER CUTTING	19

1.14	PRECAUTION OF LASER CUTTING.....	19
1.14.1	<i>Cornering & Edge Burning</i>	19
1.14.2	<i>End Discontinuity</i>	20
1.14.3	<i>Movement while Cutting</i>	20
1.14.4	<i>Damage to initial hole</i>	20
2.	LITERATURE SURVEY	22
2.1	SURVEY FROM PAST RESEARCH	22
2.2	MOTIVATION OF PRESENT RESEARCH.....	25
2.3	OBJECTIVE OF RESEARCH.....	25
3.	INTRODUCTION TO OPTIMIZATION TECHNIQUE	27
3.1	COMPONENTS OF OPTIMIZATION PROBLEM	27
3.1.1	<i>Design Variables</i>	27
3.1.2	<i>Design Constraint</i>	27
3.1.3	<i>Objective Function</i>	27
3.2	TYPES OF OPTIMIZATION TECHNIQUE	29
3.2.1	<i>Single Variable Optimization Algorithms</i>	29
3.2.2	<i>Multiple Variable Optimization Algorithms</i>	29
3.2.3	<i>Constrained Optimization Algorithms</i>	29
3.2.4	<i>Specialized Optimization Algorithms</i>	29
3.2.5	<i>Non- Traditional Optimization Algorithms</i>	29
3.3	MATLAB MODELLING	30
4.	PARTICLE SWARM OPTIMIZATION TECHNIQUE.....	32
4.1	INTRODUCTION	32
4.2	SEARCH STRATEGY.....	32
4.3	IMPLEMENTATION OF PSO	32
5.	EXPERIMENTAL STUDY AND DETAILS	36
5.1	INTRODUCTION	36
5.2	OPTIMIZATION OF THE OBJECTIVE FUNCTION.....	36
5.4	MULTIPLE OBSERVATION BY VARYING CONSTANT	37
5.4.1	<i>Observation 1</i>	37
5.4.2	<i>Observation 2</i>	40
5.4.3	<i>Observation 3</i>	43
5.4.4	<i>Observation 4</i>	46
5.4.5	<i>Observation 5</i>	49
5.4.6	<i>Observation 6</i>	57
5.4.7	<i>Observation 7</i>	65
5.4.8	<i>Observation 8</i>	74
5.5	GENERAL DISCUSSION	83
6.1	CONCLUSION	86
6.2	FUTURE SCOPE OF WORK	87
6.	APPENDICES	91
6.2	APPENDIX 2	92

TABLE OF FIGURES

FIGURE:1-	ARRANGEMENT FOR LASER CUTTING USING: A) TRANSMISSIVE OPTICS, AND B) REFLECTIVE OPTICS	2
FIGURE:2-	METHODS OF LASER CUTTING	3
FIGURE:3-	VAPORIZATION LASER CUTTING	4
FIGURE:4-	FLOW CHART OF PARTICLE SWARM OPTIMIZATION	34
FIGURE:5-	PARAMETERS OF 1 ST OBSERVATIONS	37
FIGURE:6-	GRAPH FROM 1 ST OBSERVATION WITH TAPER ANGLE VS GLASS FORMATION	37
FIGURE:7-	PARAMETERS OF 2 ND OBSERVATIONS	40
FIGURE:8-	GRAPH FROM 2 ST OBSERVATION WITH TAPER ANGLE VS GLASS FORMATION WIDTH.....	40
FIGURE:9-	PARAMETERS OF 3 RD OBSERVATIONS.....	43
FIGURE:10-	GRAPH FROM 3 RD OBSERVATION WITH TAPER ANGLE VS GLASS FORMATION	43
FIGURE:11-	PARAMETERS OF 4 TH OBSERVATIONS.....	46
FIGURE:12-	GRAPH FROM 4 TH OBSERVATION WITH TAPER ANGLE VS GLASS FORMATION	46
FIGURE:13-	PARAMETERS OF 5 TH OBSERVATIONS.....	49
FIGURE:14-	GRAPH FROM 5 TH OBSERVATION WITH TAPER ANGLE VS GLASS FORMATION	49
FIGURE:15-	PARAMETERS OF 6 TH OBSERVATIONS.....	57
FIGURE:16-	GRAPH FROM 6 TH OBSERVATION WITH TAPER ANGLE VS GLASS FORMATION	57
FIGURE:17-	PARAMETERS OF 7 TH OBSERVATIONS	65
FIGURE:18-	GRAPH FROM 7 TH OBSERVATION WITH TAPER ANGLE VS GLASS FORMATION	65
FIGURE:19-	PARAMETERS OF 8 TH OBSERVATIONS	74
FIGURE:20-	GRAPH FROM 8 TH OBSERVATION WITH TAPER ANGLE VS GLASS FORMATION	74

LIST OF TABLES

TABLE No:1-	OBSERVATION NO.1 WITH RESPECT TO INPUT PARAMETERS AND OUTPUT.....	38
TABLE No:2-	2 ND OBSERVATION WITH RESPECT TO INPUT PARAMETERS AND OUTPUT.....	41
TABLE No:3-	3 RD OBSERVATION WITH RESPECT TO INPUT PARAMETERS AND OUTPUT	44
TABLE No:4-	4 TH OBSERVATION WITH RESPECT TO INPUT PARAMETERS AND OUTPUT	47
TABLE No:5-	5 TH OBSERVATION WITH RESPECT TO INPUT PARAMETERS AND OUTPUT	50
TABLE No:6-	6 TH OBSERVATION WITH RESPECT TO INPUT PARAMETERS AND OUTPUT	58
TABLE No:7-	7 TH OBSERVATION WITH RESPECT TO INPUT PARAMETERS AND OUTPUT	66
TABLE No:8-	8 TH OBSERVATION WITH RESPECT TO INPUT PARAMETERS AND OUTPUT	75
TABLE No:9-	FINAL SET OF PARAMETERS TO GET THE OPTIMUM RESULTS	84

Abstract

Laser cutting is nowadays the most significant application of lasers in material processing. The metals that are commonly used in industries include low alloy steel, stainless steel, aluminium, ceramic tiles, etc. They prefer the laser cut for its high cutting speed which enhances the time of productivity; also it can delicately cut any fragile and ductile material.

Excellent mechanical and physical properties like high thermal resistance, high hardness, and chemical stability have encouraged the use of ceramics in various applications such as automobile engines, the electronic substrate for microwave devices, dielectric materials, etc. The hard and brittle nature of these ceramics makes them difficult to cut using conventional machining due to large cutting forces as well as several tools wear involved for hard-to-cut. Thus, non-contact laser machining utilizes to cut the hard and brittle ceramics. A highly collimated laser beam strikes the workpiece with high energy such that the temperature of the workpiece exceeds its boiling point, resulting in vaporization and ablation occurs.

In this study, concerning Pankaj Keshari's [10] thesis on “Parametric Study of Laser Cutting of Ceramic tiles” where the experimental data of the laser cutting of 7 mm thick ceramic tiles using a fiber laser is taken and will be used in the Particle Swarm optimization technique with MATLAB algorithm to minimize glass formation and taper angle in the cutting region, which in turn will improve productivity and surface finish.

Chapter 1

Introduction

1. Introduction to Laser Cutting

Laser cutting is a method of cutting material by using a laser to vaporize which results in a cut edge. A commercial laser for cutting materials uses a motion control system to follow a CNC or G-code of the pattern to be cut onto the material. The focused laser beam is directed at the material, which then either melts, burns, and vaporizes away, or is blown away by a jet of gas, giving the edge a high-quality finish.

1.1 Working Principle of Laser Cutting

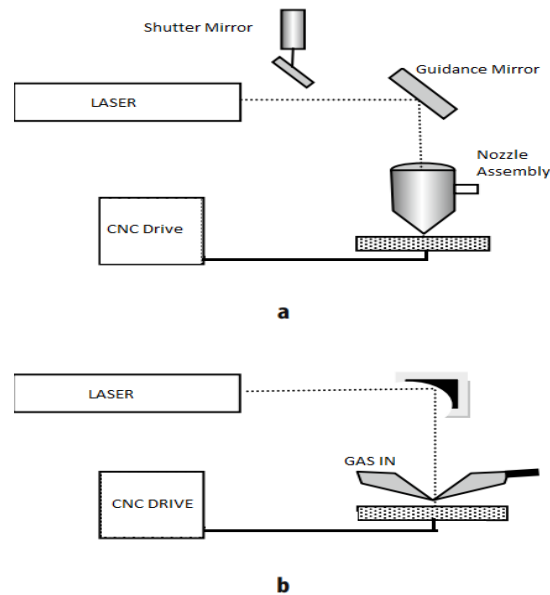


Figure:1-. Arrangement for laser cutting using: a) Transmissive Optics, and b) Reflective Optics

The general arrangement for laser cutting is shown in figure 1. The components are the laser itself with some shutter control, beam guidance train, focusing optics, and a means of moving the beam or workpiece relative to each other. The shutter is usually a retractable mirror that blocks the beam path and diverts the beam into a beam dump which doubles as a calorimeter. When the beam is required, the mirror is rapidly removed by a piston. The beam then passes to the guidance train, which directs the beam to center on a focusing optic.

The focusing optic can either be transmissive or reflective; the transmissive optics are made of ZnSe, GaAs, or CdTe for CO₂ lasers and quartz for YAG or excimer lasers; the reflective optics are spherical or parabolic off-axis mirrors. A coaxial gas jet then emerges from the nozzle from which the focused beam passes. Both the cutting process and the protection of the optics require the gas jet. An air knife is often used to deflect smoke and spatter from the exit from the metal optic train in the case of metal optics. Thus any material can be cut by different forms of cutting processes which are discussed below.

1.2 Types of Laser Cutting

There are different methods of laser cutting which are described below:


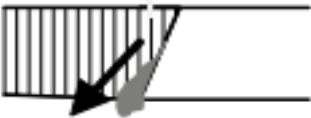
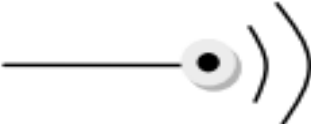


Method	Concept
Vaporisation	
Melt and blow	
Thermal stress cracking	
Scribing	 Perforation
“Cold cutting”	 high energy photons or multi photons

Figure:2-. Methods of Laser cutting

1.2.1 Vaporization Cutting

In this cutting process, a laser beam is affixed to a static area of the metal or material. As the laser remains in place, it heats the metal or material until it begins to boil, thus creating a small hole. As this hole deepens, the metal releases vapor that erodes and breaks down the adjacent walls.

Laser vaporization cutting uses a high-energy-density laser beam to heat the workpiece so that the temperature rises rapidly, reaches the boiling point of the material in a very short time, and the material begins to vaporize and form a vapor. These vapors are ejected at a high speed, and a cut is formed in the material while the vapor is ejected.

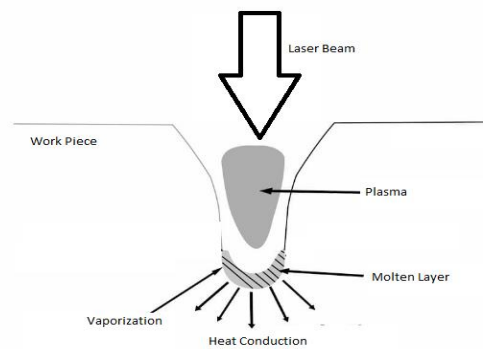


Figure:3-. Vaporization Laser Cutting

1.2.2 Fusion cutting – Melt & Blow

In this method, a penetration hole is made from the edge, with a sufficiently strong gas jet to blow the molten material out of the cut kerf. The beam arrives at the surface and most of it passes into the hole or kerf, some may be reflected off the un-melted surface and some may pass straight through. If a beam is sufficiently thin, it can pass through the kerf without touching the material at slow speeds, with the melt starting near the leading edge of the beam.

There are two mechanisms for absorption at the steeply sloped edge of the cut front (roughly 14° to the vertical): primarily Fresnel absorption - by which the beam interacts directly with the material and secondly, plasma absorption and its radiation. The gas blows the plasma away, thus reducing the build-up on a cut front. Power density is $F_0 \sin \theta \approx F_0 \times 0.24$. As soon as the melt starts, the fast-moving gas stream, pressure drop, and kerf's depth will cause the melt to blow away. At the kerf bottom, the melt gets thicker due to flow from above, formation of the film, and surface tension blocking the melt from leaving. The gas stream that ejects the molten droplets of the material at the base cut into the atmosphere. In blowing the molten part from the kerf, the gas generates a low-pressure region further up the cut length.

1.2.3 Reactive Fusion Cutting

When the gas used in the previous method also reacts exothermically with the workpiece, then another heat source is needed. The cut front becomes a focal point of many activities. In addition to pushing the melt away from the kerf, the gas passing through it reacts with the melt. It is usually oxygen or some mixture containing oxygen that is reactive. When the temperature reaches the ignition temperature, the burning reaction begins, usually at the top. As the oxide forms, it is blown into the kerf and covers the melt below. With this technique, the cutting speed is usually at least twice as fast as melt and blow cutting.

As a general rule, faster cuts lead to less heat penetration and better cuts. The workpiece may undergo some chemical changes however since there is a cutting reaction occurring. Unlike metal dross, the oxide dross has the advantage that it flows well and doesn't adhere to the base metal as strongly as if it were metal.

1.2.4 Controlled Fracture

Brittle material which is vulnerable to thermal fracture can be quickly and neatly severed by guiding a crack with a fine spot heated by a laser. The laser heats a small volume of the surface, causing it to expand and hence cause tensile stresses all around it. If there is a crack in this space, it will act as a stress raiser and the cracking will continue in the direction of the hot spot. The speed at which a crack can be guided is swift, of the order of 1 ms^{-1} . This is as hoped for until the crack approaches an edge when the stress fields become more complex and difficult to forecast. As a cutting method for glass, it is excellent. The speed, edge quality, and precision are very good. The only problem is that for straight cuts snapping is quicker and for profiled cuts, one usually needs a closed shape, as for the manufacture of car wing mirrors. This process requires that the surface is not melted since that might damage the edge. It thus requires very little power.

1.2.5 Scribing

This technique involves creating a groove or line of holes that can either penetrate fully or not penetrate at all but are sufficiently weak to allow a mechanical break. When it comes to silicon chips and alumina substrates, the quality is measured by the low levels of HAZ and debris. To remove material principally as vapor, pulses of low energy and high power density are employed.

1.2.6 Cold Cutting

In recent years, high-powered excimer lasers have been used to create extremely short, very high-power pulses in the ultraviolet range, as well as using picosecond lasers. The ultraviolet photon has an energy of 4.9 eV. This is comparable to the bond energy of many organic materials. If such a photon strikes a bond, it may break. If it did, it would reform and no one would be the wiser. In addition to sunbathing and tanning, the bond could be altered through various means, such as carcinogens (or unnatural substances). Biologically hostile radiation begins with violet light, which continues with X-rays and gamma rays. With sufficient photon flux onto the plastic, this radiation disappears from the material without heating, leaving a hole with little debris and no edge damage. A multiphoton event will occur when ultrashort powerful pulses combine to form an event with sufficient energy to cause bonds to be broken just as they do with UV light.

One of the many potential medical applications is the use of single cells in microsurgery and engineering. One of the other applications is marking.

1.2.7 LASOX

The laser-assisted oxygen cutting (LASOX) method was developed to reduce the cost and time associated with machining mild steel through the use of a low-power laser. A laser beam heats the steel to ignition temperature, and then a specially designed nozzle delivers a supersonic stream of oxygen to ignite the steel. The reaction is exothermic, resulting in sustained and controlled burning. After removing the part from the laser-burning table, it is clean and accurate to cut both square and beveled edges. At least 30% of the time can be saved by using LASOX when cleaning, fitting, and welding thick steel sections. As a result, you will be able to cut the material at speeds up to 344 inches per minute. There are, however, significant advantages for the “LASOX” process over plasma and oxy/fuel systems.

The advantages so far identified are:

- 1) Square cut top edges as opposite to curved one;
- 2) Diminished decrease, mainly inferior 2°;
- 3) Faster fierce;
- 4) Conventional incision widths of 2.5 mm when incisive in the diameter range of 20–50 mm;
- 5) Little alternative in coarseness over the smooth cut edge;
- 6) The process is omnidirectional and free of ray of light polarization;
- 7) The necessary ray of light capacity is nearly 1KW, accompanying no benefit in bearing more capacity.
- 8) Hateful speeds, are corresponding to those of skin and oxy/fuel hateful, variable from 500 mm^{-1} for a 15 mm dense plate in gentle brace to 200 mm min^{-1} for a 50-mm-dense plate; and
- 9) Skilled is less falsification on account of the lack of passionate surface jets.

1.2.8 Sublimation cutting

During this process, both the base solid and the cutting layer are vaporized. Laser beam pulses are used in conjunction with a jet of inert gas to blow away the vapor formed during the light-matter interaction, resulting in a narrow kerf width and a high-quality surface.

By using the laser, the goal is to vaporize as little material as possible while minimizing melting. As the material vapor rises, it creates high pressure that expels molten material from the top and bottom of the kerf.

Nitrogen, argon, or helium is used to shield the cut surfaces from the surrounding environment. This prevents oxide from building up. In order to meet this requirement, a pressure between 1 and 3 bar is appropriate.

A metal that is vaporized requires more energy than one that is melted. In order to achieve sublimation cutting, high laser power is needed and it takes more time. The results, however, are excellent.

In sheet metal fabrication, this process is rarely used. It becomes especially appealing when it is applied to highly delicate cutting operations. One example is the manufacture of stents.

When metal processing comes as a concept, sublimation cutting is rare. However, it is very common with non-metals. The sublimation cutting process is used to process a wide variety of non-metal materials. Examples are:

- Even small amounts of energy can vaporize plastic sheeting and textiles.
- Materials cannot be melted in wood, cardboard, or foam

1.3 Methods of Cutting

Cutting is one of the fundamental operations for industrial machining to cut different types of materials like metals, polymers, and ceramics. Cutting is the process of separating or opening a physical item into two or more parts with a sharply focused force. Cutting is a material removal process from the surface of the workpiece. Different materials have different mechanical properties (thermal conductivity, hardness, brittleness, elasticity, etc.). So, machining of different structural materials, different types of cutting methods are required:

1.4 Conventional Cutting Methods

Macroscopic chips are generally formed by shear deformation in conventional methods. In traditional machining, the tool and the workpiece come into intimate touch. The workpiece is harder than the cutting tool. Material removal occurs as a result of the application of cutting forces - this is categorized as a mechanical energy domain. In this method-surface smoothness and precision are both compromised. Conventional cutting methods are:

- Abrasive wheel cutting
- Diamond cutting
- Mechanical mounting
- Wire saw cutting, etc.

1.5 Non-Conventional Cutting Methods

Non-traditional cutting, on the other hand, is relatively new and widely used in many modern applications. Unlike traditional methods that use tool bits, non-traditional cutting techniques include various electrical, chemical, mechanical, thermal works, or a combination of these processes. Material removal may occur in conjunction with chip development, or it may not occur at all.

Non-Conventional cutting methods are as follows:

- Wire electrical discharge machining (WEDM)
- Laser Beam Machining (LBM)
- Electro discharge machining (EDM)
- Electrochemical machining (ECM), etc.

1.5.1 Hybrid Cutting Methods

Cutting methods, both conventional and non-conventional, have several restrictions that impact their cutting efficiency as well as the accuracy, precision, and quality of the cut dimension. A few novel machining techniques have been developed to improve their performance. “Hybrid machining techniques encompass the controlled and simultaneous interactions of two or more machining mechanisms, tools, and/or energy sources that alter performance parameters”. These integrate the benefits of two different processes to create a new process that is more well-organized and effective than either of the different processes.

Hybrid methods are:

- Hybrid laser-assisted water jet machining
- Electrochemical discharge assisted wire machining, etc.

1.6 Cutting with lasers

Lasers come in a variety of shapes and sizes, but the Nd:YAG and CO₂ lasers are the most commonly utilized in cutting. High-power fiber lasers have recently been used in a variety of applications. In addition, the Nd:YAG laser can produce larger peak pulse powers.

Infrared lasers typically operate at a wavelength of 1064 nm, which is shorter than that of mid-infrared lasers. The beams in this range are mostly emitted by Nd:YAG, fiber, semiconductor diode, and semiconductor lasers. This zone also includes 2nd harmonic green lasers. The majority of these lasers are Q-switched and pulsed. These laser beams have higher photon energy than mid-IR lasers. Infrared radiation wavelengths of 1064 nm and 532 nm have photon energies of 1.2 eV and 2.3 eV, respectively. Because of their excellent absorptivity and reflectivity, these lasers are particularly well suited to metals and semiconductors. However, most polymers were discovered to be incompatible with these lasers.

1.6.1 ND:YAG Laser

The most often used laser for laser cutting is the pulsed Nd-YAG laser. A YAG laser is a solid-state laser that uses an impurity in the host material as the active medium. Thus, the neodymium ion (Nd^{+3}) is utilised as a 'dopant,' or intentionally inserted impurity in either a glass crystal, and (Nd^{+3}) ions determine the 1064nm result wavelength. The lasing or lasing material With a diameter of 10 mm and a length of 150 mm, the host is formed like a cylinder. The inside and exterior of the cylinder are flattened and paralleled to extremely tight tolerances on both sides, then polished to a high shine on both sides. silvered with an optical finish to provide a reflective surface. The crystal is excited by a krypton atom. The use of a Xenon lamp aids the creation of high average power in the ND:YAG laser system. This was accomplished by combining many separately pulsed laser rods into a single resonator. Pumping and extraction efficiency are both improved as a result of this. Oscillator-amplifier systems can be utilised instead of single multirod oscillators. Nd: YAG lasers can be employed in three modes: continuous output, pulsed output, and Q switched-mode. Lasers have an average output power of 0.35 to 4.5 kW, with a peak power of up to 100 kW. One of the major advantages of the Nd: YAG laser is its ability to transport laser energy across optical fibres.

1.6.2 Co2 Laser

The CO₂ laser, which is a type of gas laser that is widely used in industrial processing, is significantly more efficient than the Nd:YAG laser and produces much greater continuous-wave output powers as well as better light quality than the Nd:YAG laser. Gas mixes mostly containing nitrogen and oxygen are used in these lasers. An electric glow discharge is used to combine helium with a little amount of carbon dioxide.CO₂ molecules are excited using this method. By continually circulating the gas blend via the optical cavity zone, the gas heating produced in this manner may be adjusted. CO₂ lasers with CW output power may produce 3-10 KW. The rapid axial flow and transverse flow CO₂ lasers, which offer the highest power outputs, are the most widely employed in the industry. CO₂ lasers have several advantages, including excellent electrical efficiency, low operating costs, and the ability to scale up to high powers.

1.6.3 Fibre Laser

The active medium in a fiber laser is the core of the laser. The fiber has been doped with a rare earth element. A single-mode optical fiber laser made of silica is the most common type. The pump beam travels the length of the fiber and is guided either by the core itself, as in Single-mode optical lasers, or by an inner cladding around the core. For many materials processing applications, fiber lasers have been touted as a viable substitute for solid-state and **CO₂**lasers.

1.7 Process Variations

1.7.1 Arc Augmented Laser Cutting

If an electric arc is present the laser-generated event, then the arc will automatically root at the high-temperature zone and the magnetic pinch created by this hot zone will constrict the arc to a size similar to the laser beam for low-current arcs up to 80 A. The cathode jet from the arc is too strong above this current and the two energy sources may not be in the same spot, nor would the arc be constricted. When the arc and the laser are on the same side of the work piece, the cut top edge will most likely be damaged because the arc will root on one side or the other. When the arc is on the bottom of the work piece, then the cutting process can be sped up by about a factor of two, which shows a plot of the cut speed vs. power. The quality of the cut different from that of a pure laser cut only when the curve begins to turn. The need for the arc to be on the side opposing the laser is a flaw in this method. Nonetheless, the procedure is available to anyone who wants to cut twice as fast for the same amount of material.

1.7.2 Hot Machining

The use of the laser to heat and soften the material is prior to mechanical machining. The technique reduces cutting force by roughly 50% if the heating is properly positioned and does not allow for quenching from the bulk material in the time between heating and machining, resulting in transformation hardening rather than softening. The laser's capital cost is more than that of a plasma torch, which could perform the same purpose.

1.8 Mechanism of material Removal

When a pulse of the proper intensity is directed to the material surface, the absorbed energy can melt or vaporize the material. These are the steps in the cutting occurs. The primary material elimination process in laser beam cutting is based on the creation of a huge high-temperature flux, which causes the material on which the laser light is focused to melt and vaporize. A suitable lasing source is employed to generate a laser beam of a suitable wavelength. A laser beam with a small-diameter emerges from a lasing medium. The beam is then focused onto the material surface using a suitable converging element, such as a lens. As a result, there is a substantial amount of energy concentrated at that location. Once the laser heat is absorbed by the surface material, the optical energy is converted to heat. Depending on the heat source and substrate material, this complete process can take the form of vaporization, boiling, ablation, or phase explosion.

1.8.1 Vaporization

When an atom or molecule is first freed from the extreme of an external surface where it is heated past its melting point to its vaporization temperature, it is said to be converted from the condensed to the vapor state. Part of the laser energy is used to liquefy the material in this situation, and the liquefied material is brought into direct contact with the substance. A portion of the molten substance is also vaporized by the laser. The created steam generates steam or backpressure, pushes the steam away from the target, and exerts strength on the molten substrate, expelling it from the side.

1.8.2 Melting/Boiling

This condition requires a comparatively long pulse time and contains the nucleation of foreign vapor bubbles that can form on the liquid's external surface, in most liquids, or at the liquid-solids boundary. At the absorption depth ($1/\alpha$, when the absorption coefficient is α), boiling occurs. The vaporization temperature, which corresponds to the surface pressure, is set, as is the surface temperature.

1.8.3 Ablation

Ablation is a technique for removing material that consists of two steps. First, a high-energy quantum is produced by a power source. If the energy of the work piece's atoms exceeds the threshold energy, every molecule can be broken into atoms and eliminated from the material. On the other hand, an energy beam with a very high power density is focused on the material. The work piece can be removed by vaporization rather than melting due to the high power. Power sources include excimer lasers and femtosecond lasers. The machined surface retains very little heat-affected layer, which is a significant feature of these processes. As a result, micro-shapes may be machined with high dimensional accuracy, and the surface layer has fewer flaws.

1.8.4 Phasor Explosion

The laser fluency must be powerful enough, and the pulse duration short enough, for the temperature of the material surface and the area immediately beneath it to achieve around 90% of the thermodynamic critical temperature. The substance swiftly transforms from a superheated liquid to a vapor or liquid droplet mixture, causing homogeneous bubble nucleation. Because the rate of occurrence increases significantly near the threshold temperature, homogeneous nucleation is conceivable. This is also known as "explosive boiling

1.9 Parameters of laser Cutting

Laser cutting has long been a good choice in industrial applications because of the advantage of fast speed. The process parameter settings must be determined in the optimal method to optimize quality with lowest manufacturing cost, time, process safety, and increased productivity. In the fully automated manufacturing process, these ideal parameters are critical for ensuring product quality, increasing productivity, and lowering production costs.

1.9.1 Beam Characteristics

1.1.1.1. Effect of beam type

Both pulsed and continuous beams can be used in laser cutting, with continuous beams being more common. The pulse duty cycle has an effect on the surface roughness, with the surface roughness decreasing as the pulse duty increases. The pulse duty cycle is defined as the ratio of pulse on time to total pulse time. Figures 12 the continuous and pulsed wave beam shapes, respectively.

1.9.1.1. Effect of Power

Increasing the power has the overall effect of allowing you to cut at faster speeds deeper depths. The potential drawback of raising the power is that the cut breadth expands, the edge finish deteriorates, and sharp corners become rounded. Another feature of high power, which is particularly relevant to high-brightness fiber lasers, is that the temperature of the melt may be high enough to stop the oxygen burning reaction and convert it to a reduction process, resulting in the loss of the extra energy mentioned in reactive fusion cutting. When approaching a corner, some laser cutting systems can switch from continuous wave to pulse mode to prevent side burning or corner rounding. Because the pulse maintains the power intensity, the depth of penetration and pulse rate can be modified in accordance with the speed to control the overall heat input. When cutting fine shapes, other technologies that aren't capable of switching during processing are frequently used in the pulsed mode. To cut, the Nd:YAG laser is commonly employed in pulsed mode. There are several types of pulsing: simple power switching, which turns the beam on and switching with excess current, which produces a "super pulse" with an energy 2–3 times that of the CW value; and switching with excess current. Q-switching, which uses a very high-speed switch in the laser cavity – such as a Pocket cell – to provide several thousand times the CW power rating in a very short time, such as a few nanoseconds; and spiking on the CW beam with short power surges to generate a "hyper-pulse," which is available on certain lasers like PRC lasers.

1.9.1.2. Effect of Beam Polarization

The cutting in one direction as opposed to one at right angles when cutting with a plane-polarized laser beam, the maximum cutting speed is doubled since the laser beam cuts in one direction rather than at right angles. The amplification of radiation whose electric vector is at right angles to the plane of incidence on the fold mirrors is favored in nearly all high-powered lasers, which contain folded cavities. That example, horizontal folding will result in a vertically polarized beam. The beam will still be plane-polarized if the cavity is not folded or if the folding has near-normal reflections, but the plane of polarization may vary unpredictably over time. As a result, even these lasers now have a fold in the entire reflecting mirror to stabilize the polarization plane from the cavity. The phenomenon is caused by a glancing angle of incidence at the cutting face, and there is a distinct difference in the reflection of a beam at such angles depending on whether the electric vector is at right angles to the plane of incidence (s-polarization) or in the plane of incidence (p-polarization). It will have a high reflectance if it is s-polarized. It will be absorbed preferentially if it is p-polarized.

1.9.1.3. Effect of Wavelength

For a particular mode of structure and optics train, the shorter the wavelength, the higher is the absorptivity, and the sharper is the focus. As a result, YAG radiation is superior to CO₂ radiation in general; however the spot diameters for both CO₂ and YAG are similar, with a little advantage for the genuine TEM₀₀ laser due to the poor mode structure of most YAG lasers of any considerable power. Fiber lasers with mono-mode fibers produce TEM₀₀ beams with much higher penetration strengths than other lasers at wavelengths of 1.03 or 1.55 μ m. The Fulham Laboratory results on cutting plastics with a CO₂ laser emitting 10.6 μ m radiation and a CO laser emitting 5.4 μ m radiation were obtained using the same resonator and optics, and thus represent a fairly good comparison between CO₂ 10.6- μ m radiation and CO laser 5.4- μ m radiation, with the shorter wavelength having an advantage.

The discrepancy is thought to be due to the absorption of the beam on the cut face. Some materials are transparent to specific wavelengths, which creates some intriguing cutting challenges. Human tissue is one such substance. In the ultraviolet, very short wavelengths have energetic photons of energy that are similar to the bond energy in biological materials (e.g., approximately 4.6 eV). As a result, they can directly break bonds. The material will effectively fall apart if a large flux of photons can concurrently rupture multiple nearby bonds, resulting in a cut without the requirement for heating. This is referred to as "cold cutting." Because some heating has been observed, it is unclear if the mechanism just described is right or not. However, this could be a secondary result rather than the main event. Multiphoton interactions with lower-energy photons can produce a similar effect.

1.9.2 Transport Characteristics

1.9.2.1. Effect of Speed

The less time the heat has to diffuse sideways and the tighter the HAZ, the faster the cutting. Due to the necessity to deposit a particular amount of energy to promote melting, the kerf is also reduced. As a result, there is a "sharpened pencil" effect with a Gaussian beam, in that as the speed increases, there is only enough energy at the tip of the Gaussian curve, not at the root, to cause melting and hence cutting.

The kerf width changes as the speed increases. The three zones depicted in the diagram are caused by side burning at slow speeds, stable cutting at medium speeds, and dross failure at higher speeds. Until this last region is reached, the faster the pace, the better the cut finish.

1.9.2.2. Effect of Focal position

The size of the surface spot dictates the intensity of the surface power and whether or not penetration will occur, although optimal cutting can be achieved by having the smallest spot size below the surface. The issue revolves around energy absorption on the sliced face and how to keep it together. Because the beam stretches out and suffers several reflections, really deep cuts are rarely achieved with high quality. There are exceptions, such as a 5-cm cut in the block board with parallel walls. How did the beam manage to do that? It must have been a wave that was guided down a slot with graphite walls - hardly a typical material for reflections.

1.9.3 Gas Characteristics

1.9.3.1. Effect of Gas Jet Velocity

The gas jet works by drawing the melt out of the cut, according to the description. The faster it can be taken out, the faster the next piece can be melted. The velocity of the gas in the slot on the cut face is critical because the drag force per unit area is $\frac{1}{2} \rho u^2$ and the drag coefficient C_d is a function of the Reynolds number ($\rho u d / \mu$) (where ρ is the gas density, u is the gas velocity, d is a typical dimension, e.g., kerf width, and μ is the gas viscosity), Researcher tried a few different angles for directing the jet into the cut front, but it had little effect. Up to a point, increasing the gas jet velocity enhanced the cutting rate. It was perplexing why there was a decrease in cutting speed as nozzle pressure increased. Some early workers speculated that the issue was one of cooling. The tests to show that there was a density gradient field close to the cut surface that may impact the focus at the cut front; however, the density gradient field was shaped like a lens, making the effect difficult to rationalize. They made surface pressure measurements and discovered a variety of shock phenomena linked with high-pressure jets.

Multiple-nozzle systems are employed in a variety of applications. The clean-cut nozzle operates at roughly 1-atm pressure for lens protection on the inner jet and around 5 atm on the outer ring jet. As a result, burr-free, striation-free cuts are produced. Amanda and Prima Industry have invented a ring nozzle with a water spray on the outer nozzle that decreases HAZ, dross, roughness, fume and smoke, as well as cutting errors caused by expansion when cutting.

1.9.3.2. Effect of Nozzle Alignment

The alignment of the nozzle with the laser beam has an impact on the cut quality. An comprehensive set of trials in which the beam and the jet were methodically mismatched. Both the roughness of the cut and the manner the dross clears the kerf are affected by the alignment.

1.9.3.3. Effect of Gas Composition

The gas composition has an effect on the cut quality in some cases. There is a benefit to using pure oxygen; even a 1% impurity will significantly degrade cutting performance when considering the natural mixing that occurs within the kerf during cutting. They demonstrated that cutting at depths more than 15 mm would be problematic due to the reactive gas's efficacy being reduced by mixing. Striations are more likely to appear while cutting reactively. Oxygen can also cause oxide layers to grow on the cut edge. As a result, cutting with inert gas is frequently preferred, especially with stainless steel, to minimize the dross problem caused by the production of high melting point chromium oxides. To increase the drag forces, inert gas cutting is commonly done at very high pressures (14 bar or so) with Laval supersonic nozzles. The cut quality might be exceptional.

1.9.4 Material Property

1.9.4.1. Optical Properties- Reflectivity

For an opaque material the absorptivity = (1–reflectivity); therefore, one may expect high-reflectivity materials to be more difficult to cut. This is true, but not as dramatically as the preceding argument implies, because reflectivity is determined not only by the material, but also by the surface shape and the presence of surface films (such as oxides), surface plasmas, and nonlinear events involving multiphoton interactions from high-intensity beams. The absorption can be substantially time-dependent due to the crucial effect of thin coatings such as oxides. There is also a temporal dependency in the absorption as the material heats up due to the coupling effect with plasmas and the recognized decrease in reflectance with temperature. In addition, the cutting rate varies significantly depending on the surface finish. Wave creation on the melt front layer should, theoretically, have a noticeable effect on absorption, but this has yet to be demonstrated. Based on the standing wave pattern on the cut front.

1.9.4.2. Thermal property

The absorptivity, melting point of the material or oxide generated, char tendency, and brittleness related with the coefficient of thermal expansion all influence how easily a material can be cut.

1.10 Characteristics of Laser Cut

The construction of a qualified cutting program, which contains the tested process parameter values or the value range for producing an end user-specified quality level cut, ensures cut quality. The development process can be carried out quickly and easily using pre-existing techniques or predictive methods. Some of them are discussed farther down

1.10.1 Kerf Depth

During through-thickness cutting, the kerf is the slot molded. The kerf width is described as the breadth of the cut at the bottom in optimal laser cutting, and it is usually much larger than the focused beam diameter. The kerf width on the bottom side of the material is typically narrower than on the top side. In gas-assisted thermal cutting procedures, the kerf width is determined by the gas jet width.

1.10.2 Heat Affected Zone

As the power incident per unit length and the cutting thickness grow, the HAZ widens. When cutting near heat components, the HAZ width is important. As a result, there are times when the maximum limit for the incident beam output or plate thickness is established, or the minimum limit for the cutting speed is set.

1.10.3 Recast Layer

The molten slag (solidified oxide) or very adherent form (hardened material) formed at the bottom of the incision is the re-melted layer. Burrs might appear as prolonged drops or as a rough covering of whiskers. Slag can be mechanically removed after cutting or separated during processing with a gas jet directed from the bottom of the material.

1.10.4 Surface Roughness

The presence of sputtering on the surface (remaining molten material ejected from the cutting) and discoloration on the surface characterize the surface condition after cutting.

1.10.5 Taper Angle

High laser power can minimize the formation of taper angles, allowing heat to penetrate the thickness of the working material. The material is penetrated more effectively with more laser power, resulting in a greater kerf with less taper. As a result, increasing the laser power increases the material removal rate while decreasing the taper development. The laser beam moves quicker at high cutting speeds, resulting in less time spent at a single point. Larger taper angles were formed at high cutting speeds as a result of the shorter energy input time, which were not adequately conveyed to the thickness of the working material.

1.11 Application of Laser Cutting

Cutting is one of the most important and effective uses for industrial lasers. Laser cutting works well with both soft and hard materials. Modern applications of laser cutting technology include medical, engineering, and several disciplines of science. In the electronics industry, laser cutting on ceramic, silicone, and polymer substrates is commonplace. In medical surgery, a laser is used to cut tents that save lives and test tubes.

1.12 Advantages of Laser cutting

The benefits of laser cutting over previous cutting methods such as plasma arc cutting, electrical discharge machining, oxyacetylene flame cutting, and mechanical cutting are summarized here.

- The kerf width is narrowed as a result, resulting in less waste;
- The heat-affected zone is quite small due to the low overall heat input. As a result, the base material sustains minimal damage, allowing it to be used in temperature-sensitive and combustible goods. Furthermore, residual stress and distortion are negligible.
- Because it's a noncontact method, there's no friction or mechanical tool forces to injure delicate work pieces.
- As a result, the cut ends are square rather than curled, as is the case with many other thermal cutting processes.
- Extremely adaptable and low-noise.

1.13 Disadvantages of Laser Cutting

The following are the main drawbacks of laser cutting:

- Cutting highly lustrous and conductive materials like Au and Ag with lasers is tough.
 - For hardening materials, the procedure's melting and rapid cooling results in a firm edge on the cut component.
 - Laser beam cutting has traditionally been used to cut thin materials with a thickness of less than a few millimetres.
 - The initial capital cost of a laser cutting system is relatively significant.
 - During laser processing, certain materials (polymers) may emit harmful exhaust fumes.

1.14 Precaution of Laser cutting

1.14.1 Cornering & Edge Burning

When cutting corners, thin slices, or anywhere the work piece temperature near the ignition point, burnout is a possibility. To some extent, this can be avoided by:

- Using pulse power;
- Ramping the power in step with the speed (some systems have this feature built in);
- Overshoot and return, resulting in a "Mickey Mouse ear" and
- Spraying water in a circular pattern around the oxygen jet.

1.14.2 End Discontinuity

At the end of a cut, there's normally a blemish on the lower side where the assist gas jet can flow on either side of the last half-thickness. With thin materials smaller than 3 mm, this is not an issue. Pulsed power should be employed for the last millimeter of thicker materials. Alternatively, this final section will have to be completed individually.

1.14.3 Movement while Cutting

The workstation's support structure must be free of vibration. For laser cutting systems, this is a fundamental design need. The work piece must not be able to slide or tip while parts are cut free due to acceleration forces on the table. As a result, it needs to be lightly fastened and supported underneath. Because X/Y tables must be rigid, many of them are heavy.

1.14.4 Damage to initial hole

A splatter will appear if you pierce the sheet anyplace other than the edge. The optics and hole quality are both endangered by the spatter. Piercing can be accomplished in numerous ways, including firing the laser as it approaches the work piece, lowering the nozzle to the work piece and then backing off to a safe height, or simply lowering to the focal position and firing. The first option is preferable if the software permits the laser to be operated while moving the workstation. The latter is risky, especially if a capacitance height sensor is employed, because the plasma might alter the height reading, causing the machine to take evasive action as if it had hit an obstacle! Some of the issues associated with piercings can be prevented by:

- piercing by careful pulsing; and
- starting on scrap metal and then progressing towards the cut line

Chapter - 2

Literature Survey

2. Literature Survey

2.1 Survey from past research

M.J.Reddy and D.N.Kumar [1] applied pareto dominance MOPSO [Multi Objective Particle Swarm Optimization] to research the extension of EM-PSO to obtain the optimal solution for the existing problems. They demonstrate the MOPSO algorithm in combination with pareto dominance criteria and external repository for elitism.

M.I.Shigur [2] wrote on RSM [Response Surface Methodology] which includes regressive analysis and objective function to get the optimal solution by using various process parameter like : laser power, Welding Speed, focal position and axial process for the fabrication of PMMA & Aluminum 6061-T6 with transmission laser welding process and using single dimensionless optimization problem to get a desired optimal solution with respect to maximize the lap shear force and minimize the weld seam width.

C.A.C. Ceollo, G.B. Lamont and D.A.V. Veldhuizen [3] applied TTLW [Transmission Laser Welding] to weld two dissimilar thermoplastic acrylic and polycarbonate material with using any filler, After the experiment they developed the mathematic model of response through Response Surface Methodology using Regression Analysis, where this Regression Equation was used in Particle Swarm Optimization to find the optimal solution for laser welding.

Bouhekara and Abido [4] used TLBO [Teaching Learning Based Optimization]to solve the optimal flow problems of power, they compared the results using this technique and with the literature which gave them a highly optimum solution even with the complexity of objective function.

Rituparna Ghosh [5] applied multi objective particle swarm optimization technique to obtain in Transmission Laser Welding to weld two dissimilar thermoplastic acrylic and polycarbonate material with using any filler, After the experiment she developed the mathematic model of response through Response Surface Methodology using Regression Analysis, where this Regression Equation was used in Particle Swarm Optimization to find the optimal solution for laser welding.

Avinash Kr Dubey and Vinod Yadav [6] conducted an experimental study of Nd:Yag laser beam machining and observed that the quality is affected by laser parameters (laser power, Wavelength) and process parameters (focal plane, feed rate, energy, pulse duration, assist gas type and gas pressure). The main quality Characteristics were Heat Affected Zone (HAZ),Taper Angle, Surface roughness, Recast Layer, Dross adherence and crack formation.

Beausoleil, Katz, Sarvestani [7] explored picosecond laser process to control the cut depth and optimize the kerf width, taper angle, crack formation and surface cleanliness of the ceramic material with the help of process parameters such as focal position, linear speed and wobble amplitude, this experiment was conducted with two laser cutting methods such as rastering and wobbling. And the quality of the cuts were measured using 3d laser scanning microscopy process.

The authors [8] had investigated about the static condition and the dynamic interaction of the assist gas with the molten material on the cutting front for which new nozzle design were improved to increase the efficiency for the removal of the molten material for which cut quality can be improved simultaneously. They also reviewed some gaps in the current scientific literature in the role of assist gas, so they worked on the interaction with the aerodynamics of the assist gas.

Norbert Ackerl and Konrad Wegener [9] experimented on ablation characteristics of alumina and zirconia ceramics from ultra-short pulsed laser to observe the multi-pass and single ablation of 515nm and 1030 nm wavelength with picosecond pulses to enhance the material removal rate. Also they refer with Raman Spectroscopy to show a negligible phase shift in the spectra using ultra-short pulses.

Pankaj Keshari from Jadavpur university [10] observed that the cutting on ceramic plates with the help of laser is possible with precise relative response parameters (Taper angle, glass formation width, kerf width on top and bottom surfaces) with the process parameters (laser power, scanning speed, frequency, and taper angle), he experimented with 7mm thickness of ceramic tiles and used a 500 watt fibre laser to cut this material along with nitrogen gas as assist gas, and the relative response parameters are minimize using Response Surface Methodology (RSM). It is a statistical method for analysing the variables whereas the DOE can solve the product design optimization projects to get a set of regression equation with the process parameter combination.

On paper [11] author has discussed about the conceptual implementation in the theory of PSO (Particle Swarm Optimization) rather than solving any practical problem. Their research included the implementation of nonlinear function optimization and neural network training.

Victor Martinez-Cagigal [12] worked and performs on MOPSO [Multi-Objective Particle Swarm Optimization] to minimize the continuous functions and implement on a cheap and compressed algorithm that can handle multiple objective functions with multiple parameters. The algorithm must be vectorized and provided with a fitness value for each particle in order to get error free results.

The Authors [13] proposed the method based on dominance for selecting guide from non-dominated archive. These methods are checked on standard test problems and found that few particles provides good convergence towards the Pareto Front. They also demonstrate the scheme which they proposed is robust in

nature with respect to the objective scaling. They tried to find the optimal solution in the feasible region close to the constraint boundaries.

The Authors [15] approach on six test problem using MOCLPSO, they found that these experiments shows a good sets of results and faster movement towards the convergence criteria when compared to another multi-objective optimization evolutionary algorithms.

The Author [16] modified the Particle Swarm optimization technique to Non-Dominated Sorting particle Swarm Optimization technique which helped them to get a better optimization by making effective use of the particle personal best. NSPSO can compare all personal best value of particle and their offspring with its population to get best results and concluded that it can make this technique more efficient than the PSO.

Jacqueline Moore and Richard Chapman [17] worked on PSO with application on impatiens plant named Bora Bora to get the best value in uniform flowering, floriferous habit and adaptability.

Sanaz Mostaghim and J.Teich [18] introduces Sigma method in MOPSO to find the local best value of each particle and compared with different function and results were compared with the Multi objective Evolutionary Algorithm technique to know the best results provided by this method, this process can be implanted when there is a lot of objective function involved in the program.

Margarita Reyes and C.Coello [19] reviewed various MOPSO approach as reported in literature, where they identify the main feature of each proposal by including a classifications of the approaches. They have also listed some of the proposal which can be very much helpful in future research.

Gregorio Toscano Pulido & Carlos Coello [20] extended the Particle Swarm Optimization technique to deal with Multi Objective Optimization Problem by using Pareto dominance to determine the direction of flight . They used a group of swarm instead of single particle to execute the information gathered from the group of Swarms and they concluded that this process gave a competitive result with compare to evolutionary optimization techniques.

Kalyan Deb [21] reported that the optimization of multiple objectives gets conflicting with each other, or absence of constraint, give rise to Pareto Optimal Solution, so he proposed to use evolutionary algorithm which uses the population approach in its search procedure.

Janez Demsar [22] examined on five statistical test and concluded the analysis of overcoming the problem of underestimated variance and evaluated the related error. They compared two or more classifiers with multiple data set and concluded that the non-parametric tests should be preferred over the parametric ones.

Yosef Hocheberg & C.Tamhane [23] worked on multiple comparison techniques to establish the drawback of reducing error rates and validate the statistical interferences. They had described numerous example for implementing the procedure which can work both practically and informatively.

2.2 Motivation of Present Research

Ceramics are one of the multipurpose materials with high thermal and electrical resistance, good chemical stability, high corrosion resistance, & hardness. Ceramics are used for electrical insulation, a high thermal application where super alloys are failed to resist heat. Ceramics are used in electronics industries as dielectric and insulators, application of heat shields for the space shuttle, heat exchanger and electronics substrate for microwave instruments, piezoelectric ceramics have wide applications in microelectronic mechanical systems (MEMS), ultrasonic measurements, strain gauge. Also, ceramics are used as mechanical tools and dies, fuel systems in space vehicles, automobile engines, defense weapon systems, biological and nuclear industries. Cutting of ceramics is a bit challenging using conventional machining techniques such as Abrasive wheel cutting; Diamond saw cutting, etc. due to their brittleness and hardness nature. Conventional techniques take more time, are noisy, and are less efficient compare to non-conventional techniques such as laser machining.

A laser is a photonic device, where we manipulate the photons using the electric signal. The laser acts as a heating point source just equivalent to machine tools in conventional techniques. The laser machining technique is eco-friendly, less noisy, very fast, and precise. In this present work ceramic tiles are used as a workpiece. Conventional techniques currently used for cutting ceramic tiles are very noisy, polluted, and less efficient in cutting speed than laser cutting.

We can easily control the response parameters such as kerf width, glass formation width, heat affected zone (HAZ), and taper angle from process parameters such as laser power, frequency, scanning speed, and gas pressure.

We simply optimize the process parameters for optimizing responses for the desired response concerning minimal laser power, maximizing scanning speed, increasing productivity, and less machining time by using Multi-Objective Particle Swarm Optimization Technique

2.3 Objective of Research

The objective of this paper is to get the optimum solution of Glass Formation Width and Taper Angle by varying the process parameters such as Laser Power, Frequency, Scanning Speed and Assist Gas pressure. The regression equation of Glass Formation Width and Taper Angle is used in MATLAB by Multi-Objective Particle Swarm Optimization to minimize the objective parameters and get a set of results by which the best sets of results will be taken as granted to get the best cutting of 7mm ceramic tiles using fiber laser with continuous Q- Switched laser beam with 1064nm and Nitrogen as an assist gas.

Chapter - 3

Introduction to Optimization Technique

3. Introduction to Optimization Technique

The design purpose in the optimization of a design could simply be to reduce production costs or to increase production efficiency. An optimization algorithm is a process that compares numerous solutions iteratively until an optimum or satisfying one is identified. Optimization has become a feature of computer-aided design activities since the invention of computers.

3.1 Components of Optimization Problem

3.1.1 Design Variables

The identification of the underlying design variables, which are primarily altered during the optimization process, is the first step in formulating an optimization problem. A design difficulty frequently involves a number of design factors, some of which are extremely important to the design's proper operation. This set of factors is referred to as design. Other design factors are usually fixed or change in response to the design variables. When formulating an optimization problem, the first rule is to use as few design variables as possible. The results of that optimization technique could indicate whether more design factors should be included in a revised formulation or whether certain previously considered design variables should be replaced with new design variables.

3.1.2 Design Constraint

The constraints are functional interactions between design variables and other design factors that fulfil specific physical phenomena and resource limits. It is depended on the user, the type and quantity of constraints to add in the formulation.

3.1.3 Objective Function

The objective function in terms of the design variables and other problem parameters is the next step in the formulation phase. Minimization of overall manufacturing costs, minimization of overall component weight, maximizing of a product's complete life cycle, and other engineering goals are prevalent. Although most of the objectives can be quantified (represented in mathematical form), and other objectives (such as the aesthetic aspect of a design, ride characteristics of a car suspension design, and design reliability) may be difficult to define mathematically. In this situation, a mathematical equation is utilized to approximate the solution.

In real-world optimization, the designer may desire to maximize more than one objective at the same time. Multiple objective optimization techniques are complicated and time-consuming to implement. As a result, the most essential goal is chosen as the objective function, and the remaining goals are incorporated as constraints by limiting their values to a specific range. Consider the difficulty of designing the best truss construction. The designer may be concerned with decreasing the total weight of the structure while also minimizing the deflection of a particular spot in the truss. The weight of the truss (as a function of the cross-sections of the members) may be used as the objective function in the optimization problem formulation, with a restriction on the deflection of the concerned point being smaller than a certain limit.

There are two kinds of objective functions. Either it must be maximized or minimized. The optimization algorithms were usually created to solve minimization or maximization problems. Although modest structural changes in some algorithms allow for either minimization (or) maximizing, this necessitates significant knowledge of the method. The duality principle assists by allowing the same algorithm to be used for both minimization and maximizing with only a tiny modification in the objective function rather than a complete method change. If the algorithm was designed to solve a minimization problem, it can simply be converted to a maximizing problem by multiplying the objective function by one, and vice versa.

3.2 Types of Optimization Technique

3.2.1 Single Variable Optimization Algorithms

These algorithms are classified into two categories

- i. Direct methods
- ii. Gradient-based methods

Direct approaches do not employ the objective function's derivative information to direct the search process; only the objective function's values are used. Gradient-based approaches, on the other hand, steer the search process using derivative information (first and/or second order). Despite the fact that engineering optimization problems typically include several variables, single-variable optimization algorithms are typically utilised as unidirectional search methods in multivariable optimization algorithms.

3.2.2 Multiple Variable Optimization Algorithms

These algorithms show how the search for the best point in several dimensions progresses. These algorithms are divided into direct and gradient-based strategies depending on whether or not gradient information is used.

3.2.3 Constrained Optimization Algorithms

These methods frequently and simultaneously apply single variable and multivariable optimization algorithms to keep the search effort within the feasible search region. The majority of the time, these techniques is employed in engineering optimization issues.

3.2.4 Specialized Optimization Algorithms

In engineering design issues, two of these algorithms, integer programming and geometric programming, are frequently utilized. With integer design variables, integer programming methods can be used to tackle optimization problems. Geometric programming approaches are used to solve optimization problems that include objective functions and constraints specified in a certain way.

3.2.5 Non- Traditional Optimization Algorithms

The optimization strategy is based on natural or natural phenomena. While these methods are quick, they do not guarantee optimal results. Approximation Methods are another name for non-traditional techniques.

3.3 MATLAB Modelling

Design optimization is the process of determining the best design parameters to suit project requirements. Engineers frequently use design of experiments (DOE), statistics, and optimization techniques to assess trade-offs and discover the best design. In design optimization, it's typical to work in a variety of design contexts to investigate the effects of design parameters across multiple physical domains.

You can import design data into MATLAB from spread sheets, text files, binary files, and other Programs. Sensitivity analysis, parameter adjustments, and design optimization may all be done with MATLAB and Simulink. Simulink is a suite of integrated tools for modelling, simulating, and optimizing multi-domain dynamic systems.

MATLAB and Simulink add-on products further extend design optimization capabilities:

- Using Statistics and Machine Learning Toolbox, perform design of experiments to establish test plans, generate random numbers for Monte Carlo simulations, apply sensitivity analysis to verify the robustness of your results, and develop response surface models.
- Use the Optimization Toolbox and Global Optimization Toolbox to optimize single and many design objectives.
- Model-Based Calibration Toolbox allows you to create test plans, statistical models, and ideal calibrations and lookup tables for complicated powertrain systems.

Chapter - 4

Particle Swarm Optimization

4. Particle Swarm Optimization Technique

4.1 Introduction

In this paper, we have used the Particle Swarm Optimization method to optimize the best result from our objective function. It is one of the non-traditional optimization technique where two or more objective function can be minimize or maximize by the help of different parameters, this method is inspired by the movement of flock of birds or swarm of fishes in a certain search space (It is a space in which the best solution can be gained), it is also assumed that it does not guarantee for an optimal solution.

4.2 Search Strategy

Suppose a flocks of birds or swarms of fishes are searching for a food in a search area, but there is only one piece of food in that search area where any of these birds don't know the position of the food, they only know the distance between them. If any of the members from the group can find the food, the remaining group will follow the lead.

Each particle /bird moves around the design space and remembers the best position and each particle communicate the information to each other and adjust their position based on their experience and hence the best result are found.

Similar to this food searching process, A random number of particles also known as population is taken and start to look for minimum or maximum point in random direction to find the best possible solution. At each step the particle search the minimum or maximum point by the entire population by changing their position and their velocity on each iteration, after certain iteration, a minimum /maximum point is achieved by them.

4.3 Implementation of PSO

Suppose an unconstrained maximization problem given as $F(X)$ with $X_L \leq X \leq X_U$, where L represents the lower bound and U represents the upper bound. This function can give the best possible maximization results which are described in multiple steps as below:

Step 1. Assume the size of the Swarm (N), where small N can have longer time to find the solution and medium N can provide a good result, usually it can be taken as 20-30 particles.

Step 2. Generate the initial position randomly between the X_L and X_U . Thus the particle can be denoted by X_{JI} , as J represent the particle and I represent the velocity.

The particle of population N can be denoted as $[X_1, X_2, X_3, \dots, X_N]$.

The design variable of 1st solution can be denoted as $X_1 = [X_{11}, X_{12}, X_{13}, \dots, X_{1K}]$.

Similarly the design variable of 2nd solution is denoted as $X_2 = [X_{21}, X_{22}, X_{23}, \dots, X_{2K}]$.

For N particle the design variable is denoted as $X_N = [X_{N1}, X_{N2}, X_{N3}, \dots, X_{NK}]$.

Step 3. To find the velocity of the particles, initially all the particle velocity are assumed to be as 0, And step by step increasing the velocity or gradually increasing. For updating the position, we can use this equation to update.

Present Position = Old position + Velocity

Step 4. Evaluate the fitness for each particle and all particle have their best position as $P_{Best, J}$. And to find the global best among the $P_{Best, J}$ which can be defined as G_{Best} . By using this we can find the function of G_{Best} as $f[X_{ji}]$.

Step 5. Calculate the updated velocity and the position of each particle using the below equations:

For updating particle we can use this equation, $X_{ji} = X_{J(i-1)} + V_{ji}$.

For updating the velocity, we can use this equation:

$$V_{ji} = V_{J(i-1)} + C_1 R_1 [P_{Best, J} - X_{J(i-1)}] + C_2 R_2 [G_{Best, J} - X_{J(i-1)}].$$

Where C_1 & C_2 can represent as Positive Constants [usually taken as 2].

R_1 & R_2 can represent as a random number between [0,1].

Step 6. Evaluate the updated fitness function as $f[X_{ji}]$ also the current best must be update from each iteration and increment the loop until the convergence is found.

Convergence Criteria: When all the particles converge to the same optimum solution, then it can said to be in a convergence criteria. In each iteration, this pollution must be updated using the local best and the global best solution and the last global best solution is accepted as optimum solution.

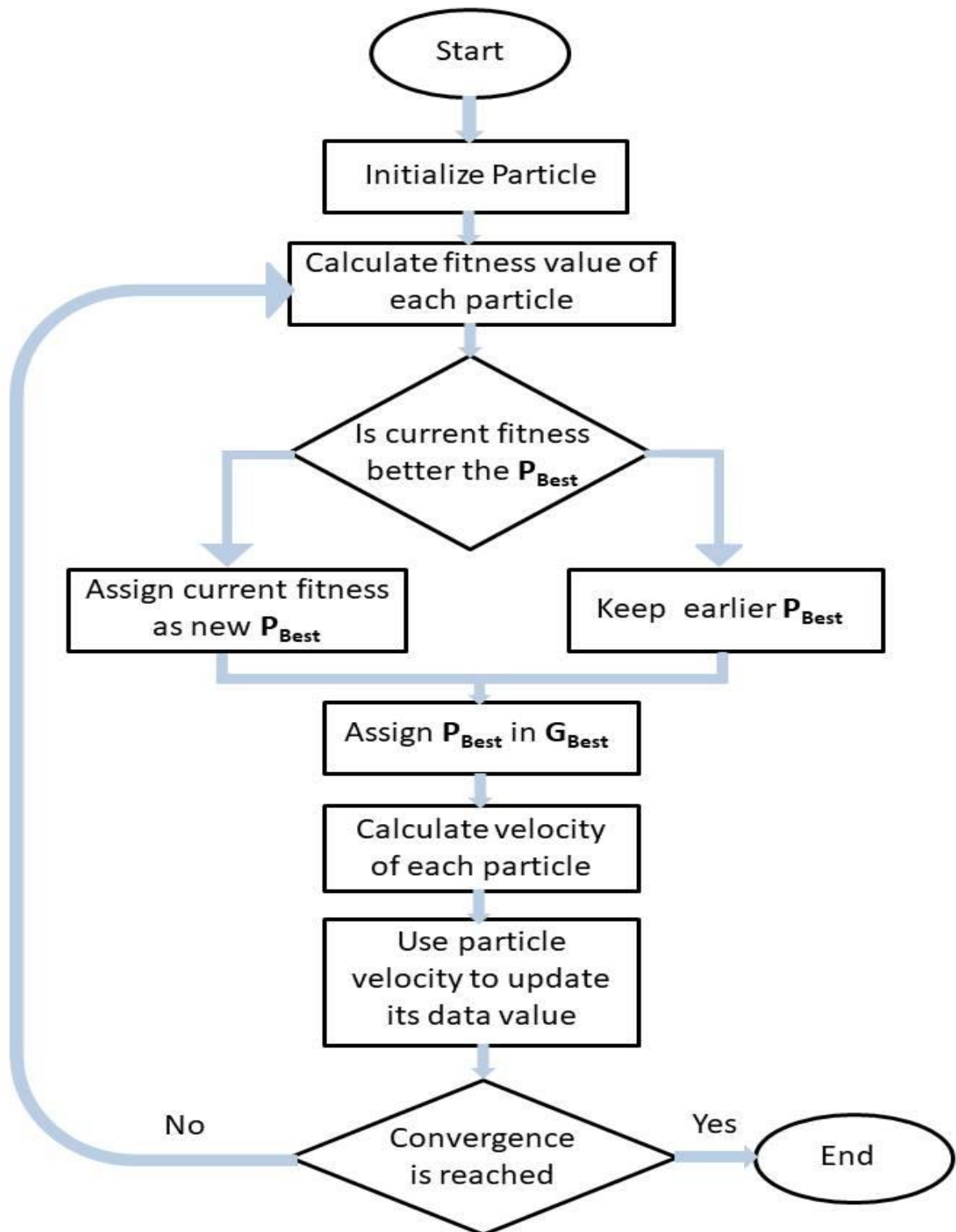


Figure:4-. Flow Chart of Particle Swarm Optimization

Chapter – 5

Results and Discussions

5. Experimental Study and Details

5.1 Introduction

In this paper, Particle Swarm Optimization is chosen to get the best solution of multi objective function with four parameters as inputs which are : Laser power (P), Scanning Speed (V), Gas Pressure (G), and Frequency (F). The objective function is taken from the regression equations of Glass formation and Taper Angle. The parameters are taken as input and Particle Swarm Optimization is used to minimize both functions.

The constant values such as Population Size (Np), Repository Size (Nr), Iteration Size (Maxgen), and Confidence Factor (C1 & C2) are varied in each observation and the minimized values of the Glass formation and Taper Angle are recorded. By comparing all the 8 observation by changing the constant values , the best value is concluded.

5.2 Optimization of the objective function

We have two objective function with all process parameters are continuous, measurable in this experiment. The first mathematical model equation for Glass Formation Width (GF) which is generated by regression analysis through MINITAB software and uses ANNOVA to generate an equation based on the output which is represented as a function $GF=f(P,V,G,F)$, the variable P,V,G,F are defined on section 5.1.

$$GF = 17725.22096 - 76.53543.*P - 1100.34431.*V - 174.18685.*G + 1.66965.*F + 2.22781.*P.*V + 0.396173.*P.*G - 0.005830.*P.*F - 21.95831.*V.*G - 0.075985.*V.*F + 0.034945.*G.*F + 0.097022.*P.*P + 51.93488.*V.*V + 0.516373.*G.*G + 0.000275.*F.*F$$

The 2nd Regression Equation is for the Taper angle(Section 1.8.5) which is taken for the same parameters using MINITAB

$$TA = 7.50882 - 0.044702.*P + 0.219641.*V + 0.064977.*G + 0.004067.*F - 0.001034.*P.*V - 0.000576.*P.*G - 0.000017.*P.*F - 0.020469.*V.*G - 0.000014.*V.*F + 0.000068.*G.*F + 0.000090.*P.*P + 0.055580.*V.*V + 0.006998.*G.*G + 0.00000149152.*F.*F$$

The both regression equation is combined in a function named as MultiObj.fun in MATLAB to get the minimum value of the Glass Formation Width and Taper Angle, also this equation will help to get the best parameter combination for getting both minimum taper angle and Glass Formation Width on the workpiece.

$$\text{MultiObj.fun} = @(P) [GF(P(:,1),P(:,2),P(:,3),P(:,4)), TA(P(:,1),P(:,2),P(:,3),P(:,4))]$$

This equation is used to generate the minimum value of both objective function in MATLAB by varying different constant value and record the value and compare the result to get the best result in all scenario.

5.4 Multiple observation by varying constant

In this experiment, a total of 8 number of observation is done to compare the best result of output from the input in MATLAB, these observations are described in the points below:

5.4.1 Observation 1

First observation is taken with the following parameters of the population size of 30 numbers , repository size of 30 numbers, iterations of 50 numbers, Inertia weight of 0.8, and the confidence factor of 2.

```
% Parameters
params.Np = 30;           % Population size
params.Nr = 30;           % Repository size
params.maxgen = 50;       % Maximum number of generations
params.W = 0.8;           % Inertia weight
params.C1 = 2;            % Individual confidence factor
params.C2 = 2;            % Swarm confidence factor
params.ngrid = 20;        % Number of grids in each dimension
params.maxvel = 5;        % Maximum vel in percentage
params.u_mut = 0.5;       % Uniform mutation percentage
```

Figure:5-. Parameters of 1st observations

The graph is gained from the following parameters with the objective function MultiObj.fun

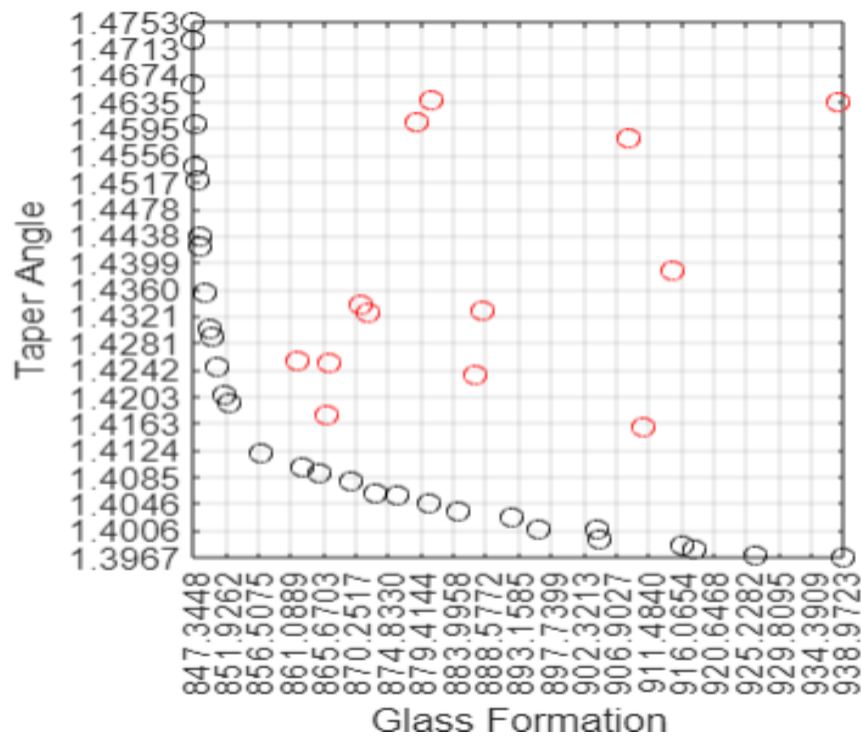


Figure:6-. Graph from 1st Observation with Taper Angle Vs Glass formation

The table is formed with respect to the other parameters are as follows:

Table No:1-. Observation No.1 with respect to input parameters and output

Laser power	Scanning speed	Gas pressure	Frequency	Glass formation width	Taper angle
$P(W)$	$V(mm/s)$	$g_p(bar)$	$f(Hz)$	(μm)	(deg)
370	4.4	12.8	680.8971	847.3448	1.4753
370	4.4	12.8	676.8215	847.3493	1.4728
370	4.4	12.8	665.5381	847.4096	1.4661
370	4.4	12.8	654.8019	847.5319	1.4602
370	4.4	12.8	643.2942	847.7334	1.4542
370	4.4	12.8	639.0469	847.8262	1.4521
370	4.4	12.8	621.6073	848.3112	1.4439
370	4.4	12.8	617.8148	848.4388	1.4423
370	4.4	12.8	601.3941	849.0825	1.4356
370	4.4	12.8	586.6078	849.7891	1.4303
370	4.4	12.8	582.8744	849.9866	1.4291
370	4.4	12.8	568.6941	850.8063	1.4248
370	4.4	12.8	552.5843	851.8717	1.4207
370	4.4	12.8	546.6599	852.2994	1.4193
370	4.4	12.8	493.2498	857.0269	1.412
370	4.3544	12.8	501.8522	862.5726	1.4101
370	4.3366	12.8	501.2051	865.1898	1.4092
370	4.3058	12.8	502.8253	869.553	1.4078
370	4.2932	12.8	486.6088	872.955	1.4062
370	4.288	12.8	463.8479	876.1084	1.4059
370	4.2583	12.8	462.0812	880.7147	1.4046
370	4.2077	12.8	501.4247	884.6975	1.4036
370	4.1956	12.7713	468.7219	892.2217	1.4027
370	4.1415	12.8	492.5916	896.1138	1.4009
370	4.1232	12.7575	477.5448	904.1993	1.4007
370	4.0933	12.8	486.9401	904.6158	1.3994
370	4.0436	12.8	453.5625	916.1103	1.3985
370	4.0172	12.8	484.8343	917.9508	1.3978
370	3.9751	12.8	470.4663	926.6164	1.3971
370	3.9105	12.8	463.9985	938.9723	1.3967

As it is observed from Fig 5 that the process parameters taken are shown as the population size / Swarm Size is taken as 30, Repository Size is taken as 30, Iteration Size is taken as 50, Inertia Weight is taken as 0.8, The confidence factor for Swarm and Individual is taken as 2, Number of Grids in each dimension is taken as 20, Maximum velocity is assumed as 5 and Uniform Mutation percentage is assumed as 0.5. By using these parameters we approach to use the Multi-Objective particle Swarm Optimization Technique.

In Fig 6 ,We can observed that the black circle on the graph represent the value of Taper angle , and the red circle represents the best values of Glass Formation Width after 50 iteration this is the best fitness graph observed using the above parameters. The maximum value of taper angle can be seen as 1.4753 degree with minimum Glass formation Width as 847.3448 μm , whereas the minimum value of taper angle (1.3967 degree) is observed with maximum value of 938.9723 μm of Glass formation Width.

If we check with the Table 1, if we take one observation taking a best result as 1st observation with glass formation width of (862.5726 μm) the taper angle is seen to be approx. 1.4101 degree which is quite nearer to the minimum value observed having a set of parameters of 370 watt of Laser Power, 4.3544 mm/s of Scanning speed, 12.8 bar of Gas pressure, 501.8522 Hz of Frequency.

Another observation can be seen when the glass formation is observed as 865.1898 μm and taper angle of 1.4092 degree also can give a comparably good result with the parameter of 370 watt of Laser Power, 4.3366 mm/s of Scanning speed, 12.8 bar of Gas pressures, 501.2051 Hz of Frequency.

So, from this 1st Table we can use these 2 sets of value for further proceeding and can conclude on a point.

5.4.2 Observation 2

This observation is taken with the following parameters of the population size of 30 numbers , repository size of 30 numbers, iterations of 50 numbers, Inertia weight of 0.4, and the confidence factor of 2.

```
% Parameters
params.Np = 30;           % Population size
params.Nr = 30;           % Repository size
params.maxgen = 50;       % Maximum number of generations
params.W = 0.4;           % Inertia weight
params.C1 = 2;            % Individual confidence factor
params.C2 = 2;            % Swarm confidence factor
params.ngrid = 20;        % Number of grids in each dimension
params.maxvel = 5;        % Maximum vel in percentage
params.u_mut = 0.5;       % Uniform mutation percentage
```

Figure:7-. Parameters of 2nd observations

The graph is gained from the following parameters with the objective function MultiObj.fun

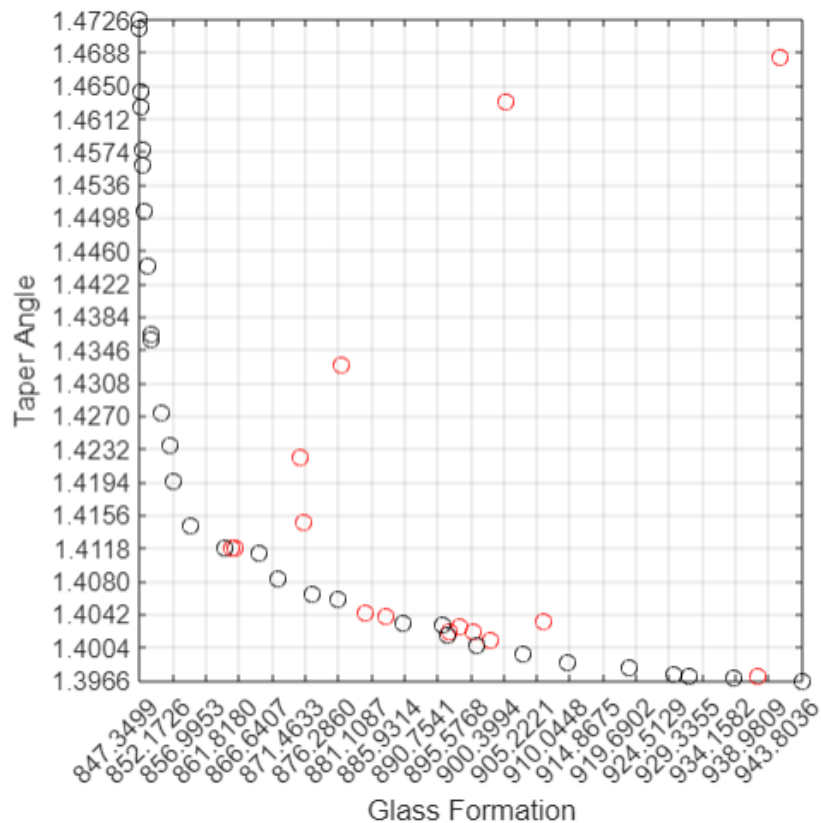


Figure:8-. Graph from 2st Observation with Taper Angle Vs Glass formation Width

The table is formed with respect to the other parameters are as follows:

Table No:2-. 2nd Observation with respect to input parameters and output

Laser power	Scanning speed	Gas pressure	Frequency	Glass formation width	Taper angle
$P(W)$	$V(mm/s)$	$g_p(bar)$	$f(Hz)$	(μm)	(deg)
370	3.9773	12.8	483.3232	925.1921	1.3973
370	3.8823	12.8	469.9194	943.8036	1.3966
370	4.4	12.8	646.7128	847.6659	1.4559
370	4.4	12.8	675.0876	847.354	1.4717
370	4.4	12.7992	636.2004	848.041	1.4507
370	4.4	12.8	676.5625	847.3499	1.4726
370	4.3035	12.8	479.1291	872.3814	1.4065
370	4.4	12.8	662.4186	847.4386	1.4644
370	4.073	12.7947	474.313	909.6164	1.3987
370	4.01	12.8	491.2131	918.7234	1.398
370	4.4	12.8	547.3703	852.2471	1.4195
370	4.4	12.7942	563.8107	851.6461	1.4236
370	4.4	12.8	577.4515	850.3738	1.4274
370	4.4	12.7985	622.227	848.4237	1.4442
370	4.3389	12.7973	478.3863	867.5025	1.4083
370	4.4	12.8	601.8482	849.0628	1.4358
370	4.1025	12.8	488.1829	903.076	1.3997
370	4.4	12.7993	518.3117	854.7074	1.4144
370	4.4	12.8	649.9916	847.655	1.4576
370	4.2228	12.8	465.5384	885.7347	1.4031
370	3.9718	12.7968	471.9017	927.3659	1.3971
370	4.4	12.8	603.2901	849.0006	1.4364
370	3.9372	12.7955	471.4592	933.9035	1.3969
370	4.149	12.8	476.3654	896.3276	1.4005
370	4.4	12.8	659.2318	847.4737	1.4626
370	4.1756	12.786	501.9919	891.3492	1.403
370	4.4	12.7891	477.767	859.7177	1.4118
370	4.2819	12.79	482.0012	876.223	1.4058
370	4.1803	12.7947	475.5372	892.227	1.4017
370	4.3293	12.7963	521.383	864.8397	1.4111

As it is observed from Fig 7 that the process parameters taken are shown as the population size / Swarm Size is taken as 30, Repository Size is taken as 30, Iteration Size is taken as 50, Inertia Weight is taken as 0.4, The confidence factor for Swarm and Individual is taken as 2, Number of Grids in each dimension is taken as 20, Maximum velocity is assumed as 5 and Uniform Mutation percentage is assumed as 0.5. By using these parameters we approach to use the Multi-Objective particle Swarm Optimization Technique.

In Fig 8, We can observe that the black circle on the graph represents the value of Taper angle, and the red circle represents the best values of Glass Formation Width after 50 iterations. This is the best fitness graph observed using the above parameters. The maximum value of taper angle can be seen as 1.4726 degree with minimum Glass formation Width as 847.3499 μm , whereas the minimum value of taper angle (1.3966 degree) is observed with maximum value of 943.8036 μm of Glass formation Width.

If we check with the Table 2, if we take one observation taking a best result as 1st observation with glass formation width of (864.8397 μm) the taper angle is seen to be approx. 1.411 degree which is quite nearer to the minimum value observed having a set of parameters of 370 watt of Laser Power, 4.3293 mm/s of Scanning speed, 12.7963 bar of Gas pressure, 521.383 Hz of Frequency.

Another observation can be seen when the glass formation is observed as 850.3738 μm and taper angle of 1.4274 degree also can give a comparably good result with the parameter of 370 watt of Laser Power, 4.4 mm/s of Scanning speed, 12.8 bar of Gas pressures, 577.4515 Hz of Frequency.

So, from this 2nd table we can use these 2 sets of value for further proceeding and can conclude on a point.

5.4.3 Observation 3

This observation is taken with the following parameters of the population size of 30 numbers, repository size of 30 numbers, iterations of 50 numbers, Inertia weight of 0.8, and the confidence factor of 1.

```
% Parameters
params.Np = 30;           % Population size
params.Nr = 30;           % Repository size
params.maxgen = 50;       % Maximum number of generations
params.W = 0.8;           % Inertia weight
params.C1 = 1;            % Individual confidence factor
params.C2 = 1;            % Swarm confidence factor
params.ngrid = 20;        % Number of grids in each dimension
params.maxvel = 5;        % Maximum vel in percentage
params.u_mut = 0.5;       % Uniform mutation percentage
```

Figure:9-. Parameters of 3rd observations

The graph is gained from the following parameters with the objective function MultiObj.fun

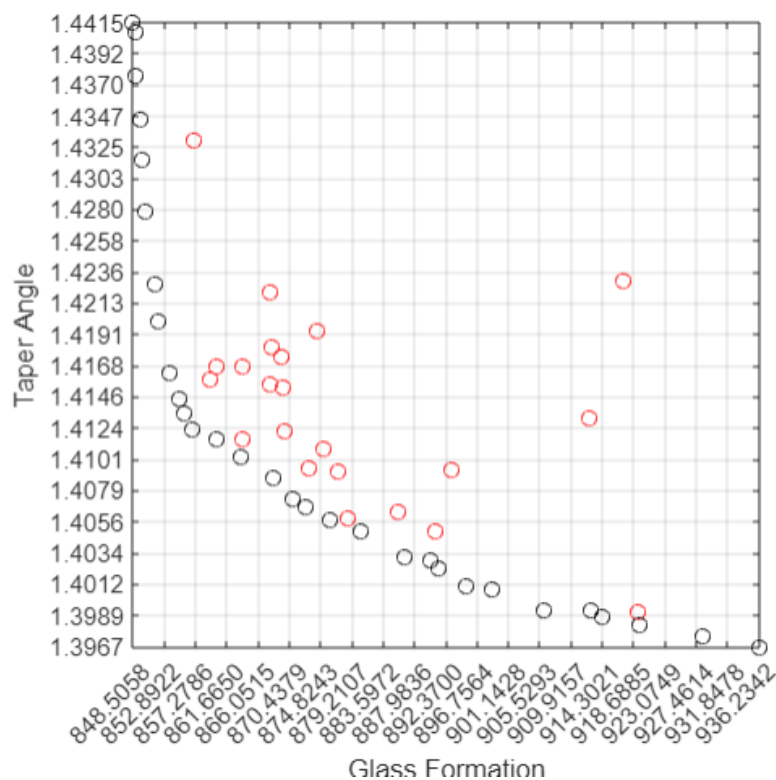


Figure:10-. Graph from 3rd Observation with Taper Angle Vs Glass formation

The table is formed with respect to the other parameters are as follows

Table No:3-. 3rd Observation with respect to input parameters and output

Laser power	Scanning speed	Gas pressure	Frequency	Glass formation width	Taper angle
P(W)	V(mm/s)	g_p(bar)	f (Hz)	(μm)	(deg)
370	4.4	12.8	549.661	852.08	1.42
370	3.9232	12.8	468.776	936.234	1.3967
370	4.3305	12.8	495.992	868.051	1.4088
370	4.4	12.8	606.656	848.86	1.4377
370	4.4	12.7983	590.333	849.756	1.4317
370	4.4	12.7999	560.674	851.487	1.4227
370	4.1315	12.7881	491.124	898.941	1.4008
370	4.158	12.8	478.85	895.15	1.401
370	4.4	12.8	510.159	855.778	1.4135
370	4.0931	12.8	477.18	906.135	1.3993
370	4.3726	12.786	480.004	863.535	1.4103
370	4.2913	12.7961	495.181	872.768	1.4067
370	4.4	12.8	530.975	853.525	1.4163
370	4.2566	12.7949	483.627	880.379	1.405
370	3.9684	12.7936	478.026	928.437	1.3974
370	4.0243	12.8	453.602	919.439	1.3982
370	4.0419	12.7946	491.096	914.29	1.3988
370	4.1832	12.7922	488.347	891.261	1.4024
370	4.4	12.7988	497.414	856.716	1.4123
370	4.4	12.8	615.912	848.506	1.4415
370	4.4	12.7974	614.109	848.807	1.4408
370	4.2871	12.7983	466.481	876.105	1.4058
370	4.4	12.8	464.408	860.232	1.4116
370	4.0647	12.8	476.46	912.711	1.3992
370	4.2163	12.7969	479.253	886.515	1.4032
370	4.3036	12.7955	495.266	870.994	1.4072
370	4.4	12.8	598.587	849.598	1.4346
370	4.4	12.8	578.99	850.2	1.4279
370	4.2023	12.7981	454.263	890.284	1.4028
370	4.4	12.7949	518.351	855.087	1.4145

As it is observed from Fig 9 that the process parameters taken are shown as the population size / Swarm Size is taken as 30, Repository Size is taken as 30, Iteration Size is taken as 50, Inertia Weight is taken as 0.8, The confidence factor for Swarm and Individual is taken as 1, Number of Grids in each dimension is taken as 20, Maximum velocity is assumed as 5 and Uniform Mutation percentage is assumed as 0.5. By using these parameters we approach to use the Multi-Objective particle Swarm Optimization Technique.

In Fig 10 ,We can observed that the black circle on the graph represent the value of Taper angle , and the red circle represents the best values of Glass Formation Width after 50 iteration this is the best fitness graph observed using the above parameters. The maximum value of taper angle can be seen as 1.4415 degree with minimum Glass formation Width as 848.506 μm , whereas the minimum value of taper angle (1.3967 degree) is observed with maximum value of 936.234 μm of Glass formation Width.

If we check with the Table 3, if we take one observation taking a best result as 1st observation with glass formation width of (860.232 μm) the taper angle is seen to be approx. 1.4116 degree which is quite nearer to the minimum value observed having a set of parameters of 370 watt of Laser Power, 4.4 mm/s of Scanning speed, 12.8 bar of Gas pressure, 464.408 Hz of Frequency.

Another observation can be seen when the glass formation is observed as 856.716 μm and taper angle of 1.4123 degree also can give a comparably good result with the parameter of 370 watt of Laser Power, 4.4 mm/s of Scanning speed, 12.7988 bar of Gas pressures, 497.414 Hz of Frequency.

So, from this 3rd table we can use these 2 sets of value for further proceeding and can conclude on a point.

5.4.4 Observation 4

This observation is taken with the following parameters of the population size of 30 numbers, repository size of 30 numbers, iterations of 50 numbers, Inertia weight of 0.4, and the confidence factor of 1.

```
% Parameters
params.Np = 30;           % Population size
params.Nr = 30;           % Repository size
params.maxgen = 50;       % Maximum number of generations
params.W = 0.4;           % Inertia weight
params.C1 = 1;            % Individual confidence factor
params.C2 = 1;            % Swarm confidence factor
params.ngrid = 20;        % Number of grids in each dimension
params.maxvel = 5;        % Maximum vel in percentage
params.u_mut = 0.5;       % Uniform mutation percentage
```

Figure:11-. Parameters of 4th observations

The graph is gained from the following parameters with the objective function MultiObj.fun

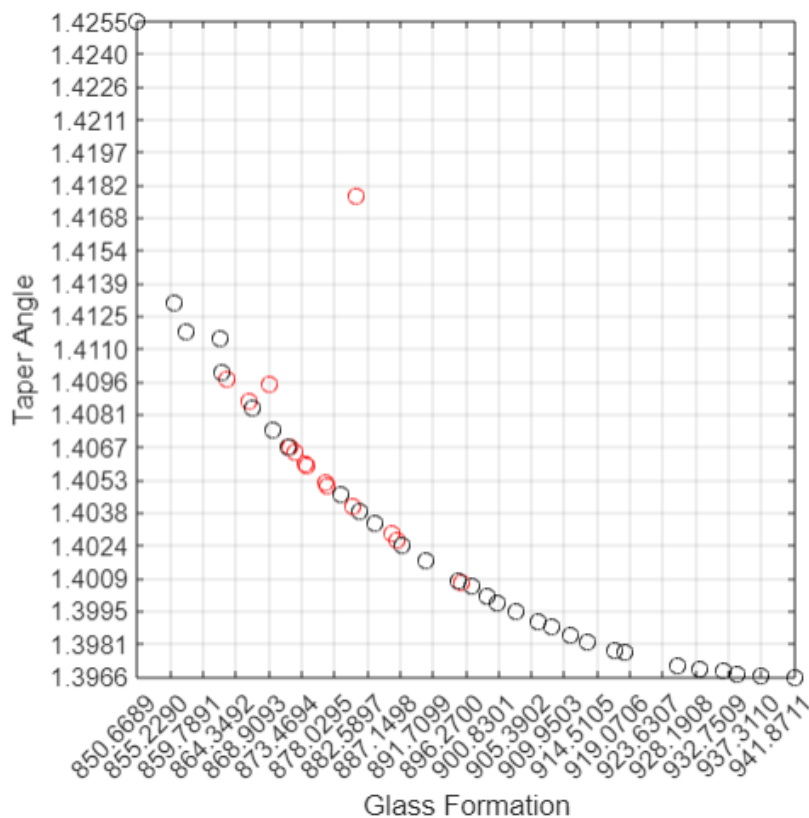


Figure:12-. Graph from 4th Observation with Taper Angle Vs Glass formation

The table is formed with respect to the other parameters are as follows

Table No:4-. 4th Observation with respect to input parameters and output

Laser power	Scanning speed	Gas pressure	Frequency	Glass formation width	Taper angle
$P(W)$	$V(mm/s)$	$g_p(bar)$	$f(Hz)$	(μm)	(deg)
370	3.914	12.8	477.6924	937.2553	1.3967
370	3.8899	12.8	476.6053	941.8711	1.3966
370	3.9334	12.8	473.0457	934.0017	1.3967
370	4.3639	12.7985	492.385	862.2885	1.41
370	4.3933	12.8	457.0359	862.025	1.4115
370	4.076	12.7993	480.2029	908.2728	1.3988
370	4.049	12.8	474.6012	913.247	1.3981
370	3.9783	12.8	475.0354	925.7001	1.3971
370	3.9613	12.7987	475.7063	928.8295	1.397
370	3.9453	12.7955	476.1752	931.959	1.3969
370	4.0615	12.7995	478.8389	910.8241	1.3984
370	4.0194	12.799	477.4835	918.3923	1.3977
370	4.028	12.7997	475.8477	916.8221	1.3978
370	4.105	12.7998	481.5146	903.1708	1.3995
370	4.1574	12.799	476.5899	895.1073	1.4008
370	4.4	12.8	488.4653	857.527	1.4118
370	4.121	12.7991	479.8863	900.6934	1.3998
370	4.2544	12.7988	487.9762	878.8235	1.4046
370	4.4	12.8	506.8002	855.679	1.4131
370	4.2264	12.7986	483.0031	883.5889	1.4033
370	4.318	12.7987	487.5477	869.3606	1.4074
370	4.1386	12.7985	487.5545	897.1907	1.4006
370	4.4	12.8	570.9438	850.6689	1.4255
370	4.2015	12.7987	483.4738	887.3922	1.4024
370	4.3013	12.7983	489.0331	871.6864	1.4067
370	4.1327	12.7984	476.1789	899.2563	1.4001
370	4.3415	12.7979	481.3213	866.7389	1.4084
370	4.0851	12.8	484.4586	906.2141	1.3991
370	4.1805	12.7988	483.4267	890.7491	1.4017
370	4.2387	12.799	484.9626	881.5718	1.4039

As it is observed from Fig 18 that the process parameters taken are shown as the population size / Swarm Size is taken as 30, Repository Size is taken as 30, Iteration Size is taken as 50, Inertia Weight is taken as 0.4, The confidence factor for Swarm and Individual is taken as 1, Number of Grids in each dimension is taken as 20, Maximum velocity is assumed as 5 and Uniform Mutation percentage is assumed as 0.5. By using these parameters we approach to use the Multi-Objective particle Swarm Optimization Technique.

In Fig 19, We can observed that the black circle on the graph represent the value of Taper angle, and the red circle represents the best values of Glass Formation Width after 50 iteration this is the best fitness graph observed using the above parameters. The maximum value of taper angle can be seen as 1.4255 degree with minimum Glass formation Width as 850.6689 μm , whereas the minimum value of taper angle (1.3966 degree) is observed with maximum value of 941.8711 μm of Glass formation Width.

If we check with the Table 4, if we take one observation taking a best result as 1st observation with glass formation width of (862.2885 μm) the taper angle is seen to be approx. 1.41 degree which is quite nearer to the minimum value observed having a set of parameters of 370 watt of Laser Power, 4.3639 mm/s of Scanning speed, 12.7985 bar of Gas pressure, 492.385 Hz of Frequency.

Another observation can be seen when the glass formation is observed as 895.5899 μm and taper angle of 1.4008 degree also can give a comparably good result with the parameter of 370 watt of Laser Power, 4.1574 mm/s of Scanning speed, 12.799 bar of Gas pressures, 476.5899 Hz of Frequency.

So, from this 4th Table, we can use these 2 sets of value for further proceeding and can conclude on a point.

5.4.5 Observation 5

This observation is taken with the following parameters of the population size of 300 numbers, repository size of 300 numbers, iterations of 500 numbers, Inertia weight of 0.8, and confidence factor of 2.

```
% Parameters
params.Np = 300;      % Population size
params.Nr = 300;      % Repository size
params.maxgen = 500;  % Maximum number of generations
params.W = 0.8;       % Inertia weight
params.C1 = 2;        % Individual confidence factor
params.C2 = 2;        % Swarm confidence factor
params.ngrid = 20;    % Number of grids in each dimension
params.maxvel = 5;    % Maximum vel in percentage
params.u_mut = 0.5;   % Uniform mutation percentage
```

Figure:13-. Parameters of 5th observations

The graph is gained from the following parameters with the objective function MultiObj.fun

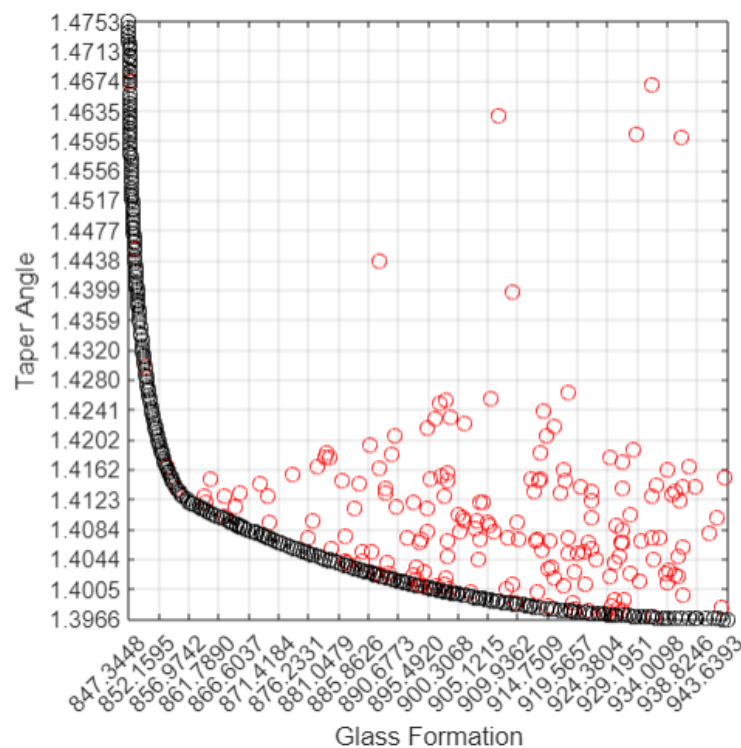


Figure:14-. Graph from 5th Observation with Taper Angle Vs Glass formation

The table is formed with respect to the other parameters are as follows

Table No:5-. 5th Observation with respect to input parameters and output

Laser power	Scanning speed	Gas pressure	Frequency	Glass formation width	Taper angle
$P(W)$	$V(mm/s)$	$g_p(bar)$	$f(Hz)$	(μm)	(deg)
370	3.9141	12.8	474.6241	937.4563	1.3966
370	3.9096	12.8	473.2956	938.4159	1.3966
370	3.9072	12.8	473.327	938.8626	1.3966
370	3.8999	12.8	472.9913	940.2531	1.3966
370	3.8928	12.8	474.6722	941.4623	1.3966
370	3.8912	12.8	469.9878	942.1268	1.3966
370	3.8858	12.8	470.8162	943.0721	1.3966
370	3.8826	12.8	471.3397	943.6393	1.3966
370	3.9312	12.8	476.0017	934.178	1.3967
370	3.9281	12.8	471.1802	935.1294	1.3967
370	3.9214	12.8	472.1724	936.2999	1.3967
370	3.9487	12.8	476.1039	930.9502	1.3968
370	3.9468	12.8	471.8953	931.6346	1.3968
370	3.9426	12.8	472.9853	932.3244	1.3968
370	3.9361	12.8	476.5186	933.2469	1.3968
370	3.9357	12.7986	472.07	933.771	1.3968
370	3.9606	12.8	475.5484	928.8345	1.3969
370	3.9592	12.8	470.1195	929.5181	1.3969
370	3.9524	12.8	476.0309	930.2913	1.3969
370	3.9732	12.8	469.8441	927.0168	1.397
370	3.9673	12.8	474.7128	927.6794	1.397
370	3.9615	12.8	477.535	928.4999	1.397
370	3.9828	12.8	473.1778	925.0049	1.3971
370	3.9797	12.8	474.997	925.4089	1.3971
370	3.9777	12.8	473.7475	925.8836	1.3971
370	3.9891	12.8	473.4737	923.86	1.3972
370	3.9864	12.8	470.7326	924.5759	1.3972
370	3.9988	12.8	475.2782	921.9768	1.3973
370	3.9962	12.8	471.6066	922.7448	1.3973
370	3.9926	12.8	474.4333	923.1475	1.3973
370	4.0041	12.8	477.4503	920.852	1.3974
370	4.003	12.8	473.0534	921.4151	1.3974
370	4.0115	12.8	474.3096	919.8032	1.3975
370	4.0185	12.8	474.7021	918.5382	1.3976
370	4.0161	12.8	474.7845	918.957	1.3976
370	4.0255	12.8	472.8925	917.4644	1.3977
370	4.0177	12.7997	479.4437	918.3042	1.3977
370	4.0287	12.8	472.9265	916.9062	1.3978
370	4.0346	12.8	480.0062	915.2762	1.3979
370	4.0345	12.8	474.3484	915.7689	1.3979
370	4.0403	12.8	477.4204	914.502	1.398
370	4.0483	12.8	474.2739	913.3845	1.3981
370	4.0516	12.8	476.2009	912.6571	1.3982

370	4.0599	12.8	469.6932	911.7989	1.3983
370	4.0563	12.8	473.1651	912.1135	1.3983
370	4.0582	12.8	479.6058	911.2238	1.3984
370	4.0671	12.8	478.0154	909.8373	1.3985
370	4.0664	12.8	469.1887	910.7292	1.3985
370	4.0718	12.8	475.4828	909.2432	1.3986
370	4.0819	12.8	476.4033	907.4532	1.3988
370	4.0763	12.8	480.7676	908.0176	1.3988
370	4.0789	12.8	467.7908	908.7439	1.3988
370	4.0891	12.8	473.4266	906.511	1.3989
370	4.0879	12.8	472.0533	906.8303	1.3989
370	4.0902	12.8	477.6806	905.9435	1.399
370	4.0926	12.8	478.2665	905.4829	1.3991
370	4.0997	12.8	478.1402	904.2941	1.3992
370	4.0961	12.8	479.1693	904.8219	1.3992
370	4.102	12.8	479.9707	903.7539	1.3993
370	4.1075	12.8	477.3354	903.0638	1.3994
370	4.1046	12.8	477.7833	903.5139	1.3994
370	4.113	12.8	471.8656	902.6534	1.3995
370	4.1067	12.8	485.7312	902.4739	1.3996
370	4.1208	12.8	475.4296	901.0331	1.3997
370	4.1141	12.7991	481.201	901.7013	1.3997
370	4.126	12.8	477.6407	899.9808	1.3999
370	4.1219	12.8	481.5389	900.2963	1.3999
370	4.1264	12.8	482.7414	899.4444	1.4
370	4.1256	12.8	482.0794	899.6447	1.4
370	4.1314	12.8	481.0186	898.7731	1.4001
370	4.137	12.8	478.9365	898.0499	1.4002
370	4.1371	12.8	474.6663	898.4294	1.4002
370	4.1427	12.8	472.7623	897.6909	1.4003
370	4.1417	12.8	481.0891	897.0917	1.4004
370	4.1483	12.8	474.3874	896.6202	1.4005
370	4.1501	12.8	478.6775	895.9371	1.4006
370	4.1432	12.8	485.6892	896.4317	1.4006
370	4.1536	12.8	476.9594	895.5226	1.4007
370	4.1519	12.8	484.9386	895.0829	1.4008
370	4.1646	12.8	477.2329	893.727	1.401
370	4.1643	12.8	483.9111	893.1582	1.4012
370	4.172	12.8	476.3554	892.6223	1.4013
370	4.1742	12.8	482.1331	891.7223	1.4014
370	4.1703	12.8	484.0483	892.1807	1.4014
370	4.1816	12.8	473.6886	891.3517	1.4015
370	4.1789	12.8	481.04	891.0851	1.4016
370	4.1828	12.7998	479.5107	890.6172	1.4017
370	4.1884	12.8	477.2662	889.9255	1.4018
370	4.1842	12.8	481.9249	890.1519	1.4018
370	4.1898	12.8	479.7612	889.4636	1.4019
370	4.1949	12.8	476.5658	888.9679	1.402
370	4.1987	12.8	480.7521	887.9664	1.4022
370	4.2054	12.8	480.4381	886.9491	1.4024
370	4.2043	12.8	477.0047	887.4412	1.4024

370	4.2058	12.8	483.953	886.5472	1.4026
370	4.2098	12.8	482.6129	886.1105	1.4027
370	4.2155	12.8	479.9164	885.4178	1.4028
370	4.2139	12.8	480.6115	885.5993	1.4028
370	4.2202	12.8	477.9507	884.8792	1.4029
370	4.2171	12.8	485.9187	884.5948	1.403
370	4.2243	12.8	479.2723	884.1126	1.4031
370	4.2238	12.8	485.6016	883.5863	1.4033
370	4.232	12.8	476.1679	883.2251	1.4034
370	4.2348	12.8	477.0176	882.7125	1.4035
370	4.2389	12.8	475.8075	882.2132	1.4036
370	4.2351	12.8	487.2265	881.6868	1.4038
370	4.2412	12.8	485.7577	880.8827	1.404
370	4.2443	12.8	486.5041	880.3349	1.4041
370	4.2523	12.8	479.9512	879.7464	1.4042
370	4.2458	12.8	492.1208	879.5813	1.4044
370	4.2521	12.8	487.8277	879.0122	1.4045
370	4.258	12.8	483.9276	878.4964	1.4046
370	4.2638	12.8	480.5736	877.9422	1.4047
370	4.2666	12.8	484.5217	877.1411	1.405
370	4.2727	12.8	480.1381	876.6553	1.4051
370	4.2778	12.8	476.7074	876.2386	1.4053
370	4.2802	12.8	477.1771	875.8451	1.4054
370	4.2808	12.8	479.9102	875.468	1.4055
370	4.2802	12.8	486.0956	874.9476	1.4056
370	4.2878	12.8	479.7511	874.4492	1.4058
370	4.288	12.8	484.5914	873.9271	1.4059
370	4.2939	12.8	481.3281	873.3784	1.4061
370	4.2934	12.8	485.5077	873.0306	1.4062
370	4.3005	12.8	483.4501	872.1946	1.4064
370	4.2995	12.8	489.7209	871.7185	1.4066
370	4.3053	12.8	485.1849	871.3171	1.4067
370	4.3061	12.8	488.9626	870.8219	1.4069
370	4.3159	12.8	479.179	870.38	1.4071
370	4.3116	12.8	489.7318	869.9301	1.4072
370	4.3198	12.8	481.2563	869.5974	1.4073
370	4.3222	12.8	482.37	869.1384	1.4074
370	4.3269	12.8	480.8106	868.6174	1.4076
370	4.3277	12.8	476.4147	868.9607	1.4076
370	4.3288	12.8	484.5668	867.9484	1.4078
370	4.325	12.8	493.2816	867.6321	1.408
370	4.3349	12.8	483.9257	867.1892	1.4081
370	4.3387	12.8	485.4646	866.4456	1.4083
370	4.3409	12.8	487.1226	865.9487	1.4085
370	4.348	12.8	479.3603	865.7517	1.4087
370	4.3477	12.8	483.9845	865.3028	1.4088
370	4.3517	12.8	479.7239	865.2237	1.4089
370	4.3476	12.8	489.4674	864.7548	1.409
370	4.3431	12.8	496.6941	864.6916	1.4091
370	4.3538	12.8	487.7947	864.0507	1.4092
370	4.3564	12.8	487.3029	863.7342	1.4093

370	4.3589	12.8	487.7236	863.3319	1.4095
370	4.3649	12.8	483.7263	862.9056	1.4097
370	4.3695	12.8	480.9231	862.5617	1.4098
370	4.3635	12.8	493.4089	862.1036	1.41
370	4.3752	12.8	483.5486	861.4811	1.4102
370	4.3774	12.8	485.609	860.958	1.4104
370	4.3809	12.8	485.2849	860.4999	1.4106
370	4.3853	12.8	483.9683	860.038	1.4108
370	4.3866	12.8	485.0424	859.743	1.4109
370	4.3903	12.8	484.2765	859.3102	1.4111
370	4.3916	12.8	485.4013	859.0013	1.4112
370	4.3966	12.8	482.9793	858.5764	1.4114
370	4.4	12.8	482.7188	858.1442	1.4116
370	4.4	12.8	485.9193	857.7982	1.4117
370	4.4	12.8	489.3613	857.4324	1.4118
370	4.4	12.8	493.3074	857.021	1.412
370	4.4	12.8	497.2042	856.6231	1.4123
370	4.4	12.8	503.1756	856.0297	1.4127
370	4.4	12.8	506.2975	855.7272	1.413
370	4.4	12.8	510.4232	855.3357	1.4134
370	4.4	12.8	511.634	855.2226	1.4136
370	4.4	12.8	516.9987	854.7311	1.4142
370	4.4	12.8	520.0018	854.4629	1.4146
370	4.4	12.8	521.6821	854.315	1.4148
370	4.4	12.8	523.7607	854.1342	1.4151
370	4.4	12.8	526.0146	853.9408	1.4155
370	4.4	12.8	528.6228	853.7205	1.4159
370	4.4	12.8	529.8918	853.6147	1.4161
370	4.4	12.8	532.0722	853.4349	1.4165
370	4.4	12.8	533.9536	853.2819	1.4168
370	4.4	12.8	536.56	853.0731	1.4173
370	4.4	12.8	538.9012	852.8888	1.4177
370	4.4	12.7988	541.482	852.7965	1.4183
370	4.4	12.8	542.6618	852.599	1.4185
370	4.4	12.8	543.7446	852.517	1.4187
370	4.4	12.8	545.3067	852.3999	1.419
370	4.4	12.8	547.042	852.2713	1.4194
370	4.4	12.8	549.1357	852.1184	1.4199
370	4.4	12.8	550.4477	852.0238	1.4202
370	4.4	12.8	552.4909	851.8783	1.4206
370	4.4	12.8	554.7975	851.7169	1.4212
370	4.4	12.8	556.6172	851.5916	1.4216
370	4.4	12.8	556.7718	851.5811	1.4217
370	4.4	12.8	559.6328	851.388	1.4224
370	4.4	12.8	561.763	851.2472	1.4229
370	4.4	12.8	563.6057	851.1274	1.4234
370	4.4	12.8	564.5235	851.0684	1.4237
370	4.4	12.8	565.6563	850.9963	1.424
370	4.4	12.8	567.371	850.8884	1.4244
370	4.4	12.8	569.6305	850.7487	1.4251
370	4.4	12.8	571.1722	850.6551	1.4255

370	4.4	12.8	572.5585	850.5719	1.4259
370	4.4	12.8	572.8414	850.5551	1.426
370	4.4	12.8	574.8175	850.4387	1.4266
370	4.4	12.8	575.1902	850.417	1.4267
370	4.4	12.8	576.7535	850.3268	1.4272
370	4.4	12.8	577.1821	850.3023	1.4273
370	4.4	12.8	578.7919	850.2112	1.4278
370	4.4	12.8	580.4839	850.117	1.4283
370	4.4	12.8	581.7032	850.0501	1.4287
370	4.4	12.8	584.0234	849.925	1.4295
370	4.4	12.8	586.2824	849.8061	1.4302
370	4.4	12.8	587.5869	849.7386	1.4307
370	4.4	12.8	588.7097	849.6814	1.4311
370	4.4	12.8	589.1809	849.6575	1.4312
370	4.4	12.8	590.696	849.5818	1.4317
370	4.4	12.8	591.6214	849.5361	1.4321
370	4.4	12.8	592.8283	849.4772	1.4325
370	4.4	12.8	594.8842	849.3788	1.4332
370	4.4	12.8	595.0026	849.3732	1.4333
370	4.4	12.7999	596.9443	849.2919	1.434
370	4.4	12.8	597.3732	849.2628	1.4341
370	4.4	12.8	599.6624	849.1591	1.435
370	4.4	12.8	599.5913	849.1623	1.435
370	4.4	12.8	601.6169	849.0728	1.4357
370	4.4	12.8	602.8542	849.0193	1.4362
370	4.4	12.8	604.6358	848.9437	1.4369
370	4.4	12.8	605.543	848.9059	1.4372
370	4.4	12.8	607.0023	848.846	1.4378
370	4.4	12.8	607.2652	848.8353	1.4379
370	4.4	12.8	608.5846	848.7824	1.4384
370	4.4	12.8	608.7939	848.7741	1.4385
370	4.4	12.8	610.314	848.7144	1.4391
370	4.4	12.8	611.6831	848.6618	1.4397
370	4.4	12.8	612.6916	848.6237	1.4401
370	4.4	12.8	613.6505	848.588	1.4405
370	4.4	12.8	614.6757	848.5504	1.4409
370	4.4	12.8	616.2862	848.4924	1.4416
370	4.4	12.8	618.0176	848.4317	1.4424
370	4.4	12.8	618.443	848.4171	1.4425
370	4.4	12.8	619.4852	848.3816	1.443
370	4.4	12.8	620.5337	848.3465	1.4435
370	4.4	12.8	621.4309	848.3169	1.4438
370	4.4	12.8	622.7144	848.2754	1.4444
370	4.4	12.8	624.2529	848.2268	1.4451
370	4.4	12.8	625.4288	848.1906	1.4456
370	4.4	12.8	626.5191	848.1576	1.4461
370	4.4	12.8	626.825	848.1485	1.4463
370	4.4	12.8	628.3392	848.1041	1.447
370	4.4	12.8	629.4193	848.0732	1.4475
370	4.4	12.8	630.5127	848.0426	1.448
370	4.4	12.8	631.0807	848.027	1.4482

370	4.4	12.8	632.1117	847.999	1.4487
370	4.4	12.8	633.1793	847.9707	1.4492
370	4.4	12.8	634.4105	847.9388	1.4498
370	4.4	12.8	635.6489	847.9076	1.4504
370	4.4	12.8	636.2021	847.8939	1.4507
370	4.4	12.8	637.7616	847.8562	1.4514
370	4.4	12.8	638.7548	847.8329	1.4519
370	4.4	12.8	639.4958	847.8159	1.4523
370	4.4	12.8	640.0743	847.8028	1.4526
370	4.4	12.8	640.7104	847.7887	1.4529
370	4.4	12.8	641.7165	847.7667	1.4534
370	4.4	12.8	643.1984	847.7354	1.4541
370	4.4	12.8	644.3029	847.7128	1.4547
370	4.4	12.8	645.43	847.6905	1.4553
370	4.4	12.8	646.3611	847.6726	1.4557
370	4.4	12.8	647.6058	847.6494	1.4564
370	4.4	12.8	648.2498	847.6377	1.4567
370	4.4	12.8	649.3309	847.6186	1.4573
370	4.4	12.8	650.4032	847.6003	1.4578
370	4.4	12.8	650.5931	847.5972	1.4579
370	4.4	12.8	651.812	847.5773	1.4586
370	4.4	12.8	652.8478	847.561	1.4591
370	4.4	12.8	654.4766	847.5366	1.46
370	4.4	12.8	655.2336	847.5258	1.4604
370	4.4	12.8	655.9165	847.5163	1.4608
370	4.4	12.8	656.6675	847.5061	1.4612
370	4.4	12.8	657.6921	847.4927	1.4617
370	4.4	12.8	658.3799	847.4841	1.4621
370	4.4	12.8	659.3774	847.472	1.4627
370	4.4	12.8	659.9192	847.4657	1.463
370	4.4	12.8	661.0193	847.4533	1.4636
370	4.4	12.8	661.9229	847.4437	1.4641
370	4.4	12.8	662.4433	847.4383	1.4644
370	4.4	12.8	663.6865	847.4261	1.4651
370	4.4	12.8	664.8965	847.4151	1.4658
370	4.4	12.8	666.9219	847.3984	1.4669
370	4.4	12.8	667.8183	847.3917	1.4674
370	4.4	12.8	668.6877	847.3857	1.4679
370	4.4	12.8	669.6763	847.3793	1.4685
370	4.4	12.8	670.0281	847.3772	1.4687
370	4.4	12.8	671.5173	847.3689	1.4696
370	4.4	12.8	672.2976	847.3651	1.4701
370	4.4	12.8	673.2859	847.3607	1.4707
370	4.4	12.8	673.6101	847.3593	1.4708
370	4.4	12.8	674.7467	847.3551	1.4715
370	4.4	12.8	675.0698	847.3541	1.4717
370	4.4	12.8	675.8396	847.3518	1.4722
370	4.4	12.8	676.7275	847.3495	1.4727
370	4.4	12.8	677.6555	847.3476	1.4733
370	4.4	12.8	678.5177	847.3463	1.4738
370	4.4	12.8	679.5563	847.3453	1.4744

As it is observed from Fig 13 that the process parameters taken are shown as the population size / Swarm Size is taken as 300, Repository Size is taken as 300, Iteration Size is taken as 500, Inertia Weight is taken as 0.8, The confidence factor for Swarm and Individual is taken as 2, Number of Grids in each dimension is taken as 20, Maximum velocity is assumed as 5 and Uniform Mutation percentage is assumed as 0.5. By using these parameters we approach to use the Multi-Objective particle Swarm Optimization Technique.

In Fig 14 ,We can observed that the black circle on the graph represent the value of Taper angle , and the red circle represents the best values of Glass Formation Width after 300 iteration this is the best fitness graph observed using the above parameters. The maximum value of taper angle can be seen as 1.4753 degree with minimum Glass formation Width as 847.3448 μm , whereas the minimum value of taper angle (1.3966 degree) is observed with maximum value of 937.4563 μm of Glass formation Width.

If we check with the Table 5, if we take one observation taking a best result as 1st observation with glass formation width of (856.6231 μm) the taper angle is seen to be approx. 1.4123 degree which is quite nearer to the minimum value observed having a set of parameters of 370 watt of Laser Power, 4.4 mm/s of Scanning speed, 12.8 bar of Gas pressure, 497.2042 Hz of Frequency.

Another observation can be seen when the glass formation is observed as 857.021 μm and taper angle of 1.412 degree also can give a comparably good result with the parameter of 370 watt of Laser Power, 4.4 mm/s of Scanning speed, 12.8 bar of Gas pressures, 476.3074 Hz of Frequency.

So, from this 5th Table, we can use these 2 sets of value for further proceeding and can conclude on a point.

5.4.6 Observation 6

This observation is taken with the following parameters of the population size of 300 numbers , repository size of 300 numbers, iterations of 500 numbers, Inertia weight of 0.4, and confidence factor of 2.

```
% Parameters
params.Np = 300;           % Population size
params.Nr = 300;           % Repository size
params.maxgen = 500;       % Maximum number of generations
params.W = 0.4;            % Inertia weight
params.C1 = 2;             % Individual confidence factor
params.C2 = 2;             % Swarm confidence factor
params.ngrid = 20;         % Number of grids in each dimension
params.maxvel = 5;         % Maximum vel in percentage
params.u_mut = 0.5;        % Uniform mutation percentage
```

Figure:15-. Parameters of 6th observations

The graph is gained from the following parameters with the objective function MultiObj.fun

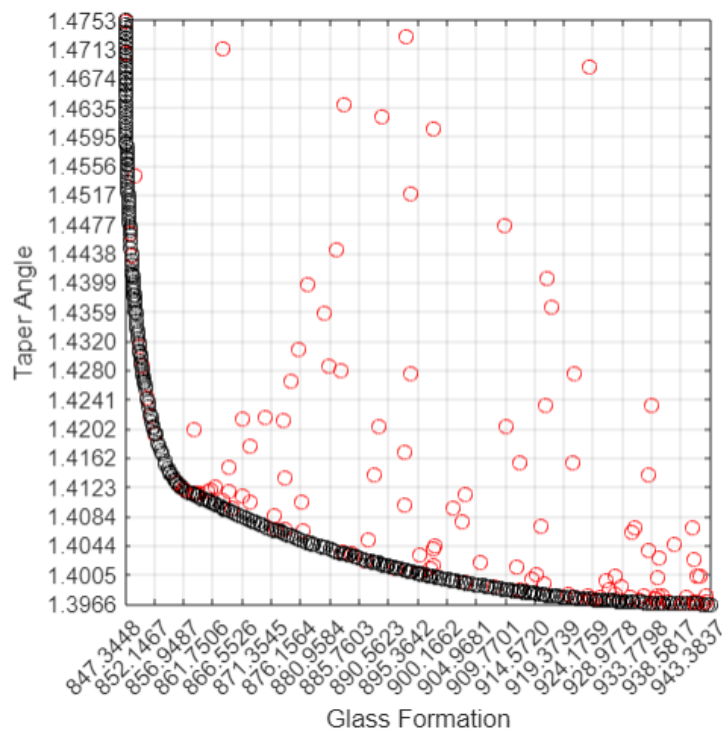


Figure:16-. Graph from 6th Observation with Taper Angle Vs Glass formation

The table is formed with respect to the other parameters are as follows

Table No:6-. 6th Observation with respect to input parameters and output

Laser power	Scanning speed	Gas pressure	Frequency	Glass formation width	Taper angle
$P(W)$	$V(mm/s)$	$g_p(bar)$	$f(Hz)$	(μm)	(deg)
370	3.8996	12.8	471.8105	940.3891	1.3966
370	3.9036	12.7997	470.7427	939.7669	1.3966
370	3.8865	12.8	471.1561	942.9197	1.3966
370	3.9125	12.8	471.89	937.9776	1.3966
370	3.915	12.7998	474.0497	937.3658	1.3966
370	3.9193	12.8	472.681	936.6479	1.3966
370	3.8838	12.8	471.7645	943.3837	1.3966
370	3.9102	12.8	470.2483	938.5282	1.3966
370	3.8905	12.8	471.8575	942.1096	1.3966
370	3.8956	12.8	471.5697	941.1615	1.3966
370	3.9286	12.8	473.0369	934.8979	1.3967
370	3.9364	12.7996	473.5328	933.4429	1.3967
370	3.925	12.7997	474.0156	935.5239	1.3967
370	3.9339	12.8	470.3939	934.1362	1.3967
370	3.9229	12.8	474.5931	935.8241	1.3967
370	3.9482	12.8	471.3413	931.4383	1.3968
370	3.9437	12.8	472.1704	932.1742	1.3968
370	3.9406	12.8	471.9318	932.779	1.3968
370	3.951	12.8	472.7048	930.8327	1.3968
370	3.961	12.8	473.411	928.922	1.3969
370	3.953	12.7999	473.4522	930.4231	1.3969
370	3.9582	12.8	473.1884	929.4536	1.3969
370	3.9627	12.8	473.6029	928.6244	1.3969
370	3.9561	12.8	472.44	929.9043	1.3969
370	3.9745	12.7999	470.6574	926.7116	1.397
370	3.9668	12.8	476.0786	927.6659	1.397
370	3.9691	12.7998	476.543	927.2813	1.397
370	3.9653	12.8	472.3248	928.2373	1.397
370	3.9764	12.8	472.0339	926.2437	1.3971
370	3.9786	12.7998	472.5257	925.822	1.3971
370	3.9798	12.8	476.5162	925.278	1.3971
370	3.9837	12.8	473.1721	924.8444	1.3971
370	3.9903	12.8	475.9176	923.4498	1.3972
370	3.9868	12.8	470.8003	924.4887	1.3972
370	3.9989	12.8	474.0782	922.0592	1.3973
370	3.9963	12.8	474.8549	922.4528	1.3973
370	3.9941	12.8	475.0156	922.841	1.3973
370	4.0039	12.8	474.9302	921.0941	1.3974
370	4.0016	12.8	473.414	921.6265	1.3974
370	4.0081	12.8	473.5825	920.4741	1.3975
370	4.0124	12.8	474.7909	919.6013	1.3975
370	4.0145	12.8	476.1338	919.1306	1.3976
370	4.0192	12.8	475.1933	918.3942	1.3976

370	4.0182	12.8	480.3798	918.1307	1.3977
370	4.0225	12.8	478.3554	917.5368	1.3977
370	4.0255	12.7991	477.2159	917.1811	1.3978
370	4.0328	12.8	474.897	916.0146	1.3978
370	4.03	12.8	474.7012	916.5327	1.3978
370	4.0384	12.7997	474.637	915.1149	1.3979
370	4.0369	12.8	469.8674	915.7494	1.3979
370	4.0422	12.7998	474.8351	914.4225	1.398
370	4.0409	12.7996	475.1504	914.6662	1.398
370	4.0447	12.7994	477.5009	913.7879	1.3981
370	4.0488	12.8	471.7186	913.5231	1.3981
370	4.054	12.8	476.6541	912.1929	1.3982
370	4.0487	12.8	480.3268	912.7995	1.3982
370	4.0511	12.8	474.327	912.9173	1.3982
370	4.0553	12.8	478.2861	911.866	1.3983
370	4.0597	12.7997	477.9338	911.1653	1.3984
370	4.0641	12.7996	475.3767	910.6555	1.3984
370	4.0658	12.8	479.635	909.9295	1.3985
370	4.0648	12.8	478.4249	910.203	1.3985
370	4.0727	12.8	478.8102	908.7988	1.3986
370	4.0733	12.8	471.0404	909.3993	1.3986
370	4.0786	12.8	473.5834	908.2594	1.3987
370	4.0817	12.8	477.9974	907.3632	1.3988
370	4.0859	12.8	476.3423	906.7935	1.3989
370	4.0904	12.7998	475.838	906.1542	1.399
370	4.0842	12.8	482.2248	906.5878	1.399
370	4.0915	12.8	479.8734	905.5342	1.3991
370	4.0938	12.7995	476.8157	905.4493	1.3991
370	4.0969	12.8	477.6704	904.8828	1.3992
370	4.1038	12.7999	472.1087	904.1937	1.3993
370	4.1058	12.7999	476.9698	903.415	1.3994
370	4.1092	12.7999	476.2948	902.9029	1.3995
370	4.1093	12.8	481.3351	902.4424	1.3996
370	4.1197	12.8	469.8736	901.7652	1.3997
370	4.1165	12.8	481.7412	901.1835	1.3997
370	4.1209	12.8	477.4062	900.8348	1.3998
370	4.1255	12.7998	474.9819	900.3227	1.3999
370	4.1294	12.8	475.8281	899.5737	1.4
370	4.1343	12.7991	473.9052	899.0461	1.4001
370	4.1324	12.8	482.1803	898.5477	1.4002
370	4.1378	12.7998	480.3907	897.8557	1.4003
370	4.1424	12.7991	475.3847	897.5707	1.4004
370	4.1409	12.7998	481.7166	897.1861	1.4004
370	4.145	12.7997	478.9343	896.7792	1.4005
370	4.1499	12.7995	478.167	896.0638	1.4006
370	4.152	12.7996	478.5033	895.6828	1.4007
370	4.1537	12.7998	479.5397	895.3227	1.4007
370	4.1594	12.8	477.9084	894.5095	1.4009
370	4.1564	12.8	485.9532	894.2596	1.401
370	4.165	12.7998	474.6663	893.9186	1.401
370	4.1661	12.7987	477.6301	893.579	1.4011

370	4.1669	12.8	480.5598	893.1068	1.4012
370	4.1748	12.7999	474.0953	892.4057	1.4013
370	4.1734	12.7988	482.3773	891.9381	1.4014
370	4.1799	12.8	475.4462	891.473	1.4015
370	4.1832	12.8	475.7341	890.8986	1.4016
370	4.1859	12.7998	475.9479	890.4777	1.4017
370	4.1871	12.7997	481.0127	889.809	1.4018
370	4.1852	12.8	480.5174	890.13	1.4018
370	4.1898	12.7998	482.9615	889.2132	1.402
370	4.1962	12.7998	480.9491	888.3647	1.4021
370	4.1977	12.7996	471.9863	889.0208	1.4021
370	4.1994	12.8	480.9365	887.8909	1.4023
370	4.2002	12.799	482.8741	887.6895	1.4024
370	4.2068	12.8	476.5517	887.0945	1.4024
370	4.2082	12.7999	479.4343	886.6267	1.4025
370	4.2131	12.8	480.4259	885.7541	1.4027
370	4.2203	12.7996	475.576	885.1442	1.4029
370	4.223	12.7998	473.3908	884.9209	1.403
370	4.2231	12.8	480.1812	884.2163	1.4031
370	4.2271	12.8	474.8456	884.1221	1.4032
370	4.2281	12.7997	480.1819	883.4666	1.4033
370	4.2295	12.8	479.4411	883.3398	1.4033
370	4.2335	12.7999	478.3721	882.7912	1.4035
370	4.2342	12.8	485.7697	881.987	1.4037
370	4.2413	12.8	479.8061	881.4439	1.4038
370	4.2469	12.7991	476.8873	880.9902	1.404
370	4.2492	12.8	479.9914	880.2212	1.4041
370	4.253	12.7999	479.6132	879.6967	1.4043
370	4.2594	12.7991	474.3502	879.3466	1.4045
370	4.2609	12.8	480.4369	878.4059	1.4046
370	4.2604	12.8	483.6983	878.1503	1.4047
370	4.2645	12.8	485.001	877.4084	1.4049
370	4.2677	12.7986	476.8226	877.8776	1.4049
370	4.2703	12.8	481.0862	876.9205	1.405
370	4.2737	12.7999	484.4305	876.0939	1.4053
370	4.2782	12.8	482.4118	875.6111	1.4054
370	4.2779	12.7997	484.5266	875.468	1.4055
370	4.2812	12.8	484.5227	874.9505	1.4056
370	4.2846	12.7999	484.696	874.4488	1.4058
370	4.2891	12.8	482.5093	873.9905	1.4059
370	4.2929	12.7996	481.9907	873.5265	1.4061
370	4.2902	12.7998	490.2764	873.0569	1.4062
370	4.3025	12.8	479.6718	872.287	1.4064
370	4.2911	12.8	491.9754	872.7422	1.4064
370	4.3018	12.8	485.0886	871.8433	1.4066
370	4.3055	12.8	484.768	871.3364	1.4067
370	4.3095	12.8	486.0303	870.6171	1.4069
370	4.3154	12.7996	485.651	869.8196	1.4072
370.	4.3165	12.7999	485.6645	869.6291	1.4073
370	4.3238	12.8	481.7088	868.9891	1.4075
370	4.326	12.8	481.5397	868.6708	1.4076

370	4.3299	12.7998	480.195	868.2655	1.4078
370	4.3286	12.8	486.1631	867.8243	1.4079
370	4.3329	12.7996	484.9368	867.3591	1.4081
370	4.3381	12.8	481.8385	866.9021	1.4082
370	4.344	12.8	481.8485	866.0578	1.4085
370	4.344	12.8	485.1808	865.7196	1.4086
370	4.344	12.7998	492.0334	865.0551	1.4089
370	4.344	12.8	495.5079	864.6891	1.4091
370	4.3558	12.7998	484.828	864.1001	1.4092
370	4.358	12.8	486.7084	863.5684	1.4094
370	4.3637	12.7998	481.7604	863.3268	1.4095
370	4.3581	12.7991	492.3976	863.0786	1.4097
370	4.3645	12.7999	488.6681	862.4586	1.4098
370	4.3741	12.8	478.2291	862.212	1.41
370	4.3736	12.8	481.7763	861.8888	1.4101
370	4.3745	12.7997	485.3173	861.4286	1.4102
370	4.3772	12.7999	487.1234	860.8432	1.4104
370	4.3799	12.7992	481.0584	861.1705	1.4104
370	4.3791	12.7997	489.0758	860.3744	1.4106
370	4.3831	12.8	487.5523	859.9542	1.4108
370	4.3892	12.7999	485.6803	859.3077	1.4111
370	4.3889	12.7998	488.8897	859.0332	1.4112
370	4.395	12.8	485.3434	858.5457	1.4114
370	4.4	12.8	480.7084	858.3645	1.4115
370	4.4	12.7999	484.4422	857.9638	1.4116
370	4.4	12.8	489.4345	857.4982	1.4118
370	4.4	12.7995	498.9814	856.4943	1.4124
370	4.4	12.7996	500.8872	856.3062	1.4125
370	4.4	12.7996	503.5943	856.0235	1.4128
370	4.4	12.8	507.3275	855.635	1.4131
370	4.4	12.8	510.6924	855.3208	1.4135
370	4.4	12.7994	513.7832	855.0778	1.4138
370	4.4	12.7998	517.0875	854.7724	1.4142
370	4.4	12.8	518.5498	854.592	1.4144
370	4.4	12.7993	521.1757	854.4873	1.4148
370	4.4	12.8	525.8163	853.9607	1.4155
370	4.4	12.7991	527.6913	853.8826	1.4158
370	4.4	12.7993	533.7842	853.3681	1.4168
370	4.4	12.8	535.8016	853.1519	1.4171
370	4.4	12.7998	539.8359	852.8312	1.4179
370	4.4	12.8	542.0395	852.6464	1.4184
370	4.4	12.7995	546.9171	852.3239	1.4194
370	4.4	12.8	548.0151	852.1999	1.4196
370	4.4	12.7999	550.967	851.9975	1.4203
370	4.4	12.8	552.2303	851.8967	1.4206
370	4.4	12.7998	554.2593	851.7681	1.4211
370	4.4	12.8	557.2718	851.5611	1.4218
370	4.4	12.7999	558.9098	851.4486	1.4222
370	4.4	12.7997	562.9059	851.2456	1.4232
370	4.4	12.7998	564.5495	851.0844	1.4237
370	4.4	12.8	566.2634	850.9579	1.4241

370	4.4	12.7998	571.0362	850.6793	1.4255
370	4.4	12.7995	572.857	850.5971	1.426
370	4.4	12.8	573.9785	850.4879	1.4263
370	4.4	12.8	574.5951	850.4517	1.4265
370	4.4	12.7999	575.9009	850.3879	1.4269
370	4.4	12.8	577.6532	850.3162	1.4275
370	4.4	12.8	579.1283	850.1967	1.4279
370	4.4	12.8	580.2727	850.1287	1.4283
370	4.4	12.8	581.8661	850.0412	1.4288
370	4.4	12.7999	583.4733	849.9597	1.4293
370	4.4	12.8	585.1191	849.867	1.4299
370	4.4	12.7998	585.7393	849.8509	1.4301
370	4.4	12.8	586.7	849.7844	1.4304
370	4.4	12.8	587.8132	849.727	1.4308
370	4.4	12.8	590.587	849.5872	1.4317
370	4.4	12.8	592.1554	849.5099	1.4323
370	4.4	12.8	593.7795	849.4314	1.4328
370	4.4	12.7998	595.1196	849.3877	1.4333
370	4.4	12.8	596.433	849.3138	1.4338
370	4.4	12.8	597.5949	849.2526	1.4342
370	4.4	12.8	599.1865	849.1804	1.4348
370	4.4	12.7998	601.5063	849.1002	1.4357
370	4.4	12.8	602.419	849.0469	1.436
370	4.4	12.8	603.4725	848.9929	1.4364
370	4.4	12.8	604.8751	848.9337	1.437
370	4.4	12.7999	606.1505	848.8909	1.4375
370	4.4	12.8	606.3294	848.8735	1.4375
370	4.4	12.7997	607.8049	848.8606	1.4381
370	4.4	12.7999	607.9691	848.8167	1.4382
370	4.4	12.8	609.4835	848.7469	1.4388
370	4.4	12.8	610.3575	848.7128	1.4392
370	4.4	12.8	611.3269	848.6754	1.4396
370	4.4	12.7998	612.4723	848.6528	1.44
370	4.4	12.7999	613.8402	848.5962	1.4406
370	4.4	12.8	614.2931	848.5643	1.4408
370	4.4	12.7998	615.1696	848.5512	1.4412
370	4.4	12.8	615.8732	848.5072	1.4415
370	4.4	12.8	617.8565	848.4373	1.4423
370	4.4	12.8	619.4642	848.3823	1.443
370	4.4	12.8	621.012	848.3307	1.4437
370	4.4	12.8	623.0134	848.2659	1.4445
370	4.4	12.8	625.3659	848.195	1.4456
370	4.4	12.8	625.4245	848.1907	1.4456
370	4.4	12.8	627.1083	848.1401	1.4464
370	4.4	12.8	628.3414	848.1041	1.447
370	4.4	12.8	629.3176	848.084	1.4474
370	4.4	12.8	630.7649	848.0356	1.4481
370	4.4	12.8	631.811	848.0071	1.4486
370	4.4	12.7998	632.9355	847.9982	1.4491
370	4.4	12.7999	633.6813	847.9641	1.4495
370	4.4	12.8	634.7171	847.931	1.45

370	4.4	12.7999	636.2815	847.9055	1.4507
370	4.4	12.8	637.1662	847.8704	1.4511
370	4.4	12.8	638.265	847.8593	1.4517
370	4.4	12.8	639.1474	847.8239	1.4521
370	4.4	12.8	639.7381	847.8132	1.4524
370	4.4	12.8	640.7009	847.7889	1.4529
370	4.4	12.8	642.0994	847.7585	1.4536
370	4.4	12.8	643.3187	847.7329	1.4542
370	4.4	12.8	644.3385	847.7121	1.4547
370	4.4	12.8	645.2259	847.6945	1.4552
370	4.4	12.8	646.3611	847.6726	1.4557
370	4.4	12.8	646.7	847.6662	1.4559
370	4.4	12.8	647.8621	847.6447	1.4565
370	4.4	12.8	648.308	847.642	1.4567
370	4.4	12.8	649.0904	847.6228	1.4571
370	4.4	12.8	649.9239	847.6084	1.4576
370	4.4	12.8	650.9329	847.5915	1.4581
370	4.4	12.8	651.9579	847.5749	1.4587
370	4.4	12.8	652.378	847.5683	1.4589
370	4.4	12.8	653.5505	847.5503	1.4595
370	4.4	12.8	654.4403	847.5371	1.46
370	4.4	12.8	655.0638	847.5282	1.4603
370	4.4	12.8	656.0768	847.5141	1.4609
370	4.4	12.8	656.988	847.5019	1.4614
370	4.4	12.8	658.5781	847.4816	1.4622
370	4.4	12.8	658.766	847.4793	1.4623
370	4.4	12.8	659.6889	847.4684	1.4628
370	4.4	12.8	660.3081	847.4612	1.4632
370	4.4	12.8	661.3085	847.4502	1.4637
370	4.4	12.8	662.3796	847.439	1.4643
370	4.4	12.8	663.7013	847.426	1.4651
370	4.4	12.8	663.9115	847.424	1.4652
370	4.4	12.8	664.979	847.4144	1.4658
370	4.4	12.8	666.2896	847.4034	1.4666
370	4.4	12.8	666.4768	847.4019	1.4667
370	4.4	12.8	667.5662	847.3936	1.4673
370	4.4	12.8	668.1033	847.3897	1.4676
370	4.4	12.8	669.1373	847.3843	1.4682
370	4.4	12.8	670.1093	847.3767	1.4688
370	4.4	12.8	670.922	847.3721	1.4693
370	4.4	12.8	671.7701	847.3676	1.4698
370	4.4	12.8	672.4017	847.3646	1.4701
370	4.4	12.8	673.1606	847.3612	1.4706
370	4.4	12.8	674.0329	847.3577	1.4711
370	4.4	12.8	674.7402	847.3552	1.4715
370	4.4	12.8	675.7557	847.352	1.4721
370	4.4	12.8	675.9013	847.3516	1.4722
370	4.4	12.8	676.9181	847.3491	1.4728
370	4.4	12.8	677.9022	847.3472	1.4734
370	4.4	12.8	678.3487	847.3465	1.4737
370	4.4	12.8	679.3425	847.3454	1.4743

As it is observed from Fig 15 that the process parameters taken are shown as the population size / Swarm Size is taken as 300, Repository Size is taken as 300, Iteration Size is taken as 500, Inertia Weight is taken as 0.4, The confidence factor for Swarm and Individual is taken as 2, Number of Grids in each dimension is taken as 20, Maximum velocity is assumed as 5 and Uniform Mutation percentage is assumed as 0.5. By using these parameters we approach to use the Multi-Objective particle Swarm Optimization Technique.

In Fig 16 ,We can observed that the black circle on the graph represent the value of Taper angle , and the red circle represents the best values of Glass Formation Width after 300 iteration this is the best fitness graph observed using the above parameters. The maximum value of taper angle can be seen as 1.4753 degree with minimum Glass formation Width as 847.3448 μm , whereas the minimum value of taper angle (1.3966 degree) is observed with maximum value of 943.3837 μm of Glass formation Width.

If we check with the Table 6, if we take one observation taking a best result as 1st observation with glass formation width of (851.9975 μm) the taper angle is seen to be approx. 1.4203 degree which is quite nearer to the minimum value observed having a set of parameters of 370 watt of Laser Power, 4.4 mm/s of Scanning speed, 12.7999 bar of Gas pressure, 550.967 Hz of Frequency.

Another observation can be seen when the glass formation is observed as 851.8967 μm and taper angle of 1.4206 degree also can give a comparably good result with the parameter of 370 watt of Laser Power, 4.4 mm/s of Scanning speed, 12.8 bar of Gas pressures, 552.2303 Hz of Frequency.

So, from this 6th Table, we can use these 2 sets of value for further proceeding and can conclude on a point.

5.4.7 Observation 7

This observation is taken with the following parameters of the population size of 300 numbers, repository size of 300 numbers, iterations of 500 numbers, Inertia weight of 0.8, and confidence factor of 1.

```
% Parameters
params.Np = 300;           % Population size
params.Nr = 300;           % Repository size
params.maxgen = 500;       % Maximum number of generations
params.W = 0.8;            % Inertia weight
params.C1 = 1;             % Individual confidence factor
params.C2 = 1;             % Swarm confidence factor
params.ngrid = 20;        % Number of grids in each dimension
params.maxvel = 5;         % Maximum vel in percentage
params.u_mut = 0.5;        % Uniform mutation percentage
```

Figure:17-. Parameters of 7th observations

The graph is gained from the following parameters with the objective function MultiObj.fun

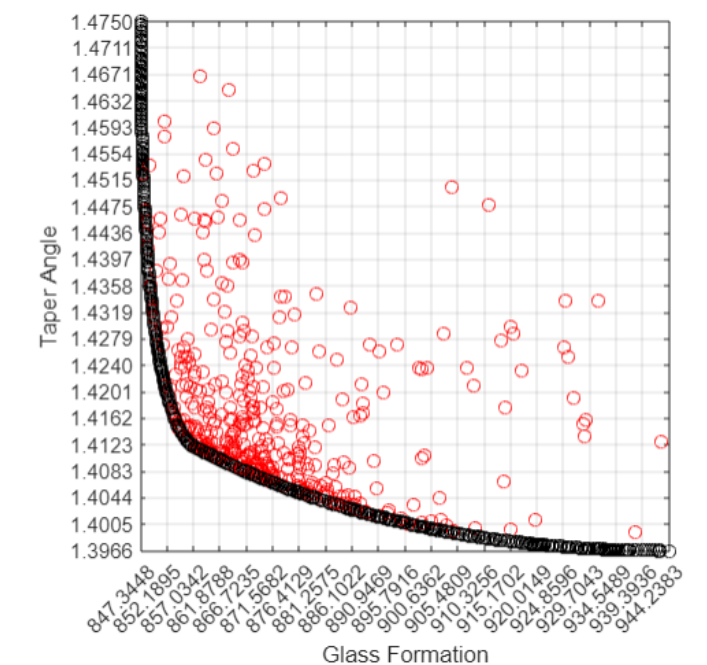


Figure:18-. Graph from 7th Observation with Taper Angle Vs Glass formation

The table is formed with respect to the other parameters are as follows

Table No:7-. 7th Observation with respect to input parameters and output

Laser power	Scanning speed	Gas pressure	Frequency	Glass formation width	Taper angle
$P(W)$	$V(mm/s)$	$g_p(bar)$	$f(Hz)$	(μm)	(deg)
370	4.4	12.8	680.44	847.34	1.475
370	4.4	12.8	678.79	847.35	1.474
370	4.4	12.8	677.79	847.35	1.4734
370	4.4	12.8	676.73	847.35	1.4727
370	4.4	12.8	675.94	847.35	1.4722
370	4.4	12.8	675.54	847.35	1.472
370	4.4	12.8	674.39	847.36	1.4713
370	4.4	12.8	673.98	847.36	1.4711
370	4.4	12.8	673.1	847.36	1.4705
370	4.4	12.8	672.27	847.37	1.47
370	4.4	12.8	671.29	847.37	1.4695
370	4.4	12.8	670.41	847.38	1.469
370	4.4	12.8	669.4	847.38	1.4684
370	4.4	12.8	669.12	847.38	1.4682
370	4.4	12.8	668.12	847.39	1.4676
370	4.4	12.8	667.67	847.4	1.4674
370	4.4	12.8	666.85	847.4	1.4669
370	4.4	12.8	665.58	847.41	1.4662
370	4.4	12.8	664.6	847.42	1.4656
370	4.4	12.8	663.44	847.43	1.4649
370	4.4	12.8	662.44	847.44	1.4644
370	4.4	12.8	662.1	847.44	1.4642
370	4.4	12.8	660.8	847.46	1.4635
370	4.4	12.8	660	847.46	1.463
370	4.4	12.8	659.23	847.48	1.4626
370	4.4	12.8	658.14	847.49	1.462
370	4.4	12.8	657.9	847.49	1.4619
370	4.4	12.8	656.52	847.51	1.4611
370	4.4	12.8	655.82	847.52	1.4607
370	4.4	12.8	655.21	847.53	1.4604
370	4.4	12.8	654.09	847.56	1.4598
370	4.4	12.8	653.1	847.56	1.4593
370	4.4	12.8	652.71	847.57	1.4591

370	4.4	12.8	650.01	847.61	1.4576
370	4.4	12.8	649.29	847.62	1.4572
370	4.4	12.8	648.27	847.64	1.4567
370	4.4	12.8	647.28	847.66	1.4562
370	4.4	12.8	645.62	847.69	1.4554
370	4.4	12.8	644.27	847.71	1.4547
370	4.4	12.8	643.68	847.73	1.4544
370	4.4	12.8	642.99	847.74	1.454
370	4.4	12.8	642.05	847.77	1.4535
370	4.4	12.8	641.5	847.78	1.4533
370	4.4	12.8	640.6	847.79	1.4528
370	4.4	12.8	639.49	847.82	1.4523
370	4.4	12.8	638.64	847.84	1.4519
370	4.4	12.8	637.57	847.87	1.4513
370	4.4	12.8	635.75	847.91	1.4504
370	4.4	12.8	634.15	847.95	1.4497
370	4.4	12.8	633.14	847.97	1.4492
370	4.4	12.8	631.97	848	1.4486
370	4.4	12.8	631.01	848.03	1.4482
370	4.4	12.8	630	848.06	1.4477
370	4.4	12.8	628.89	848.09	1.4472
370	4.4	12.8	627.96	848.12	1.4468
370	4.4	12.8	626.28	848.17	1.446
370	4.4	12.8	624.41	848.22	1.4452
370	4.4	12.8	623.42	848.25	1.4447
370	4.4	12.8	622.19	848.3	1.4442
370	4.4	12.8	620.96	848.34	1.4436
370	4.4	12.8	619.66	848.38	1.4431
370	4.4	12.8	618.51	848.41	1.4426
370	4.4	12.8	617.54	848.45	1.4422
370	4.4	12.8	615.92	848.54	1.4415
370	4.4	12.8	615.67	848.55	1.4414
370	4.4	12.8	614.35	848.56	1.4408
370	4.4	12.8	613.51	848.59	1.4405
370	4.4	12.8	612.3	848.65	1.44
370	4.4	12.8	611.25	848.68	1.4395
370	4.4	12.8	608.94	848.77	1.4386
370	4.4	12.8	608.16	848.8	1.4383
370	4.4	12.8	606.74	848.89	1.4377
370	4.4	12.8	606.74	848.86	1.4377
370	4.4	12.8	605.27	848.92	1.4371
370	4.4	12.8	603.59	848.99	1.4365
370	4.4	12.8	602.16	849.07	1.4359
370	4.4	12.8	600.84	849.11	1.4354
370	4.4	12.8	599.1	849.23	1.4348

370	4.4	12.8	599.15	849.2	1.4348
370	4.4	12.8	597.3	849.28	1.4341
370	4.4	12.8	595.37	849.37	1.4334
370	4.4	12.8	594.03	849.42	1.4329
370	4.4	12.8	592.72	849.48	1.4325
370	4.4	12.8	591.22	849.56	1.4319
370	4.4	12.8	589.95	849.62	1.4315
370	4.4	12.8	588.42	849.7	1.431
370	4.4	12.8	587.27	849.8	1.4306
370	4.4	12.8	585.6	849.84	1.43
370	4.4	12.8	584.17	849.93	1.4295
370	4.4	12.8	582.6	850.03	1.429
370	4.4	12.8	581	850.1	1.4285
370	4.4	12.8	579.38	850.18	1.428
370	4.4	12.8	577.87	850.3	1.4275
370	4.4	12.8	575.44	850.44	1.4268
370	4.4	12.8	574.74	850.46	1.4266
370	4.4	12.8	573.3	850.53	1.4261
370	4.4	12.8	571.98	850.61	1.4258
370	4.4	12.8	570.23	850.71	1.4253
370	4.4	12.8	568.34	850.83	1.4247
370	4.4	12.8	566.44	850.96	1.4242
370	4.4	12.8	565.89	851.05	1.424
370	4.4	12.8	564.38	851.08	1.4236
370	4.4	12.8	562.91	851.2	1.4232
370	4.4	12.8	559.77	851.38	1.4224
370	4.4	12.799	558.42	851.56	1.4221
370	4.4	12.8	556.43	851.6	1.4216
370	4.4	12.8	554.61	851.73	1.4211
370	4.4	12.8	553.48	851.84	1.4209
370	4.4	12.8	551.49	851.96	1.4204
370	4.4	12.8	549.42	852.1	1.4199
370	4.4	12.8	547.54	852.23	1.4195
370	4.4	12.8	546.78	852.35	1.4194
370	4.4	12.8	544.92	852.44	1.419
370	4.4	12.8	544.36	852.5	1.4188
370	4.4	12.8	541.76	852.72	1.4183
370	4.4	12.8	538.79	852.9	1.4177
370	4.4	12.8	537.75	853.03	1.4175
370	4.4	12.8	535.18	853.18	1.417
370	4.4	12.8	532.95	853.44	1.4166
370	4.4	12.8	530.67	853.55	1.4162
370	4.4	12.8	528.38	853.74	1.4159
370	4.4	12.8	524.11	854.1	1.4152
370	4.4	12.8	522.75	854.26	1.415

370	4.4	12.8	520.88	854.39	1.4147
370	4.4	12.8	517.11	854.75	1.4142
370	4.4	12.8	514.22	854.98	1.4139
370	4.4	12.8	511.68	855.25	1.4136
370	4.4	12.8	507.16	855.64	1.4131
370	4.4	12.8	505.99	855.77	1.413
370	4.4	12.799	503.77	856.04	1.4128
370	4.4	12.799	500.12	856.42	1.4125
370	4.4	12.8	496.72	856.67	1.4122
370	4.4	12.8	490.75	857.35	1.4119
370	4.4	12.8	485.86	857.81	1.4117
370	4.4	12.8	484.87	857.96	1.4116
370	4.3932	12.8	489.02	858.44	1.4114
370	4.3926	12.799	485.54	858.92	1.4113
370	4.3941	12.8	480.07	859.24	1.4112
370	4.3826	12.8	493.22	859.5	1.411
370	4.3799	12.8	493.15	859.86	1.4109
370	4.388	12.8	478.68	860.27	1.4108
370	4.3775	12.8	491.43	860.35	1.4107
370	4.3746	12.8	490.37	860.88	1.4104
370	4.3758	12.8	484.22	861.37	1.4103
370	4.3741	12.8	484	861.64	1.4102
370	4.3629	12.8	493.35	862.23	1.41
370	4.3654	12.8	486.93	862.55	1.4098
370	4.3598	12.8	490.66	863	1.4097
370	4.3616	12.797	483.81	863.64	1.4096
370	4.3588	12.8	481.78	864.01	1.4093
370	4.3475	12.799	491.21	864.69	1.4091
370	4.3462	12.8	488	865.11	1.4088
370	4.3437	12.8	486.82	865.64	1.4087
370	4.3429	12.799	483.32	866.19	1.4085
370	4.3398	12.799	482.87	866.64	1.4084
370	4.3313	12.799	489.33	867.2	1.4082
370	4.334	12.8	481.06	867.7	1.408
370	4.3285	12.8	484.24	868.12	1.4078
370	4.3183	12.8	493.36	868.64	1.4077
370	4.3201	12.8	486.55	869.01	1.4075
370	4.322	12.799	481.6	869.31	1.4074
370	4.3206	12.8	478.22	869.86	1.4073
370	4.3169	12.799	478.68	870.35	1.4071
370	4.3145	12.8	481.33	870.37	1.407
370	4.3101	12.797	481.9	871.23	1.4069
370	4.302	12.8	487.99	871.58	1.4067
370	4.3019	12.799	483.63	872.1	1.4065
370	4.2963	12.8	486.24	872.58	1.4063

370	4.2944	12.8	484.56	873.03	1.4062
370	4.2914	12.8	483.3	873.61	1.406
370	4.289	12.8	482.02	874.09	1.4059
370	4.2868	12.8	482.36	874.33	1.4058
370	4.2836	12.8	483.28	874.72	1.4057
370	4.278	12.799	486.49	875.36	1.4056
370	4.2768	12.799	489.03	875.25	1.4056
370	4.2812	12.8	474.69	875.97	1.4054
370	4.2728	12.8	486.35	876.05	1.4053
370	4.2717	12.799	484.29	876.47	1.4052
370	4.265	12.8	488.29	877.05	1.405
370	4.2638	12.8	481.67	877.9	1.4048
370	4.2598	12.799	483.28	878.38	1.4047
370	4.2513	12.8	489.93	878.98	1.4046
370	4.2563	12.799	480.45	879.15	1.4044
370	4.254	12.8	478.25	879.69	1.4043
370	4.2498	12.8	480.14	880.18	1.4042
370	4.2436	12.8	485.35	880.58	1.404
370	4.2447	12.8	478.69	881.08	1.4039
370	4.241	12.8	477.69	881.72	1.4038
370	4.238	12.8	481.02	881.87	1.4037
370	4.2363	12.8	474.54	882.8	1.4036
370	4.2264	12.799	482.02	883.67	1.4033
370	4.2154	12.799	491.35	884.43	1.4032
370	4.2201	12.8	476.98	885.05	1.403
370	4.2146	12.8	482.82	885.34	1.4029
370	4.2121	12.8	481.57	885.82	1.4027
370	4.204	12.8	488.71	886.39	1.4027
370	4.2077	12.8	481.7	886.52	1.4026
370	4.2053	12.799	479.59	887.15	1.4025
370	4.2052	12.8	474.83	887.52	1.4024
370	4.2018	12.8	477.29	887.81	1.4023
370	4.191	12.8	485.96	888.72	1.4021
370	4.1946	12.8	476	889.07	1.402
370	4.186	12.8	483.89	889.68	1.4019
370	4.1923	12.8	476.81	889.41	1.4019
370	4.1862	12.8	478.9	890.13	1.4018
370	4.1828	12.8	479.49	890.64	1.4017
370	4.1808	12.8	479.23	890.96	1.4016
370	4.1761	12.799	482.53	891.54	1.4015
370	4.1727	12.799	479.51	892.34	1.4013
370	4.1743	12.8	477.11	892.24	1.4013
370	4.166	12.8	481.65	893.12	1.4012
370	4.1632	12.8	480.51	893.67	1.401
370	4.1636	12.8	473.85	894.21	1.401

370	4.1588	12.8	475.07	894.96	1.4009
370	4.1541	12.8	478.71	895.37	1.4007
370	4.1504	12.799	481.22	895.75	1.4007
370	4.1456	12.8	484.56	896.16	1.4006
370	4.1484	12.8	472.44	896.83	1.4005
370	4.1436	12.799	476.64	897.31	1.4004
370	4.1402	12.799	477.24	897.82	1.4003
370	4.1323	12.8	481.43	898.6	1.4002
370	4.1331	12.8	473.32	899.27	1.4001
370	4.1315	12.8	473.73	899.44	1.4
370	4.1258	12.8	477.68	900.04	1.3999
370	4.1232	12.8	475.25	900.69	1.3998
370	4.1184	12.799	480.26	901.11	1.3998
370	4.1165	12.8	478	901.55	1.3997
370	4.1124	12.798	481.17	902.06	1.3997
370	4.1096	12.8	478.03	902.72	1.3995
370	4.1089	12.8	473.45	903.18	1.3994
370	4.103	12.8	478.39	903.79	1.3993
370	4.1	12.8	476.89	904.37	1.3992
370	4.0952	12.8	479.64	904.95	1.3992
370	4.0965	12.8	472.86	905.35	1.3991
370	4.0914	12.8	476.76	905.85	1.399
370	4.0866	12.799	479.91	906.41	1.399
370	4.0834	12.8	479.75	906.97	1.3989
370	4.0808	12.8	474.54	907.85	1.3988
370	4.0832	12.8	474.95	907.4	1.3988
370	4.0746	12.8	479.26	908.46	1.3987
370	4.0691	12.8	482.74	909.15	1.3987
370	4.0702	12.8	477.37	909.36	1.3986
370	4.067	12.8	474.63	910.18	1.3985
370	4.0647	12.8	479.16	910.14	1.3985
370	4.0621	12.8	474.57	911.07	1.3984
370	4.0561	12.8	473	912.2	1.3983
370	4.0528	12.8	481.75	911.98	1.3983
370	4.0495	12.8	478.81	912.82	1.3982
370	4.0424	12.8	479.09	914	1.3981
370	4.0464	12.8	478.69	913.37	1.3981
370	4.0419	12.8	473.31	914.63	1.398
370	4.0376	12.8	474.97	915.19	1.3979
370	4.0247	12.8	478.92	917.14	1.3978
370	4.0324	12.8	474.65	916.11	1.3978
370	4.0305	12.8	475.11	916.42	1.3978
370	4.02	12.799	471.68	918.62	1.3977
370	4.0245	12.8	475.37	917.46	1.3977
370	4.0196	12.8	478.53	918.09	1.3977

370	4.0173	12.798	475.58	918.86	1.3976
370	4.0093	12.8	475.48	920.13	1.3975
370	4.0138	12.8	471.99	919.63	1.3975
370	3.9983	12.8	475.21	922.14	1.3974
370	4.0037	12.8	474.73	921.19	1.3974
370	4.0061	12.8	474.7	920.74	1.3974
370	4.0017	12.799	475.35	921.53	1.3974
370	3.9983	12.8	472.37	922.32	1.3973
370	3.9947	12.8	470.56	923.11	1.3973
370	3.9902	12.8	474.58	923.57	1.3972
370	3.9867	12.799	471.96	924.49	1.3972
370	3.9824	12.8	474.36	925.03	1.3971
370	3.9769	12.799	474.19	926.05	1.3971
370	3.9657	12.8	474.2	928	1.397
370	3.9704	12.8	473.33	927.25	1.397
370	3.9681	12.799	475.07	927.57	1.397
370	3.9745	12.8	472.41	926.58	1.397
370	3.9589	12.8	475.29	929.17	1.3969
370	3.9571	12.8	472.1	929.74	1.3969
370	3.9535	12.8	471.54	930.49	1.3969
370	3.9627	12.8	473.36	928.65	1.3969
370	3.9392	12.8	474	932.89	1.3968
370	3.9453	12.8	475.59	931.64	1.3968
370	3.9435	12.8	472.02	932.23	1.3968
370	3.9484	12.8	475.33	931.08	1.3968
370	3.9238	12.8	473.25	935.8	1.3967
370	3.9286	12.8	472.16	934.96	1.3967
370	3.9373	12.8	472.25	933.38	1.3967
370	3.9197	12.8	475.02	936.41	1.3967
370	3.9184	12.8	472.2	936.9	1.3967
370	3.9322	12.8	472.09	934.35	1.3967
370	3.9339	12.799	472.42	934.02	1.3967
370	3.9103	12.8	471.43	938.43	1.3966
370	3.8972	12.8	472.68	940.79	1.3966
370	3.8996	12.8	473.7	940.27	1.3966
370	3.8943	12.8	471.71	941.42	1.3966
370	3.9057	12.8	471.96	939.25	1.3966
370	3.9032	12.8	470.84	939.81	1.3966
370	3.914	12.8	471.87	937.7	1.3966
370	3.8885	12.8	472.53	942.46	1.3966
370	3.8921	12.8	472.39	941.77	1.3966
370	3.8798	12.8	470.43	944.24	1.3966

As it is observed from Fig 17 that the process parameters taken are shown as the population size / Swarm Size is taken as 300, Repository Size is taken as 300, Iteration Size is taken as 500, Inertia Weight is taken as 0.8, The confidence factor for Swarm and Individual is taken as 1, Number of Grids in each dimension is taken as 20, Maximum velocity is assumed as 5 and Uniform Mutation percentage is assumed as 0.5. By using these parameters we approach to use the Multi-Objective particle Swarm Optimization Technique.

In Fig 18 ,We can observed that the black circle on the graph represent the value of Taper angle , and the red circle represents the best values of Glass Formation Width after 300 iteration this is the best fitness graph observed using the above parameters. The maximum value of taper angle can be seen as 1.475 degree with minimum Glass formation Width as 847.345 μm , whereas the minimum value of taper angle (1.3966 degree) is observed with value of 938.426 μm of Glass formation Width.

If we check with the Table 7, if we take one observation taking a best result as 1st observation with glass formation width of (856.672 μm) the taper angle is seen to be approx. 1.4122 degree which is quite nearer to the minimum value observed having a set of parameters of 370 watt of Laser Power, 4.4 mm/s of Scanning speed, 12.8 bar of Gas pressure, 496.718 Hz of Frequency.

Another observation can be seen when the glass formation is observed as 857.348 μm and taper angle of 1.4119 degree also can give a comparably good result with the parameter of 370.005 watt of Laser Power, 4.4 mm/s of Scanning speed, 12.7997 bar of Gas pressures, 490.753 Hz of Frequency.

So, from this 7th Table, we can use these 2 sets of value for further proceeding and can conclude on a point.

5.4.8 Observation 8

This observation is taken with the following parameters of the population size of 300 numbers , repository size of 300 numbers, iterations of 500 numbers, Inertia weight of 0.4, and confidence factor of 1.

```
% Parameters
params.Np = 300;           % Population size
params.Nr = 300;           % Repository size
params.maxgen = 500;       % Maximum number of generations
params.W = 0.4;            % Inertia weight
params.C1 = 1;             % Individual confidence factor
params.C2 = 1;             % Swarm confidence factor
params.ngrid = 20;         % Number of grids in each dimension
params.maxvel = 5;         % Maximum vel in percentage
params.u_mut = 0.5;        % Uniform mutation percentage
```

Figure:19-. Parameters of 8th observations

The graph is gained from the following parameters with the objective function MultiObj.fun

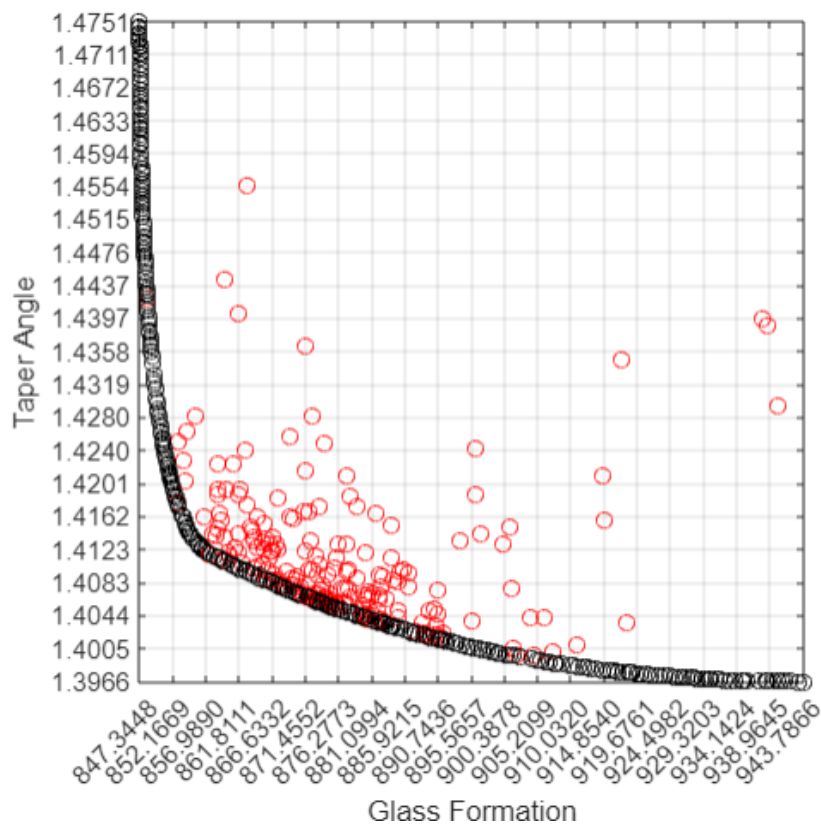


Figure:20-. Graph from 8th Observation with Taper Angle Vs Glass formation

The table is formed with respect to the other parameters are as follows

Table No:8-. 8th Observation with respect to input parameters and output

Laser power	Scanning speed	Gas pressure	Frequency	Glass formation width	Taper angle
$P(W)$	$V(mm/s)$	$g_p(bar)$	$f(Hz)$	(μm)	(deg)
370	3.9011	12.8	471.4754	940.1346	1.3966
370	3.8915	12.8	473.552	941.7854	1.3966
370	3.8959	12.8	472.2887	941.0664	1.3966
370	3.8982	12.8	471.6879	940.6645	1.3966
370	3.885	12.8	472.1768	943.124	1.3966
370	3.9081	12.8	472.7039	938.7368	1.3966
370	3.9046	12.8	471.4076	939.495	1.3966
370	3.9111	12.8	471.2855	938.2861	1.3966
370	3.8819	12.8	471.1949	943.7866	1.3966
370	3.9156	12.8	471.4595	937.4399	1.3966
370	3.8918	12.8	472.0974	941.8469	1.3966
370	3.9255	12.8	469.6098	935.7349	1.3967
370	3.9382	12.8	472.1118	933.1936	1.3967
370	3.9278	12.8	472.4357	935.0918	1.3967
370	3.9342	12.8	472.5014	933.9022	1.3967
370	3.9287	12.8	473.8141	934.8087	1.3967
370	3.9453	12.8	474.7654	931.69	1.3968
370	3.9498	12.8	472.528	931.0346	1.3968
370	3.9424	12.8	473.559	932.3175	1.3968
370	3.958	12.8	472.7433	929.5215	1.3969
370	3.9539	12.8	474.8573	930.0953	1.3969
370	3.9527	12.8	474.88	930.3122	1.3969
370	3.9707	12.8	476.3575	926.9233	1.397
370	3.9634	12.8	475.3969	928.324	1.397
370	3.9627	12.8	468.2625	929.0392	1.397
370	3.9682	12.8	471.3777	927.7824	1.397
370	3.9689	12.8	471.4026	927.6626	1.397
370	3.9813	12.8	473.6504	925.2382	1.3971
370	3.9786	12.8	472.6755	925.8139	1.3971
370	3.9745	12.8	475.0675	926.3426	1.3971
370	3.9823	12.8	473.1744	925.0974	1.3971
370	3.9842	12.8	477.5956	924.3944	1.3972
370	3.99	12.8	472.5991	923.7722	1.3972
370	3.9928	12.8	476.8378	922.9124	1.3973
370	3.9965	12.8	476.2004	922.3058	1.3973
370	4.0041	12.8	475.335	921.0377	1.3974
370	4.0001	12.8	475.0533	921.7669	1.3974

370	4.0105	12.8	472.1796	920.1735	1.3975
370	4.0131	12.8	473.8008	919.5686	1.3975
370	4.019	12.8	473.3322	918.5675	1.3976
370	4.0145	12.8	477.8662	918.9802	1.3976
370	4.0211	12.8	471.6477	918.3498	1.3976
370	4.0238	12.8	475.2122	917.5655	1.3977
370	4.0302	12.8	474.783	916.4877	1.3978
370	4.0277	12.8	474.0608	916.9831	1.3978
370	4.0347	12.8	478.3925	915.4007	1.3979
370	4.0338	12.8	474.0801	915.9156	1.3979
370	4.0402	12.8	474.5481	914.7622	1.398
370	4.0482	12.8	471.5354	913.6458	1.3981
370	4.0475	12.8	479.9783	913.0336	1.3982
370	4.0541	12.8	472.9821	912.4961	1.3982
370	4.0535	12.8	476.5662	912.2886	1.3982
370	4.0569	12.8	475.3028	911.8107	1.3983
370	4.0598	12.8	477.9611	911.0837	1.3984
370	4.0664	12.8	471.4359	910.5309	1.3985
370	4.0687	12.8	473.4677	909.9657	1.3985
370	4.0731	12.8	480.8978	908.5666	1.3987
370	4.0774	12.8	480.156	907.8883	1.3988
370	4.082	12.8	475.0104	907.5688	1.3988
370	4.0868	12.8	471.8953	907.0318	1.3989
370	4.0881	12.8	477.1568	906.3433	1.399
370	4.0903	12.8	480.9972	905.6302	1.3991
370	4.0981	12.8	479.5978	904.4454	1.3992
370	4.0914	12.8	484.251	905.173	1.3992
370	4.1092	12.8	477.5041	902.7764	1.3995
370	4.1171	12.8	474.4996	901.7389	1.3996
370	4.1186	12.8	478.0031	901.1628	1.3997
370	4.1211	12.8	478.8332	900.6729	1.3998
370	4.1296	12.8	476.6359	899.4662	1.4
370	4.1252	12.8	482.5876	899.6692	1.4
370	4.1305	12.8	480.7001	898.957	1.4001
370	4.1324	12.8	482.853	898.4538	1.4002
370	4.1372	12.8	478.6945	898.0339	1.4002
370	4.1417	12.8	481.0513	897.0925	1.4004
370	4.1447	12.8	481.4493	896.5558	1.4005
370	4.15	12.8	478.5154	895.9731	1.4006
370	4.1546	12.8	476.6551	895.3892	1.4007
370	4.1546	12.8	482.1709	894.8835	1.4008
370	4.1589	12.8	481.4111	894.2532	1.4009
370	4.1621	12.8	484.0303	893.5093	1.4011
370	4.1704	12.8	473.5172	893.1505	1.4012
370	4.1672	12.8	483.741	892.7077	1.4013

370	4.1726	12.8	483.3062	891.8805	1.4014
370	4.1743	12.8	483.1673	891.6226	1.4015
370	4.181	12.8	479.7092	890.8726	1.4016
370	4.1794	12.8	480.2176	891.0701	1.4016
370	4.1811	12.8	484.2485	890.4406	1.4017
370	4.1872	12.8	481.939	889.6759	1.4019
370	4.1905	12.8	481.4039	889.1957	1.402
370	4.1958	12.8	479.0512	888.5886	1.4021
370	4.1972	12.8	483.1325	887.973	1.4022
370	4.2005	12.8	482.5818	887.5143	1.4023
370	4.2059	12.8	478.9418	887.0119	1.4024
370	4.2084	12.8	477.0637	886.8063	1.4025
370	4.2132	12.8	478.7467	885.8878	1.4027
370	4.2147	12.8	484.0578	885.1488	1.4029
370	4.2214	12.8	479.2581	884.5661	1.403
370	4.2199	12.8	484.4104	884.2992	1.4031
370	4.2245	12.8	482.5965	883.7562	1.4032
370	4.2248	12.8	480.4373	883.9179	1.4032
370	4.225	12.8	486.8192	883.2769	1.4034
370	4.2365	12.8	473.5584	882.7992	1.4035
370	4.2247	12.8	489.7485	883.0559	1.4035
370	4.235	12.8	480.2425	882.3677	1.4036
370	4.2321	12.8	487.3097	882.1341	1.4037
370	4.2368	12.8	485.0857	881.6217	1.4038
370	4.2469	12.8	476.7549	880.899	1.404
370	4.2489	12.8	481.2186	880.1503	1.4041
370	4.2519	12.8	483.2169	879.4952	1.4043
370	4.2541	12.8	475.295	879.9533	1.4043
370	4.257	12.8	481.4946	878.8891	1.4045
370	4.2563	12.8	485.4654	878.6108	1.4046
370	4.2577	12.8	488.5548	878.0994	1.4047
370	4.2643	12.8	483.1709	877.6098	1.4048
370	4.2682	12.8	484.2074	876.9255	1.405
370	4.2709	12.8	484.694	876.4782	1.4051
370	4.2756	12.8	481.973	876.0387	1.4053
370	4.274	12.8	487.0937	875.7666	1.4054
370	4.282	12.8	479.7378	875.305	1.4055
370	4.2811	12.8	484.0413	875.0034	1.4056
370	4.2838	12.8	484.009	874.6148	1.4057
370	4.2866	12.8	483.8983	874.1984	1.4058
370	4.2866	12.8	486.8464	873.9083	1.4059
370	4.294	12.8	482.1622	873.2784	1.4061
370	4.2951	12.8	477.1292	873.6332	1.4061
370	4.2968	12.8	479.3455	873.1547	1.4062
370	4.2965	12.8	486.8824	872.4451	1.4064

370	4.3042	12.8	481.6211	871.8312	1.4066
370	4.3097	12.8	484.4343	870.7453	1.4069
370	4.3125	12.8	483.8344	870.3906	1.407
370	4.3148	12.8	481.7265	870.2777	1.4071
370	4.3093	12.8	492.6769	869.9866	1.4072
370	4.3152	12.8	487.6919	869.6142	1.4073
370	4.3219	12.8	485.7784	868.8327	1.4075
370	4.3256	12.8	484.2964	868.4397	1.4077
370	4.3234	12.8	490.2859	868.161	1.4078
370	4.3288	12.8	486.7315	867.7321	1.4079
370	4.3288	12.8	490.6568	867.335	1.4081
370	4.3365	12.8	484.6715	866.8405	1.4082
370	4.3418	12.8	480.4952	866.5141	1.4084
370	4.3362	12.8	493.7682	865.9652	1.4086
370	4.3453	12.8	485.7318	865.4631	1.4087
370	4.3471	12.8	489.8587	864.7895	1.409
370	4.3431	12.8	497.3958	864.6192	1.4092
370	4.3525	12.8	491.3093	863.8693	1.4093
370	4.3568	12.8	484.904	863.9223	1.4093
370	4.3562	12.8	490.7015	863.4162	1.4095
370	4.358	12.8	492.7604	862.947	1.4097
370	4.3688	12.8	480.3391	862.7176	1.4098
370	4.3689	12.8	486.1533	862.0857	1.41
370	4.3691	12.8	489.0381	861.7637	1.4101
370	4.3739	12.8	487.7613	861.2144	1.4103
370	4.3771	12.8	486.2512	860.9323	1.4104
370	4.3802	12.8	485.08	860.6181	1.4105
370	4.3897	12.8	480.6863	859.7838	1.4109
370	4.3832	12.8	491.3958	859.5396	1.411
370	4.3938	12.8	482.8455	858.9832	1.4112
370	4.3955	12.8	483.8372	858.6462	1.4113
370	4.4	12.8	482.8407	858.1309	1.4116
370	4.4	12.8	491.6101	857.1969	1.4119
370	4.4	12.8	493.9505	856.9553	1.4121
370	4.4	12.8	499.0446	856.4381	1.4124
370	4.3998	12.8	500.1586	856.3552	1.4125
370	4.4	12.8	502.7576	856.0709	1.4127
370	4.4	12.8	504.7614	855.8759	1.4129
370	4.4	12.8	507.2915	855.632	1.4131
370	4.4	12.8	511.6281	855.2237	1.4136
370	4.4	12.8	513.6415	855.038	1.4138
370	4.4	12.8	516.0086	854.8211	1.4141
370	4.4	12.8	518.6667	854.582	1.4144
370	4.4	12.8	521.4565	854.3348	1.4148
370	4.4	12.8	523.0966	854.1925	1.415

370	4.4	12.8	525.3333	853.9998	1.4154
370	4.4	12.8	526.3226	853.9149	1.4155
370	4.4	12.8	529.9058	853.6142	1.4161
370	4.4	12.8	531.4871	853.4829	1.4164
370	4.4	12.8	536.7441	853.0589	1.4173
370	4.4	12.8	538.3652	852.9313	1.4176
370	4.4	12.8	540.1694	852.7906	1.418
370	4.4	12.8	542.4555	852.6154	1.4184
370	4.4	12.8	542.8891	852.5824	1.4185
370	4.4	12.8	544.6141	852.4527	1.4189
370	4.4	12.8	547.0823	852.2686	1.4194
370	4.4	12.8	547.8461	852.2127	1.4196
370	4.4	12.8	550.3332	852.0328	1.4201
370	4.4	12.8	551.9027	851.9205	1.4205
370	4.4	12.8	553.1347	851.8335	1.4208
370	4.4	12.8	553.9167	851.7787	1.421
370	4.4	12.8	555.3121	851.6813	1.4213
370	4.4	12.8	556.0121	851.6336	1.4215
370	4.4	12.8	557.5432	851.5292	1.4219
370	4.4	12.8	559.2907	851.4112	1.4223
370	4.4	12.8	560.1087	851.3563	1.4225
370	4.4	12.8	561.7217	851.2503	1.4229
370	4.4	12.8	563.4685	851.1362	1.4234
370	4.4	12.8	564.7904	851.0519	1.4237
370	4.4	12.8	566.5013	850.9432	1.4242
370	4.4	12.8	568.0812	850.8446	1.4246
370	4.4	12.8	568.7386	850.8045	1.4248
370	4.4	12.8	570.1395	850.7179	1.4252
370	4.4	12.8	571.3967	850.6422	1.4256
370	4.4	12.8	572.916	850.5516	1.426
370	4.4	12.8	574.1059	850.4807	1.4264
370	4.4	12.8	576.1305	850.3628	1.427
370	4.4	12.8	577.9799	850.2575	1.4276
370	4.4	12.8	579.8197	850.1544	1.4281
370	4.4	12.8	580.0136	850.1436	1.4282
370	4.4	12.8	581.4394	850.0649	1.4287
370	4.4	12.8	582.6098	850.0014	1.429
370	4.4	12.8	585.1018	849.8683	1.4298
370	4.4	12.8	586.3083	849.8052	1.4302
370	4.4	12.8	589.5201	849.641	1.4313
370	4.4	12.8	591.6869	849.5329	1.4321
370	4.4	12.8	592.7218	849.4833	1.4325
370	4.4	12.8	594.4182	849.4016	1.4331
370	4.4	12.8	598.2868	849.2214	1.4345
370	4.3996	12.8	600.4803	849.1779	1.4353

370	4.4	12.8	602.2485	849.0456	1.436
370	4.4	12.8	603.6879	848.9843	1.4365
370	4.4	12.8	604.2548	848.96	1.4367
370	4.4	12.8	605.0589	848.9263	1.4371
370	4.4	12.8	606.4246	848.8699	1.4376
370	4.4	12.8	607.7344	848.8164	1.4381
370	4.4	12.8	608.2813	848.7951	1.4383
370	4.4	12.8	610.4235	848.7109	1.4392
370	4.4	12.8	611.3989	848.6731	1.4396
370	4.4	12.8	612.0931	848.6469	1.4399
370	4.4	12.8	614.2853	848.5647	1.4408
370	4.4	12.8	615.4318	848.5232	1.4413
370	4.4	12.8	616.5563	848.4833	1.4417
370	4.4	12.8	618.3355	848.4216	1.4425
370	4.4	12.8	618.8569	848.4032	1.4427
370	4.4	12.8	620.083	848.3625	1.4433
370	4.4	12.8	620.9662	848.3328	1.4436
370	4.4	12.8	621.937	848.301	1.4441
370	4.4	12.8	622.9274	848.2686	1.4445
370	4.4	12.8	623.2642	848.2581	1.4447
370	4.4	12.8	624.3467	848.2243	1.4451
370	4.4	12.8	626.3103	848.1639	1.446
370	4.4	12.8	627.2395	848.1363	1.4465
370	4.4	12.8	627.9071	848.1174	1.4468
370	4.4	12.8	629.0186	848.0854	1.4473
370	4.4	12.8	629.7508	848.0642	1.4476
370	4.4	12.8	630.6024	848.0406	1.448
370	4.4	12.8	632.0624	848.0008	1.4487
370	4.4	12.8	632.3787	847.9923	1.4488
370	4.4	12.8	633.6088	847.96	1.4494
370	4.4	12.8	634.8661	847.9278	1.45
370	4.4	12.8	636.3473	847.8908	1.4507
370	4.4	12.8	637.3208	847.8676	1.4512
370	4.4	12.8	638.7542	847.8336	1.4519
370	4.4	12.8	639.6352	847.8128	1.4523
370	4.4	12.8	640.7591	847.7882	1.4529
370	4.4	12.8	641.5874	847.7695	1.4533
370	4.4	12.8	641.9422	847.7623	1.4535
370	4.4	12.8	642.9047	847.7415	1.454
370	4.4	12.8	643.6617	847.7262	1.4544
370	4.4	12.8	644.9025	847.7014	1.455
370	4.4	12.8	645.7119	847.685	1.4554
370	4.4	12.8	646.457	847.6708	1.4558
370	4.4	12.8	647.1359	847.6583	1.4561
370	4.4	12.8	648.7601	847.6289	1.457

370	4.4	12.8	649.0184	847.6243	1.4571
370	4.4	12.8	650.0544	847.6065	1.4577
370	4.4	12.8	651.1208	847.5888	1.4582
370	4.4	12.8	652.1662	847.5719	1.4588
370	4.4	12.8	653.2628	847.5555	1.4594
370	4.4	12.8	655.146	847.527	1.4604
370	4.4	12.8	655.8151	847.5179	1.4607
370	4.4	12.8	656.7838	847.5053	1.4613
370	4.4	12.8	657.7152	847.493	1.4618
370	4.4	12.8	658.5896	847.4816	1.4622
370	4.4	12.8	659.1653	847.4753	1.4626
370	4.4	12.8	659.7386	847.4687	1.4629
370	4.4	12.8	660.6013	847.4579	1.4634
370	4.4	12.8	661.5812	847.4477	1.4639
370	4.4	12.8	663.0964	847.4337	1.4648
370	4.4	12.8	663.419	847.4292	1.4649
370	4.4	12.8	664.3426	847.4203	1.4655
370	4.4	12.8	665.1678	847.4128	1.4659
370	4.4	12.8	666.0056	847.4057	1.4664
370	4.4	12.8	666.8519	847.3995	1.4669
370	4.4	12.8	668.313	847.3883	1.4677
370	4.4	12.8	669.227	847.383	1.4683
370	4.4	12.8	669.9451	847.3777	1.4687
370	4.4	12.8	671.0852	847.3722	1.4694
370	4.4	12.8	671.2347	847.3704	1.4694
370	4.4	12.8	672.2514	847.3657	1.47
370	4.4	12.8	673.4782	847.3602	1.4708
370	4.4	12.8	674.3027	847.3569	1.4713
370	4.4	12.8	674.6016	847.3564	1.4714
370	4.4	12.8	675.4775	847.3538	1.472
370	4.4	12.8	675.8382	847.3521	1.4722
370	4.4	12.8	676.4442	847.3502	1.4725
370	4.4	12.8	677.2292	847.3486	1.473
370	4.4	12.8	677.7866	847.3474	1.4734
370	4.4	12.8	678.2057	847.3468	1.4736
370	4.4	12.8	679.1624	847.3457	1.4742
370	4.4	12.8	679.7469	847.3457	1.4746
370	4.4	12.8	680.5842	847.3448	1.4751

As it is observed from Fig 19 that the process parameters taken are shown as the population size / Swarm Size is taken as 300, Repository Size is taken as 300, Iteration Size is taken as 500, Inertia Weight is taken as 0.4, The confidence factor for Swarm and Individual is taken as 1, Number of Grids in each dimension is taken as 20, Maximum velocity is assumed as 5 and Uniform Mutation percentage is assumed as 0.5. By using these parameters we approach to use the Multi-Objective particle Swarm Optimization Technique.

In Fig 20 ,We can observed that the black circle on the graph represent the value of Taper angle , and the red circle represents the best values of Glass Formation Width after 300 iteration this is the best fitness graph observed using the above parameters. The maximum value of taper angle can be seen as 1.4751 degree with minimum Glass formation Width as 847.3448 μm , whereas the minimum value of taper angle (1.3966 degree) is observed with value of 940.1346 μm of Glass formation Width.

If we check with the Table 8, if we take one observation taking a best result as 1st observation with glass formation width of (856.4381 μm) the taper angle is seen to be approx. 1.4124 degree which is quite nearer to the minimum value observed having a set of parameters of 370 watt of Laser Power, 4.4 mm/s of Scanning speed, 12.8 bar of Gas pressure, 499.0446 Hz of Frequency.

Another observation can be seen when the glass formation is observed as 856.3552 μm and taper angle of 1.4125 degree also can give a comparably good result with the parameter of 370 watt of Laser Power, 4.3998 mm/s of Scanning speed, 12.8 bar of Gas pressures, 500.1586 Hz of Frequency.

So, from this 8th Table, we can use these 2 sets of value for further proceeding and can conclude on a point.

5.5 General Discussion

The criterion is to find the optimal parameters for minimizing taper angle at relatively low operating energy cost by minimizing the line energy, i.e., by minimizing laser power, P and maximizing scanning speed, V . Maximizing the scan speed, also helps to minimize the machining time, thereby increases productivity.

As we can see that all the 8 observation conducted gave the same set of results, also the minimum value of glass formation width is found to be as 847.3448 μm and the minimum value of taper angle is found to be 1.3967 degree. But the minimum glass formation value gives different sets of parameters as compared to minimum taper angle.

As all observation table shows the same results, we can take the two observation from each table to elaborate the issue. As we can see that the glass formation width is minimum where the set of parameters are seen on red row, that is: laser power is 370 watt, Scanning Speed is 4.4 mm/s, Gas Pressure is 12.8 bar, Frequency is 680.8971 Hz and Taper Angle is 1.4753. This parameter clearly shows that when glass formation width is low, scanning speed is maximum which is extremely good, but the taper angle is maximum.

In case of lower taper angle as shown with blue row, indicates that when the taper angle is minimized the scanning speed is 3.9105 mm/s with high glass formation width which is high as compared to the 1st row.

So, we can take a range of the parameters to balance each other to get a optimum result as shown in the table given below:

Table No:9-. Final Set of parameters to get the optimum results

Table. No	Laser power	Scanning speed	Gas pressure	Frequency	Glass formation width	Taper angle
	$P(W)$	$V(mm/s)$	$g_p(bar)$	$f(Hz)$	(μm)	(deg)
1	370	4.4	12.8	680.8971	847.3448	1.4753
	370	4.3544	12.8	501.8522	862.5726	1.4101
2	370.013	4.4	12.8	577.4515	850.3738	1.4274
	370.003	4.3293	12.7963	521.383	864.8397	1.4111
3	370	4.4	12.8	464.4081	860.2322	1.4116
	370	4.4	12.7988	497.4139	856.7161	1.4123
4	370.01	4.1574	12.799	476.5899	895.1073	1.4008
	370	4.3639	12.7985	492.385	862.2885	1.41
5	370	4.4	12.8	493.3074	857.021	1.412
	370	4.4	12.8	497.2042	856.6231	1.4123
6	370	4.4	12.7999	550.967	851.9975	1.4203
	370	4.4	12.8	552.2303	851.8967	1.4206
7	370	4.4	12.8	496.7177	856.6723	1.4122
	370.005	4.4	12.7997	490.7533	857.3479	1.4119
8	370	4.4	12.8	499.0446	856.4381	1.4124
	370	4.3998	12.8	500.1586	856.3552	1.4125

This range of parameters are taken on an average of both the parameters can be used to meet the needs.

Chapter – 6

Conclusions and Future Scope

6.1 Conclusion

The total 16 numbers of observations is taken from two from each table showing the best results from each table. Since we have to take a certain pair of parameters where we can get a minimized value of taper angle and glass formation width by which we can conclude from the above table that, some observation having or tending towards a minimum value can be taken. So, the minimized value can be seen as 1.4125 degree for taper angle and 856.3552 μm for Glass formation Width with the set of these parameters are 370 Watt for Laser Power, 4.3998 mm/s for Scanning Speed, 12.8 for Gas Pressure and 500.1586 Hz for Frequency.

One more parameter can be taken for our conclusion is 1.4119 degree for taper angle and 857.3479 μm for Glass formation Width with the set of these parameters are 370.005 Watt for Laser Power, 4.4 mm/s for Scanning Speed, 12.7997 for Gas Pressure and 490.7533 Hz for Frequency.

6.2 Future Scope of Work

After the completion of the study, there are few more scope of work which can be done are as follows:

- Since there is a limitation of this project that we are getting minimized value of taper angle with different parameters and different sets of parameter for minimizing glass formation width. So, we can write another program to get more focused solution or exactly one solution with their respective parameters.
- As theoretical and practical values may vary, the future scope of the work would be doing practical and check the results values with the parameters as shown in Table -9 and verify the conclusion to be correct or not.
- We have concluded with only two parameters that is Glass Formation Width and Taper angle, we can include the HAZ (Heat Affected Zone), BL (Breaking Load),Recast Layer, Surface Roughness etc., as per our requirements to get maximum benefit from a single program.
- Since Particle Swarm Optimization does not guarantee with an optimal solution, So, we can check with other Traditional or Non-Traditional Optimization technique to compare the results with this value and check the percentage of error with the practical values.
- Since this value might differ from material to material during cutting, welding or marking, so as the composition, hardness, brittleness, malleability and ductility may differ, so we can develop an Optimization program to give an exact and one solution for all different parameters.

References

- [1].M. J. Reddy and D. N. Kumar, “An efficient multi-objective optimization algorithm based on swarm intelligence for engineering design,” IISC Bangalore, India, Engineering Optimization Vol. 39, No. 1, January 2007, 49–68
- [2].M. I. Shirgur, “Optimization of Laser Transmission Welding Process Parameters Using Single Objective and Multi Objective Optimization Technique,” International Research Journal of Engineering and Technology (IRJET) Volume: 06 Issue: 10 | Oct 2019
- [3].C. A. C. Ceollo, G. B. Lamont, D. A. V. Veldhuizen, “Evolutionary Algorithms for Solving Multi-objective Problems,” 2nd edition, ISBN 978-0-387-33254-3, 2007 Springer Science+Business Media, LLC
- [4].H. R. E. H. Boucekara, M.A. Abido, M. Boucherma , “Optimal power flow using Teaching-Learning-Based Optimization technique,” Electric Power Systems Research 114 (2014) 49–59
- [5].Rituparna Ghosh,Parametric Study of Through Transmission Laser Welding using Particle Swarm Optimization, 2021 6th International conference on Inventive Computational Technologies (ICICT) , 978-1-7281-8501-9/21/S31.00 IEEE.
- [6].Dubey, A. K., & Yadava, V. (2008). Experimental study of Nd: YAG laser beam machining—An overview. Journal of materials processing technology, 195(1-3), 15-26.
- [7].Beausoleil, C., Sarvestani, H. Y., Katz, Z., Gholipour, J., & Ashrafi, B. (2020). Deep and high precision cutting of alumina ceramics by picosecond laser. Ceramics International, 46(10), 15285-15296.
- [8].Riveiro, A., Mejías, A., Soto, R., Quintero, F., Del Val, J., Boutinguiza, M. & Pou, J. (2016). CO2 laser cutting of natural granite. Optics & Laser Technology, 76, 19-28.
- [9].Ackerl, N., & Wegener, K. (2019). Ablation characteristics of alumina and zirconia ceramics on ultra-short pulsed laser machining. Journal of Laser Micro Nano engineering, 14(2), 168-172.
- [10]. Pankaj Keshari from Jadavpur University entitled Parametric study of Laser cutting of Ceramic Tiles (2019-21).

- [11]. J. Kennedy and R. Eberhart, "Particle swarm optimization, "Washington, DC 20212, IEEE Publications 0-7803-2768-3/95/\$4.00 0 1995 IEEE.
- [12]. Víctor Martínez-Cagigal (2022). Multi-Objective Particle Swarm Optimization (MOPSO) MATLAB Central File Exchange. Retrieved June 20, 2022.
- [13]. Álvarez-Benítez, J.E., Everson, R.M., Fieldsend, J.E.: A MOPSO Algorithm Based Exclusively on Pareto Dominance Concepts. In: Coello Coello, C.A., Hernández Aguirre, A., Zitzler, E. (eds.) EMO 2005. LNCS, vol. 3410, pp. 459–473. Springer, Heidelberg (2005).
- [14]. Durillo, J.J., García-Nieto, J., Nebro, A.J., Coello, C.A.C., Luna, F., Alba, E. (2009). Multi-Objective Particle Swarm Optimizers: An Experimental Comparison. In: Ehrgott, M., Fonseca, C.M., Gandibleux, X., Hao, J.K., Sevaux, M. (eds) Evolutionary Multi-Criterion Optimization. EMO 2009. Lecture Notes in Computer Science, vol 5467. Springer, Berlin, Heidelberg.
- [15]. Huang, V.L., Suganthan, P.N., Liang, J.J.: Comprehensive learning particle swarm optimizer for solving multiobjective optimization problems. *Int. J. Intell. Syst.* 21(2), 209–226 (2006).
- [16]. Li, X.: A Non-dominated Sorting Particle Swarm Optimizer for Multiobjective Optimization. In: Cantú-Paz, E., Foster, J.A., Deb, K., Davis, L., Roy, R., O'Reilly, U.-M., Beyer, H.-G., Kendall, G., Wilson, S.W., Harman, M., Wegener, J., Dasgupta, D., Potter, M.A., Schultz, A., Dowsland, K.A., Jonoska, N., Miller, J., Standish, R.K. (eds.) GECCO 2003. LNCS, vol. 2723, pp. 37–48. Springer, Heidelberg (2003).
- [17]. Moore, J., Chapman, R.: Application of particle swarm to multiobjective optimization. Technical report, Department of Computer Science and Software Engineering, Auburn University (1999).
- [18]. Mostaghim, S., Teich, J.: Strategies for finding good local guides in multi-objective particle swarm optimization (MOPSO). In: Proceedings of the IEEE Swarm Intelligence Symposium, SIS 2003, pp. 26–33 (2003).
- [19]. Reyes Sierra, M., Coello Coello, C.A.: Improving PSO-based multi-objective optimization using crowding, mutation and ε -dominance. In: Coello Coello, C.A., Hernández Aguirre, A., Zitzler, E. (eds.) EMO 2005. LNCS, vol. 3410, pp. 505–519. Springer, Heidelberg (2005)

- [20]. Toscano, G., Coello, C.: Using Clustering Techniques to Improve the Performance of a Multi-objective Particle Swarm Optimizer. In: Deb, K., et al. (eds.) GECCO 2004. LNCS, vol. 3102, pp. 225–237. Springer, Heidelberg (2004)
- [21]. Deb, K.: Multi-Objective Optimization Using Evolutionary Algorithms. John Wiley & Sons, Chichester (2001).
- [22]. Demšar, J.: Statistical comparisons of classifiers over multiple data sets. *J. Mach. Learn. Res.* 7, 1–30 (2006)
- [23]. Hochberg, Y., Tamhane, A.C.: Multiple Comparison Procedures. Wiley, Chichester (1987).
- [24]. Kennedy, J., Eberhart, R.C.: Swarm Intelligence. Morgan Kaufmann Publishers, San Francisco (2001).
- [25]. Knowles, J., Thiele, L., Zitzler, E.: A Tutorial on the Performance Assessment of Stochastic Multiobjective Optimizers. Technical Report 214, Computer Engineering and Networks Laboratory (TIK), ETH Zurich (2006)

6. Appendices

A

Ablation	18, 71
air knife	9
ANNOVA	37

B

beam guidance train	9
---------------------------	---

C

CO2 lasers	9, 15, 16
coaxial gas jet	9
confidence factor	39, 42, 45, 48, 51, 55, 59, 63
Confidence Factor	37
constraints	27, 28, 29

D

Direct methods	29
DOE	30
dopant	16

E

exciter lasers	18
explosive boiling	18

F

femtosecond lasers	18
focusing optics	9
Fresnel absorption	11

G

Gaussian beam	21
Gaussian curve	21
G-code	9
Glass Formation Width	37, 38
Gradient-based methods	29

H

HAZ	12, 21, 22, 24
hyper-pulse	19

I

Infrared lasers	15
Iteration Size	37

K

kerf width	13, 21, 22, 23, 25
krypton atom	16

L

LASOX	13
-------------	----

M

MINITAB	37
Multiple-nozzle systems	22

P

Particle Swarm Optimization	34, 36, 37, 71
plasma torch	17
Pocket cell	19
Population Size	37
p-polarisation	20
PRC lasers	19
pulse duty cycle	19

Q

Q-switching	19
-------------------	----

R

radio waves	23
reflectivity	15, 23
regression equation	38
repository size	39, 42, 45, 48, 51, 55, 59, 63
Reynolds number	22

S

Simulink	30
solidified oxide	24
s-polarisation	20
sublimation cutting	14

T

Taper Angle	24, 37, 38, 39, 42, 45, 48, 51, 55, 59, 63
transmissive	9

6.2 Appendix 2

The Main program where we gave regression equation as objective function denoted by “TA & GW” and save as MAIN.m file in MATLAB.

```
clear; clc;
switch MultiObjFnc
    case 'MOPSO'
        GW = @(x,y,z,w) 17725.22096 - 76.53543.*x - 1100.34431.*y - 174.18685.*z + 1.66965.*w +
        2.22781.*x.*y + 0.396173.*x.*z - 0.005830.*x.*w - 21.95831.*y.*z - 0.075985.*y.*w +
        0.034945.*z.*w + 0.097022.*x.*x + 51.93488.*y.*y + 0.516373.*z.*z + 0.000275.*w.*w;
        TA = @(x,y,z,w) 7.50882 - 0.044702.*x + 0.219641.*y + 0.064977.*z + 0.004067.*w -
        0.001034.*x.*y - 0.000576.*x.*z - 0.000017.*x.*w - 0.020469.*y.*z - 0.000014.*y.*w +
        0.000068.*z.*w + 0.000090.*x.*x + 0.055580.*y.*y + 0.006998.*z.*z + 0.00000149152.*w.*w;
        MultiObj.fun = @(x) [GW(x(:,1),x(:,2),x(:,3),x(:,4)), TA(x(:,1),x(:,2),x(:,3),x(:,4))];
        MultiObj.nVar = 4;
        MultiObj.var_min = [370 1.6 7.2 230];
        MultiObj.var_max = [440 4.4 12.8 720];
    end

% Parameters
params.Np = 300;    % Population size
params.Nr = 300;    % Repository size
params.maxgen = 50; % Maximum number of generations
params.W = 0.4;    % Inertia weight
params.C1 = 1;     % Individual confidence factor
params.C2 = 1;     % Swarm confidence factor
params.ngrid = 20; % Number of grids in each dimension
params.maxvel = 5; % Maximum velocity in percentage
params.u_mut = 0.5; % Uniform mutation percentage
% MOPSO
REP = MOPSO(params,MultiObj);
display('Repository fitnez values are stored in REP.pos_fit');
display('Repository particles positions are store in REP.pos');
```

The 2nd Part in the Function part named as MOPSO.m file in MATLAB

```
function REP = MOPSO(params,MultiObj)
```

```
    % Parameters
```

```
    Np    = params.Np;
```

```
    Nr    = params.Nr;
```

```
    maxgen = params.maxgen;
```

```
    W     = params.W;
```

```
    C1    = params.C1;
```

```
    C2    = params.C2;
```

```
    ngrid = params.ngrid;
```

```
    maxvel = params.maxvel;
```

```
    u_mut  = params.u_mut;
```

```
    fun    = MultiObj.fun;
```

```
    nVar   = MultiObj.nVar;
```

```
    var_min = MultiObj.var_min(:);
```

```
    var_max = MultiObj.var_max(:);
```

```
    % Initialization
```

```
    POS = repmat((var_max-var_min)',Np,1).*rand(Np,nVar) + repmat(var_min',Np,1);
```

```
    VEL = zeros(Np,nVar);
```

```
    POS_fit = fun(POS);
```

```
    if size(POS,1) ~= size(POS_fit,1)
```

```
        warning(['The objective function is badly programmed. It is not returning a value for each  
particle, please check it.']);
```

```
end
```

```
    PBEST = POS;
```

```
    PBEST_fit= POS_fit;
```

```
    DOMINATED= checkDomination(POS_fit);
```

```
    REP.pos = POS(~DOMINATED,:);
```

```
    REP.pos_fit = POS_fit(~DOMINATED,:);
```

```
    REP     = updateGrid(REP,ngrid);
```

```
    maxvel = (var_max-var_min).*maxvel./100;
```

```
    gen    = 1;
```

```

% Plotting and verbose
if(size(POS_fit,2)==2)
    h_fig = figure(1);
    h_par = plot(POS_fit(:,1),POS_fit(:,2),'or'); hold on;
    h_rep = plot(REP.pos_fit(:,1),REP.pos_fit(:,2),'ok'); hold on;
    try
        set(gca,'xtick',REP.hypercube_limits(:,1),'ytick',REP.hypercube_limits(:,2));
        axis([min(REP.hypercube_limits(:,1)) max(REP.hypercube_limits(:,1)) ...
            min(REP.hypercube_limits(:,2)) max(REP.hypercube_limits(:,2))]);
        grid on; xlabel('f1'); ylabel('f2');
    end
    drawnow;
end
if(size(POS_fit,2)==3)
    h_fig = figure(1);
    h_par = plot3(POS_fit(:,1),POS_fit(:,2),POS_fit(:,3),'or'); hold on;
    h_rep = plot3(REP.pos_fit(:,1),REP.pos_fit(:,2),REP.pos_fit(:,3),'ok'); hold on;
    try
        set(gca,'xtick',REP.hypercube_limits(:,1),'ytick',REP.hypercube_limits(:,2)),...
            'ztick',REP.hypercube_limits(:,3));
        axis([min(REP.hypercube_limits(:,1)) max(REP.hypercube_limits(:,1)) ...
            min(REP.hypercube_limits(:,2)) max(REP.hypercube_limits(:,2))]);
    end
    grid on; xlabel('f1'); ylabel('f2'); zlabel('f3');
    drawnow;
    axis square;
end
display(['Generation #0 - Repository size: ' num2str(size(REP.pos,1))]);

% Main MPSO loop
stopCondition = false;
while ~stopCondition
    % Select leader
    h = selectLeader(REP);

```

```

% Update speeds and positions
VEL = W.*VEL + C1*rand(Np,nVar).*(PBEST-POS) ...
      + C2*rand(Np,nVar).*(repmat(REP.pos(h,:),Np,1)-POS);
POS = POS + VEL;

% Perform mutation
POS = mutation(POS,gen,maxgen,Np,var_max,var_min,nVar,u_mut);

% Check boundaries
[POS,VEL] = checkBoundaries(POS,VEL,maxvel,var_max,var_min);

% Evaluate the population
POS_fit = fun(POS);

% Update the repository
REP = updateRepository(REP,POS,POS_fit,ngrid);
if(size(REP.pos,1)>Nr)
    REP = deleteFromRepository(REP,size(REP.pos,1)-Nr,ngrid);
end

% Update the best positions found so far for each particle
pos_best = dominates(POS_fit, PBEST_fit);
best_pos = ~dominates(PBEST_fit, POS_fit);
best_pos(rand(Np,1)>=0.5) = 0;
if(sum(pos_best)>1)
    PBEST_fit(pos_best,:) = POS_fit(pos_best,:);
    PBEST(pos_best,:) = POS(pos_best,:);
end

if(sum(best_pos)>1)
    PBEST_fit(best_pos,:) = POS_fit(best_pos,:);
    PBEST(best_pos,:) = POS(best_pos,:);
end

% Plotting and verbose
if(size(POS_fit,2)==2)
    figure(h_fig); delete(h_par); delete(h_rep);
    h_par = plot(POS_fit(:,1),POS_fit(:,2),'or'); hold on;
    h_rep = plot(REP.pos_fit(:,1),REP.pos_fit(:,2),'ok'); hold on;
    try
        set(gca,'xtick',REP.hypercube_limits(:,1),'ytick',REP.hypercube_limits(:,2));
        axis([min(REP.hypercube_limits(:,1)) max(REP.hypercube_limits(:,1)) ...
              min(REP.hypercube_limits(:,2)) max(REP.hypercube_limits(:,2))]);
    end
end

```



```

end

if(isfield(MultiObj,'truePF'))
    try delete(h_pf); end
    h_pf = plot(MultiObj.truePF(:,1),MultiObj.truePF(:,2),'.','color',0.8.*ones(1,3)); hold on;
end
grid on; xlabel('f1'); ylabel('f2');
drawnow;
axis square;
end
if(size(POS_fit,2)==3)
    figure(h_fig); delete(h_par); delete(h_rep);
    h_par = plot3(POS_fit(:,1),POS_fit(:,2),POS_fit(:,3),'or'); hold on;
    h_rep = plot3(REP.pos_fit(:,1),REP.pos_fit(:,2),REP.pos_fit(:,3),'ok'); hold on;
    try

        set(gca,'xtick',REP.hypercube_limits(:,1),'ytick',REP.hypercube_limits(:,2),'ztick',REP.hypercube_limits(:,3));
        axis([min(REP.hypercube_limits(:,1)) max(REP.hypercube_limits(:,1)) ...
            min(REP.hypercube_limits(:,2)) max(REP.hypercube_limits(:,2)) ...
            min(REP.hypercube_limits(:,3)) max(REP.hypercube_limits(:,3))]);
    end
    if(isfield(MultiObj,'truePF'))
        try delete(h_pf); end
        h_pf= plot3(MultiObj.truePF(:,1),MultiObj.truePF(:,2),MultiObj.truePF(:,3),.....
            '','color',0.8.*ones(1,3));
        hold on;
    end
    grid on; xlabel('f1'); ylabel('f2'); zlabel('f3');
    drawnow;
    axis square;
end
display(['Generation #' num2str(gen) ' - Repository size: ' num2str(size(REP.pos,1))]);
    % Update generation and check for termination
    gen = gen + 1;
    if(gen>maxgen), stopCondition = true; end

```

```

end
hold off;
end
% Function that updates the repository given a new population and its fitness
function REP = updateRepository(REP,POS,POS_fit,ngrid)
    % Domination between particles
    DOMINATED = checkDomination(POS_fit);
    REP.pos = [REP.pos; POS(~DOMINATED,:)];
    REP.pos_fit = [REP.pos_fit; POS_fit(~DOMINATED,:)];
    % Domination between non-dominated particles and the last repository
    DOMINATED = checkDomination(REP.pos_fit);
    REP.pos_fit = REP.pos_fit(~DOMINATED,:);
    REP.pos = REP.pos(~DOMINATED,:);
    % updating the grid
    REP = updateGrid(REP,ngrid);
end
% Function that corrects the positions and velocities of the particles that exceed the boundaries
function [POS,VEL] = checkBoundaries(POS,VEL,maxvel,var_max,var_min)
    % Useful matrices
    Np = size(POS,1);
    MAXLIM = repmat(var_max(:)',Np,1);
    MINLIM = repmat(var_min(:)',Np,1);
    MAXVEL = repmat(maxvel(:)',Np,1);
    MINVEL = repmat(-maxvel(:)',Np,1);
    % correct positions and velocities
    VEL(VEL>MAXVEL) = MAXVEL(VEL>MAXVEL);
    VEL(VEL<MINVEL) = MINVEL(VEL<MINVEL);
    VEL(POS>MAXLIM) = (-1).*VEL(POS>MAXLIM);
    POS(POS>MAXLIM) = MAXLIM(POS>MAXLIM);
    VEL(POS<MINLIM) = (-1).*VEL(POS<MINLIM);
    POS(POS<MINLIM) = MINLIM(POS<MINLIM);
end
% Function for checking the domination between the population. It
% returns a vector that indicates if each particle is dominated (1) or not
function dom_vector = checkDomination(fitness)
    Np = size(fitness,1);

```

```

    dom_vector = zeros(Np,1);
    all_perm = nchoosek(1:Np,2); % Possible permutations
    all_perm = [all_perm; [all_perm(:,2) all_perm(:,1)]];
    d = dominates(fitness(all_perm(:,1),:),fitness(all_perm(:,2),:));
    dominated_particles = unique(all_perm(d==1,2));
    dom_vector(dominated_particles) = 1;
end

% Function that returns 1 if x dominates y and 0 otherwise
function d = dominates(x,y)
    d = all(x<=y,2) & any(x<y,2);
end

% Function that updates the hypercube grid, the hypercube where belongs
% each particle and its quality based on the number of particles inside it
function REP = updateGrid(REP,ngrid)
    % Computing the limits of each hypercube
    ndim = size(REP.pos_fit,2);
    REP.hypercube_limits = zeros(ngrid+1,ndim);
    for dim = 1:1:ndim
        REP.hypercube_limits(:,dim) = linspace(min(REP.pos_fit(:,dim)),...
            max(REP.pos_fit(:,dim)),ngrid+1)';
    end

    % Computing where belongs each particle
    npar = size(REP.pos_fit,1);
    REP.grid_idx = zeros(npar,1);
    REP.grid_subidx = zeros(npar,ndim);
    for n = 1:1:npar
        idnames = [];
        for d = 1:1:ndim
            REP.grid_subidx(n,d) = find(REP.pos_fit(n,d)<=REP.hypercube_limits(:,d)',1,'first')-1;
            if(REP.grid_subidx(n,d)==0), REP.grid_subidx(n,d) = 1; end
            idnames = [idnames ' ' num2str(REP.grid_subidx(n,d))];
        end
        REP.grid_idx(n) = eval(['sub2ind(ngrid.*ones(1,ndim)' idnames ')']);
    end
end

```

```

        % Quality based on the number of particles in each hypercube
        REP.quality = zeros(ngrid,2);
        ids = unique(REP.grid_idx);
        for i = 1:length(ids)
            REP.quality(i,1) = ids(i); % First, the hypercube's identifier
            REP.quality(i,2) = 10/sum(REP.grid_idx==ids(i)); % Next, its quality
        end
    end

% Function that selects the leader performing a roulette wheel selection
% based on the quality of each hypercube
function selected = selectLeader(REP)
    % Roulette wheel
    prob = cumsum(REP.quality(:,2)); % Cumulated probs
    sel_hyp = REP.quality(find(rand(1,1)*max(prob)<=prob,1,'first'),1); % Selected hypercube
    % Select the index leader as a random selection inside that hypercube
    idx = 1:1:length(REP.grid_idx);
    selected = idx(REP.grid_idx==sel_hyp);
    selected = selected(randi(length(selected)));
end

% Function that deletes an excess of particles inside the repository using
% crowding distances
function REP = deleteFromRepository(REP,n_extra,ngrid)
    % Compute the crowding distances
    crowding = zeros(size(REP.pos,1),1);
    for m = 1:1:size(REP.pos_fit,2)
        [m_fit,idx] = sort(REP.pos_fit(:,m),'ascend');
        m_up = [m_fit(2:end); Inf];
        m_down = [Inf; m_fit(1:end-1)];
        distance = (m_up-m_down)./(max(m_fit)-min(m_fit));
        [~,idx] = sort(idx,'ascend');
        crowding = crowding + distance(idx);
    end

    crowding(isnan(crowding)) = Inf;
    % Delete the extra particles with the smallest crowding distances

```

```

[~,del_idx] = sort(crowding,'ascend');
del_idx = del_idx(1:n_extra);
REP.pos(del_idx,:) = [];
REP.pos_fit(del_idx,:) = [];
REP = updateGrid(REP,ngrid);
end

```

%Function that performs the mutation of the particles depending on the current generation

```
function POS = mutation(POS,gen,maxgen,Np,var_max,var_min,nVar,u_mut)
```

```
% Sub-divide the swarm in three parts [2]
```

```
fract = Np/3 - floor(Np/3);
```

```
if(fract<0.5), sub_sizes =[ceil(Np/3) round(Np/3) round(Np/3)];
```

```
else sub_sizes =[round(Np/3) round(Np/3) floor(Np/3)];
```

```
end
```

```
cum_sizes = cumsum(sub_sizes);
```

```
% First part: no mutation
```

```
% Second part: uniform mutation
```

```
nmut = round(u_mut*sub_sizes(2));
```

```
if(nmut>0)
```

```
idx = cum_sizes(1) + randperm(sub_sizes(2),nmut);
```

```
POS(idx,:) = repmat((var_max-var_min)',nmut,1).*rand(nmut,nVar) +
```

```
repmat(var_min',nmut,1);
```

```
end
```

```
% Third part: non-uniform mutation
```

```
per_mut = (1-gen/maxgen)^(5*nVar); % Percentage of mutation
```

```
nmut = round(per_mut*sub_sizes(3));
```

```
if(nmut>0)
```

```
idx = cum_sizes(2) + randperm(sub_sizes(3),nmut);
```

```
POS(idx,:) = repmat((var_max-var_min)',nmut,1).*rand(nmut,nVar) +
```

```
repmat(var_min',nmut,1);
```

```
end
```

```
end
```